U.S. DEPARTMENT OF COMMERCE
National Technical Information Service

PB-288 791

Seasonal Distribution, Trajectory Studies, and Sorption Characteristics of Suspended Particulate Matter in the Northern Puget Sound Region

(U.S.) National Oceanic and Atmospheric Admin., Seattle, WA

Prepared for

Environmental Protection Agency, Washington, DC

Jul 78

PB 288791

DOC

EPA

United States
Department of
Commerce

National Oceanic and Atmospheric Administration
Environmental Research Laboratories
Seattle WA 98115

United States
Environmental Protection
Agency

Office of Energy, Minerals, and
Industry
Washington DC 20460

EPA-600/7-78-126
July 1978

Research and Development

Seasonal Distribution, Trajectory Studies, and Sorption Characteristics of Suspended Particulate Matter in the Northern Puget Sound Region

Interagency Energy/Environment R&D Program Report

REPRODUCED BY
NATIONAL TECHNICAL
INFORMATION SERVICE
U. S. DEPARTMENT OF COMMERCE
SPRINGFIELD, VA. 22161

TECHNICAL REPORT DATA

(Please read Instructions on the reverse before completing)

1. REPORT NO.
EPA-600/7-78-126

2.

3. RECIPIENT'S ACCESSION NO.
PB288791

4. TITLE AND SUBTITLE
Seasonal Distribution, Trajectory Studies, and Sorption Characteristics of Suspended Particulate Matter in the Northern Puget Sound Region

5. REPORT DATE
July 1978 issuing date

6. PERFORMING ORGANIZATION CODE

7. AUTHOR(S)
Baker, Edward T., Cline, Joel D., Feely, Richard A. and Quan, Joyce

8. PERFORMING ORGANIZATION REPORT NO.

9. PERFORMING ORGANIZATION NAME AND ADDRESS
Pacific Marine Environmental Laboratory
Environmental Research Laboratories, NOAA
7600 Sand Point Way NE
Seattle, Washigton 98115

10. PROGRAM ELEMENT NO.
EHE 625-A

11. CONTRACT/GRANT NO.
NA
(IAG No. D6-E693-EN)

12. SPONSORING AGENCY NAME AND ADDRESS
U.S. Environmental Protection Agency
Office of Research & Development
Office of Energy, Minerals & Industry
Washington, D.C. 20460

13. TYPE OF REPORT AND PERIOD COVERED

14. SPONSORING AGENCY CODE
EPA-ORD

15. SUPPLEMENTARY NOTES
This project is part of the EPA-planned and coordinated Federal Interagency Energy/Environment R&D Program.

16. ABSTRACT

With the development of petroleum and natural gas reserves in Alaska, the waters of northern Puget Sound and the Strait of Juan de Fuca have become major transportation routes through which Alaskan petroleums are delivered to Washington State. The increased tanker traffic undoubtedly will result in significant addition of petroleum hydrocarbons to the marine ecosystem. Once petroleum hydrocarbons are introduced into the marine environment, a combination of physical, chemical, and biological processes become operative in the destruction and removal of the oil.

This study focuses on the spatial and seasonal distributions of suspended particulate matter and its adsorption characteristics relative to Alaskan crude oils. Seasonal distributions of total suspended solids were determined for the area north of Admiralty Inlet, east of Port Angeles, and south of the Fraser River between November 1976 and August 1977. Also, LANDSAT images were utilized to study surface trajectories of sediment plumes originating from the Fraser and Skagit Rivers. The composition and abundance of hydrocarbons associated with suspended matter was evaluated at five strategic locations in the northern Puget Sound region. Laboratory measurements were also performed under simulated natural conditions to investigate the short-term interaction between Prudhoe Bay crude oil and two locally-derived riverine sediments.

17. (Circle One or More) KEY WORDS AND DOCUMENT ANALYSIS

a. DESCRIPTORS

Ecology
[✓ Environments]
Earth Atmosphere
Environmental Engineering
Geography
Hydrology, Limnology
Biochemistry
Earth Hydrosphere
Combustion
Refining
Energy Conversion
[✓ Physical Chemistry]
Materials Handling
[✓ Inorganic Chemistry]
[✓ Organic Chemistry]
Chemical Engineering
Other

b. IDENTIFIERS/OPEN ENDED TERMS

[illegible]
Other Transport Processes
Ecological Effects

c. COSATI Field/Group

6F [✓ 8A] 8F
8H 10A 10B
[✓ 7B] [✓ 7C] 13B
[✓ 97E]

18. DISTRIBUTION STATEMENT
Release Unlimited

19. SECURITY CLASS (This Report)
Unclassified

20. SECURITY CLASS (This page)
Unclassified

21. NO. OF PAGES
156

22. PRICE
PC A08/MF A01

EPA Form 2220-1 (9-73)

EPA-600/7-78-126
July 1978

SEASONAL DISTRIBUTION, TRAJECTORY STUDIES, AND SORPTION CHARACTERISTICS OF SUSPENDED PARTICULATE MATTER IN THE NORTHERN PUGET SOUND REGION

by

Edward T. Baker, Joel D. Cline, Richard A. Feely, and Joyce Quan

Pacific Marine Environmental Laboratory
Environmental Research Laboratories
National Oceanic and Atmospheric Administration
7600 Sand Point Way N.E.
Seattle, Washington 98115

Prepared for the MESA (Marine Ecosystems Analysis) Puget Sound Project, Seattle, Washington in partial fulfillment of

EPA Interagency Agreement No. D6-E693-EN
Program Element No. EHE625-A

This study was conducted
as part of the Federal
Interagency Energy/Environment
Research and Development Program

Prepared for

OFFICE OF ENERGY, MINERALS, AND INDUSTRY
OFFICE OF RESEARCH AND DEVELOPMENT
U.S. ENVIRONMENTAL PROTECTION AGENCY
WASHINGTON, D.C. 20460

February 1978

UNITED STATES DEPARTMENT OF COMMERCE
Juanita M. Kreps, Secretary

NATIONAL OCEANIC AND ATMOSPHERIC ADMINISTRATION
Richard A. Frank, Administrator

Environmental Research Laboratories
Wilmot N. Hess, Director

Completion Report Submitted to
PUGET SOUND ENERGY-RELATED RESEARCH PROJECT
MARINE ECOSYSTEMS ANALYSIS PROGRAM
ENVIRONMENTAL RESEARCH LABORATORIES

by

Pacific Marine Environmental Laboratory
Environmental Research Laboratories
National Oceanic and Atmospheric Administration
7600 Sand Point Way N.E.
Seattle, Washington 98115

This work is the result of research sponsored by the Environmental Protection Agency and administered by the Environmental Research Laboratories of the National Oceanic and Atmospheric Administration.

The Environmental Research Laboratories do not approve, recommend, or endorse any proprietary product or proprietary material mentioned in this publication. No reference shall be made to the Environmental Research Laboratories or to this publication furnished by the Environmental Research Laboratories in any advertising or sales promotion which would indicate or imply that the Environmental Research Laboratories approve, recommend, or endorse any proprietary product or proprietary material mentioned herein, or which has as its purpose an intent to cause directly or indirectly the advertised product to be used or purchased because of this Environmental Research Laboratories publication.

CONTENTS

Figures . . . v
Tables . . . ix
Abstract . . . xi

1. Introduction . . . 1
    1.1 General Statement . . . 1
    1.2 Objectives . . . 2
2. Geography, Physical Oceanography, and Hydrology . . . 4
    2.1 Physiographic Setting . . . 4
    2.2 Circulation Patterns and Hydrography . . . 4
    2.3 River Runoff and Sediment Discharge . . . 6
3. Conclusions . . . 12
    3.1 Suspended Matter Distributions . . . 12
    3.2 Suspended Hydrocarbons . . . 12
    3.3 Oil-Sediment Interaction Studies . . . 13
    3.4 LANDSAT Imagery . . . 13
4. Recommendations . . . 15
    4.1 Suspended Matter Distributions . . . 15
    4.2 Characterization of Suspended Hydrocarbons . . . 15
    4.3 Oil-Sediment Interaction Studies . . . 16
    4.4 LANDSAT Studies . . . 16
5. Suspended Matter Distributions . . . 17
    5.1 Station Locations and Sampling Rationale . . . 17
    5.2 Observational Procedures . . . 19
    5.3 Results and Discussion . . . 22
        5.3.1 Suspended Particulate Matter Concentrations - Areal Distributions . . . 22
            5.3.1.1 Seasonal surface values . . . 22
            5.3.1.2 Seasonal near-bottom values . . . 22
        5.3.2 Suspended Particulate Matter Distribution - Seasonal Nephelometer Transects . . . 22
            5.3.2.1 Transect A (sta. 4-7) . . . 26
            5.3.2.2 Transect B (sta. 11-15) . . . 26
            5.3.2.3 Transect C (sta. 17-21) . . . 26
            5.3.2.4 Transect D (sta. 24-27) . . . 30
        5.3.3 Suspended Particulate Matter Distribution - Time Series Measurements . . . 32
            5.3.3.1 Strait of Juan de Fuca (sta. 9/10) . . . 32
            5.3.3.2 Deception Pass (sta. 15) . . . 32
            5.3.3.3 Cherry Point (sta. 17) . . . 37
            5.3.3.4 Fraser River (sta. 26) . . . 37

    - 5.3.4 Suspended Particulate Matter - X-ray Mineralogy . . . 37
    - 5.3.5 Particle Size Distributions 44
  - 5.4 Summary 44
- 6. Oil-Sediment Interactions 46
  - 6.1 General Statement 46
  - 6.2 Laboratory Study 47
  - 6.3 Methodology 47
    - 6.3.1 Petroleum Hydrocarbon Analysis 47
    - 6.3.2 Oil Recovery Efficiency 48
    - 6.3.3 Sediment-Sea Water Organic Matter Corrections 49
    - 6.3.4 Sediment Morphology and Compositional Characteristics 50
  - 6.4 Results 57
    - 6.4.1 Skagit River Sediments 57
    - 6.4.2 Fraser River Sediments 62
  - 6.5 Discussion 64
  - 6.6 Summary 67
- 7. Natural Distributions of Hydrocarbons on Suspended Matter 68
  - 7.1 General Statement 68
  - 7.2 Field Studies 69
  - 7.3 Methodology 69
    - 7.3.1 Sample Collection 69
    - 7.3.2 Sample Preparation and Analysis 70
  - 7.4 Results 73
    - 7.4.1 Field Sampling 73
    - 7.4.2 Suspended Hydrocarbons - MESA I 73
    - 7.4.3 Suspended Hydrocarbons - MESA II 76
    - 7.4.4 Suspended Hydrocarbons - MESA III 82
  - 7.5 Discussion 87
  - 7.6 Summary 90
- 8. LANDSAT Imagery 91
  - 8.1 Introduction 91
  - 8.2 Seasonal Variations 93
  - 8.3 Tidal Variations 103
  - 8.4 Summary and Conclusions 105

- Acknowledgments 107
- Bibliography 108
- Appendix A Seasonal Distributions and Abundances of Low Molecular Weight Aliphatics in the Waters of Northern Puget Sound 114
  - A.1 Introduction 115
  - A.2 Methodology 116
  - A.3 Results and Discussion 116
    - A.3.1 LMWH - MESA I 118
    - A.3.2 LMWH - MESA II 123
    - A.3.3 LMWH - MESA III 123
  - A.4 Summary 132

FIGURES

Number		Page
2.1	Physical setting of the study region	5
2.2	Monthly range, mean, and standard deviation of: a. water discharge and b. suspended sediment discharge for the Fraser River at Hope, B.C. for the period from January 1967 through September 1977	8
2.3	Monthly mean discharge of water and suspended sediments of the Skagit River at Mt. Vernon during 1975	11
5.1	Station locations for MESA I, II, and III. Light scattering measurements were made at all stations	18
5.2	Scatter plot of nephelometer data versus particulate concentration in the study area	20
5.3	Scatter plot of nephelometer data versus particulate concentration for some Gulf of Mexico samples collected simultaneously with the light scattering measurements	21
5.4	Concentration contours (mg/l) of particulate matter for surface and near bottom samples from MESA I	23
5.5	Concentration contours (mg/l) of particulate matter for surface and near bottom samples from MESA II	24
5.6	Concentration contours (mg/l) of particulate matter for surface and near bottom samples from MESA III	25
5.7	Light scattering values, Transect A	27
5.8	Temperature values (°C), Transect A	28
5.9	Light scattering values, Transect B	29
5.10	Temperature values (°C), Transect B	30
5.11	Light scattering values, Transect C	31

Number Page

5.12 Temperature values ($^{\circ}C$), Transect C 33

5.13 Light scattering values, Transect D 34

5.14 Temperature values ($^{\circ}C$), Transect C 35

5.15 Time series light scattering measurements, station 9/10A 36

5.16 Time series light scattering measurements, station 15 38

5.17 Time series light scattering measurements, station 17 39

5.18 Time series light scattering measurements, station 26 40

5.19 Coulter Counter particle size distributions from six centrifuge samples 45

6.1 Evaporative weight loss of Prudhoe Bay crude oil 48

6.2 Suspended matter recovery system 51

6.3 Scanning electron micrographs of Skagit River suspended matter showing particles recovered in the ambient water (a) and in the effluent from the centrifuge (b) 54

6.4 Scanning electron micrographs of Fraser River suspended matter showing particles recovered in the ambient water (a) and in the effluent from the centrifuge (b) 56

6.5 Concentration of accommodated Prudhoe Bay crude oil (L_a) on Skagit River suspended sediments as a function of the initial oil loading (L_o) 59

6.6 Gas chromatogram of the extracted aliphatic fraction taken from oil flocculated sediments 60

6.7 Gas chromatogram of the aliphatic fraction of Prudhoe Bay crude oil 61

6.8 Concentration of accommodated Prudhoe Bay crude oil (L_a) on Fraser River suspended sediments as a function of the initial oil loading (L_o) 63

Number Page

7.1 Chromatograms of the (a) alkane standard (ALK-9) and (b) the arene standard (PAH-6) 72

7.2 Gas chromatogram of the saturated hydrocarbon fraction from station 15 75

7.3 Gas chromatograms of the (a) saturated and (b) unsaturated fraction from station 9 located near Port Angeles (MESA-II) 78

7.4 Gas chromatograms of the (a) saturated and (b) unsaturated fractions from station 17 located near Cherry Point (MESA-II) 81

7.5 Gas chromatograms of the (a) saturated and (b) unsaturated fractions from station 17 located near Cherry Point (MESA-III) 83

7.6 Gas chromatograms of the (a) saturated and (b) unsaturated fractions from station 26 located near the mouth of the Fraser River (MESA-III) 86

8.1 MSS Band 5 of LANDSAT image 1169-18373 on Jan. 8, 1973 between slack water and major ebb current 94

8.2 MSS Band 5 of LANDSAT image 1187-18374 on Jan. 26, 1973 95

8.3 MSS Band 4 of LANDSAT image 2417-18220 on Mar. 14, 1976 96

8.4 MSS Band 5 of LANDSAT image 2111-18254 on May 13, 1975 97

8.5 MSS Band 5 of LANDSAT image 2129-18254 on May 31, 1975 98

8.6 MSS Band 5 of LANDSAT image 1727-18290 on July 20, 1974 99

8.7 MSS Band 5 of LANDSAT image 5465-17484 on July 27, 1976 100

8.8 MSS Band 4 of LANDSAT image 2921-18025 on July 31, 1977 101

8.9 MSS Band 5 of LANDSAT image 2957-18004 on Sept. 5, 1977 102

Number Page

Appendix

A.1 Locations selected for seasonal LMW hydrocarbon observations 117

A.2 Areal surface distribution of dissolved methane (nℓ/ℓ, STP) during 16-22 Nov. 1976 (MESA-I) 119

A.3 Distribution of dissolved methane (nℓ/ℓ, STP) within 5 m of the bottom during 16-22 Nov. 1976 (MESA-I) 120

A.4 Areal surface distribution of dissolved ethane (nℓ/ℓ, STP) during 16-22 Nov. 1976 (MESA-I) 121

A.5 Areal surface distribution of dissolved ethene (nℓ/ℓ, STP) during 16-22 Nov. 1976 (MESA-I) 122

A.6 Areal surface distribution of dissolved methane (nℓ/ℓ, STP) during 10-17 Mar. 1977 (MESA-II) 124

A.7 Distribution of dissolved methane (nℓ/ℓ, STP) within 5 m of the bottom during 10-17 Mar. 1977 (MESA-II) 125

A.8 Areal surface distribution of dissolved ethane (nℓ/ℓ, STP) during 10-17 Mar. 1977 (MESA-II) 126

A.9 Areal surface distribution of dissolved ethene (nℓ/ℓ, STP) during 10-17 Mar. 1977 (MESA-II) 127

A.10 Areal surface distribution of dissolved methane (nℓ/ℓ, STP) during 8-14 Aug. 1977 (MESA-III) 128

A.11 Distribution of dissolved methane (nℓ/ℓ, STP) within 5 m of the bottom during 8-14 Aug. 1977 (MESA-III) 129

A.12 Areal surface distribution of dissolved ethane (nℓ/ℓ, STP) during 8-14 Aug. 1977 (MESA-III) 130

A.13 Areal surface distribution of dissolved ethane (nℓ/ℓ, STP) during 8-14 Aug. 1977 (MESA-III) 131

A.14 The areal surface ethane/ethene ratio ($C_{2:0}/C_{2:1}$) during 8-14 Aug. 1977 (MESA-III) 133

TABLES

Number		Page
2.1	Average annual runoff from the major rivers discharging into the study region	7
2.2	Comparison of water and sediment discharge for the Fraser and Skagit Rivers during period of record (1967-1976)	9
5.1	X-ray mineralogy of selected water samples and centrifuge samples	41
6.1	Extraction and concentration step efficiencies	49
6.2	Comparison of the concentration of total suspended matter (TSM) in the ambient water with that in the centrifuge effluent. Also shown are the concentrations of total carbon in the suspended material, its carbon:nitrogen ratio (C:N), and the chlorite:illite, quartz:illite, and feldspar:illite ratios	53
6.3	Representative particle size distributions from the Skagit and Fraser Rivers	55
6.4	The concentration of sediment-accommodated Prudhoe Bay crude oil for various initial oil loadings	57
6.5	Accommodation of Prudhoe Bay crude oil on Fraser River suspended sediments at 10°C and 32°/oo	64
7.1	Component listing and concentrations for aliphatic standard (ALK-9) and arene standard (PAH-6)	71
7.2	Sampling protocol for suspended hydrocarbons at each of the time series stations	74
7.3	Concentrations of saturated and unsaturated hydrocarbons at stations sampled	77
7.4	Concentrations of normal alkanes and the isoprenoid hydrocarbons pristane and phytane at stations occupied during MESA-II	79

Number		Page
7.5	Concentrations of normal alkanes and the isoprenoid hydrocarbons pristane and phytane at stations occupied during MESA-III	84
7.6	Summary of hydrocarbon concentrations, organic carbon, carbon:nitrogen ratios, and the ratio of extractable hydrocarbons to organic carbon at selected stations	89
8.1	Principal characteristics of the LANDSAT satellite and multispectral scanner	92
Appendix	
A.1	Seasonal distributions of selected hydrocarbons at station 2 (48°11.3'N 122°48.6'W)	134
A.2	Seasonal distributions of selected hydrocarbons at station 5 (48°14.0'N 123°17.2'W)	135
A.3	Seasonal distributions of selected hydrocarbons at station 15 (48°24.2'N 122°41.0'W)	136
A.4	Seasonal distributions of selected hydrocarbons at station 17 (48°50.6'N 122°46.2'W)	137
A.5	Seasonal distributions of selected hydrocarbons at station 23 (48°55.0'N 123°6.5'W)	138
A.6	Seasonal distributions of selected hydrocarbons at station 26 (49°2.0'N 123°15.5'W)	139
A.7	Seasonal distributions of selected hydrocarbons at station 32 (48°34.3'N 123°13.5'W)	140

ABSTRACT

With the projected development of petroleum and natural gas reserves in Alaska, the waters of northern Puget Sound and the Strait of Juan de Fuca may become major transportation routes through which Alaskan petroleums are delivered to Washington State refineries. Associated with increased production of the refineries will be the exportation of refined products to markets outside the State of Washington.

The seasonal distributions of total suspended solids were determined for the area north of Admiralty Inlet, east of Port Angeles, and south of the Fraser River between November 1976 and August 1977. Typical values ranged from 0.5 to 2 mg/ℓ with the highest concentrations observed near the Fraser River (8 mg/ℓ) and Deception Pass (2-3 mg/ℓ). Vertical distributions of suspended particulate matter (SPM) showed highest values in the surface and near bottom waters. High surface concentrations are believed to be due to seasonal/temporal fresh water runoff and primary production; elevated levels near the bottom are probably related to resuspension processes. Seasonal variability was insignificant on a regional basis except for areas directly influenced by river runoff. Diurnal variability was most pronounced near major sediment sources and at stations characterized by large tidal excursions.

In a complementary study, LANDSAT images were utilized to study surface trajectories of sediment plumes originating from the Fraser and Skagit Rivers. Major sediment plumes originating from the Fraser River can be traced across the Strait of Georgia and through Porlier, Active, and Boundary Passes. Trajectories during the ebb tide are southeast along the coast; but during flood tide, the trajectory is west and northwest along the northern coast of Galiano Island. Sediment plumes originating from the distributaries of the Skagit River are most pronounced in early summer. At this time suspended sediments from the Skagit River can be traced as far south as the middle of Saratoga Passage and as far north as Deception Pass.

As a corollary to the suspended sediment distribution studies, the composition and abundance of hydrocarbons associated with suspended matter was evaluated at five strategic locations in the northern Puget Sound region. Hydrocarbons extracted from suspended matter ranged from 0.2 mg/g to 1.4 mg/g dry weight. Major identifiable paraffins were largely biogenic (e.g., pentadecane, heptadecane, pristane, etc.), although one sample taken near the Fraser River may have been contaminated with motor oil. Similarly, samples taken from the Strait of Juan de Fuca show the possible presence of weathered petroleum residues (i.e., tar balls), which is not unexpected given the level of transportation activity in this area. Within the limits of these few data, we conclude that suspended matter in these waters is not obviously contaminated with petroleum hydrocarbons, but low levels of contaminants may be present that were not identifiable because of the modicum concentrations of suspended matter present.

Laboratory measurements also were performed under simulated natural conditions to investigate the short-term interaction between Prudhoe Bay crude oil and two locally-derived riverine sediments. These experiments showed that significant concentrations of crude oil may be accommodated on suspended matter under optimum conditions. Skagit River sediments, being significantly coarser than suspended material from the Fraser River, accommodated and settled up to 100% its weight in oil at 10°C (S = 32°/oo), but only 40% at 15°C (S = 32°/oo). When smaller particles (Fraser River) were subjected to the same experimental conditions, considerably less oil was sedimented (up to 17%). However, much of the remaining oil and sediment was present in a surface slick. Experiments show that significant amounts of oil may be accommodated on suspended sediments, but the quantity retained will depend on the isoelectric point of the oil and sediment particles, particle size, temperature, and the concentration of oil relative to that of sediments.

1. INTRODUCTION

1.1 GENERAL STATEMENT

With the recent development of petroleum reserves at Prudhoe Bay and the projected development of petroleum and natural gas reserves on the OCS of Alaska, northern Puget Sound and the Strait of Juan de Fuca may become a major transportation route through which Alaskan petroleums are delivered to Washington State refineries or transshipped to northern tier states. Refining of petroleum is presently carried out at Cherry Point, Ferndale, and Anacortes refineries. Associated with increased production of these refineries will be the exportation of refined products (e.g., gasoline, diesel fuel, lubricating oils, etc.) to markets outside the State of Washington. A portion of the products undoubtedly will be transported by water, thus creating an increase potential for hydrocarbon loading of the local marine waters through minor chronic spillage or a major tanker accident.

With few notable exceptions, the region has not been plagued with massive oil spills, although the effects of chronic, low level inputs of petroleum and refined products have not been adequately assessed. In the past, much of the crude oil was delivered to Washington State refineries by pipeline from Canada, but plans announced by the National Energy Board of Canada will systematically curtail and finally terminate all exports of crude oil by 1982 (EPA, 1977). This alone will result in a significant increase in tranker traffic to meet local domestic needs. This event will not affect the marine shipment of refined products from the local refineries, whose production schedules should increase with the availability of Alaskan crude oil.

At the present time, the proven reserves of Prudhoe Bay are 9.6 billion barrels with an additional estimated reserve of 3.2 billion barrels locked up in other north slope reserves (EPA, 1977). By 1985, it is estimated that approximately 3.1 million barrels per day will be produced from Alaska, the bulk of it derived from the north slope via the trans-Alaskan pipeline (EPA, 1977). Numerous scenarios governing the allocation and transportation of this crude oil to west coast ports and elsewhere are currently being debated. While no firm estimates are available on the quantity of crude oil that will be shipped to and/or through Washington State, it remains clear that ever increasing amounts of petroleum will be moved through the Strait of Juan de Fuca and San Juan Passages via tankers to meet local demand.

Once petroleum hydrocarbons are introduced into the marine environment, a combination of physical, chemical, and biological processes become operative in the destruction and removal of the oil. These processes include spreading, dispersion, atmospheric injection, evaporation, chemical and biochemical oxidation, emulsification, and the physical sedimentation of oil on particles (NAS, 1975). While all of these processes are of special interest, this study addresses the temporal and spatial distributions of suspended particulate matter and its adsorption characteristics relative to a typical Alaskan crude oil.

1.2 OBJECTIVES

Oil spilled onto the surface of the ocean is acted upon by several physical processes, including solution, emulsification, attachment to suspended particles, evaporation, and aerosol formation. The latter two processes represent a physical transfer of oil from the aquatic environment, thus reducing its potential impact on marine organisms. In contrast, petroleum in true solution, emulsified or sorbed to sediments represents a direct impact on marine organisms.

Of the water accommodated fraction, oil sorbed to particles represents a potential impact of longer duration than either oil in true solution or emulsified. Most of the components of oil are sparingly soluble in natural waters (McAuliffe, 1977), the exceptions being the low molecular weight aromatics. Thus, their impact is minimal both in terms of concentration and duration. Likewise, oil-in-water emulsion is thermodynamically unstable in sea water (Huang and Elliott, 1977), thus oil droplets would tend to coalesce into a surface slick when the turbulent energy is diminished.

On the other hand, oil agglutinated to particles is stabilized by the association (Huang and Elliott, 1977) and results in wide dispersal of oiled particles that may impact a range of planktonic and benthic organisms. Recent studies of oil spills in coastal regions containing high suspended matter concentrations clearly have indicated rapid dispersal of the oil by adsorption onto particles (Forrester, 1971; Farrington and Quinn, 1973). However, other investigators have observed surface oil slicks coexisting with suspended matter plumes (Kolpack, 1971). Apparently, the dispersal of oil does not always result from a simplistic model of adsorption and transport in association with suspended particles.

The major objectives of this multidisciplinary study are directed toward a better understanding of the importance of suspended matter in the transport of crude oil. Recognizing the importance of suspended matter in the transport and dispersal of sorbed hydrocarbons, an element of this study addresses the distributions, mineralogical compositions, and trajectories of marine and riverine suspended matter in the waters of "northern Puget Sound." Synoptic trajectories and distributions were evaluated photographically using LANDSAT imagery, augmented with sea truth measurements taken seasonally.

In concert with these activities, the oil loading capacity of both Fraser and Skagit River sediments was studied under simulated environmental conditions. Prudhoe Bay crude oil was used as the adsorbed phase.

The third major thrust of the study deals with natural hydrocarbon-particulate matter associations. Because the Strait of Juan de Fuca, San Juan passages, and the southern Strait of Georgia (referred to here as northern Puget Sound) represent major transportation waterways to British

Columbia and the State of Washington, the compositions and ambient concentrations of sorbed hydrocarbons on suspended solids were investigated.

In a related study, the seasonal distributions of the dissolved low molecular weight aliphatic hydrocarbons (LMWH) were determined in order to quantify the baseline levels of these components and to make a preliminary assessment of the current levels of petroleum input into these waters. Because this subprogram is not directly related to the question of suspended matter transport of petroleum, it was included in Appendix A.

For clarity, the results of this research are described in four separate sections (Chapters 5-8). The first section discusses the seasonal and diurnal distributions of suspended matter. This discussion is followed by a preliminary treatment of the absorptive behavior of river-derived sediments toward Prudhoe Bay crude oil. The third section discusses and evaluates the current levels of sorbed hydrocarbons and their probable sources. Lastly, a synoptic overview of the surface suspended sediment distributions and probable trajectories of riverine material are provided as a focus for probable areas of impact. The purpose of the study and research objectives are outlined in Chapter 1, followed by a summary of conclusions and recommended research activities in Chapters 3 and 4. For the purpose of continuity, the geographical and hydrological setting of the Strait of Juan de Fuca, San Juan passages, and the lower Strait of Georgia are reserved for Chapter 2.

2. GEOGRAPHY, PHYSICAL OCEANOGRAPHY, AND HYDROLOGY

2.1 PHYSIOGRAPHIC SETTING

Figure 2.1 shows the physical setting of the study region. The area is an inland sea with access to the open Pacific Ocean through two major waterways, the Strait of Georgia and the Strait of Juan de Fuca. The Strait of Georgia, to the north, is one of the largest inland waterways on the west coast of North America. It is partially enclosed with Vancouver Island forming the western boundary and the mainland of British Columbia and northwestern Washington forming the eastern boundary. The Strait of Georgia is about 220 km long, 33 km wide, and has an average depth of about 150 m. The San Juan Archipelago and the Canadian Gulf Islands separate the Strait of Georgia from the Strait of Juan de Fuca. Passage between these major waterways is primarily accomplished through Haro Strait to the west and Rosario Strait to the east.

The Strait of Juan de Fuca, to the south, is a submarine valley extending from the Pacific Ocean to Whidbey Island and Rosario Strait, about 145 km long. The width varies between 20 and 24 km from the entrance to the Port Angeles area, where it narrows to 16 km near Victoria, B.C., before widening to about 40 km. The Strait contains two basins which are separated by a cross-channel ridge or sill. The ridge extends southward from Victoria, at an approximate depth of 60 m. The western basin or Outer Strait slopes gradually in a seaward direction. The eastern basin or Inner Strait contains several channels which lead into Haro Strait, Rosario Strait, and Admiralty Inlet.

2.2 CIRCULATION PATTERNS AND HYDROGRAPHY

Circulation patterns and hydrography for the study region have been studied and reviewed by several authors (Tully, 1942; Waldichuk, 1957; Herlinveaux and Tully, 1961; Chang et al., 1976; Parker, 1977; Schumacher et al., 1978), and only a brief summary is deemed necessary for the purpose of this report.

The primary factors that control circulation and the distribution of properties in the study region include tides, fresh water, runoff, winds and atmospheric pressure variations, with secondary influences due to coriolis force, centrifugal force, and topography. The Strait of Georgia is characterized by a strong vertical stratification which results from fresh water input from numerous mainland rivers, the Fraser River being the most important. Driven by estuarine flow, the brackish water moves progressively seaward, primarily through the San Juan passages into the Strait of Juan de Fuca, where mixing occurs as a result of turbulent tidal energy. As the brackish water mixes with the saline Pacific Ocean water, part of it is returned to the deeper waters of the Strait of Georgia. However, the major portion escapes to the Pacific Ocean in the upper layer. Salt balance is maintained by the intrusion of colder, more saline water from the Pacific at mid-depths in the Strait of Juan de Fuca during the summer months (Waldichuk, 1957). This water

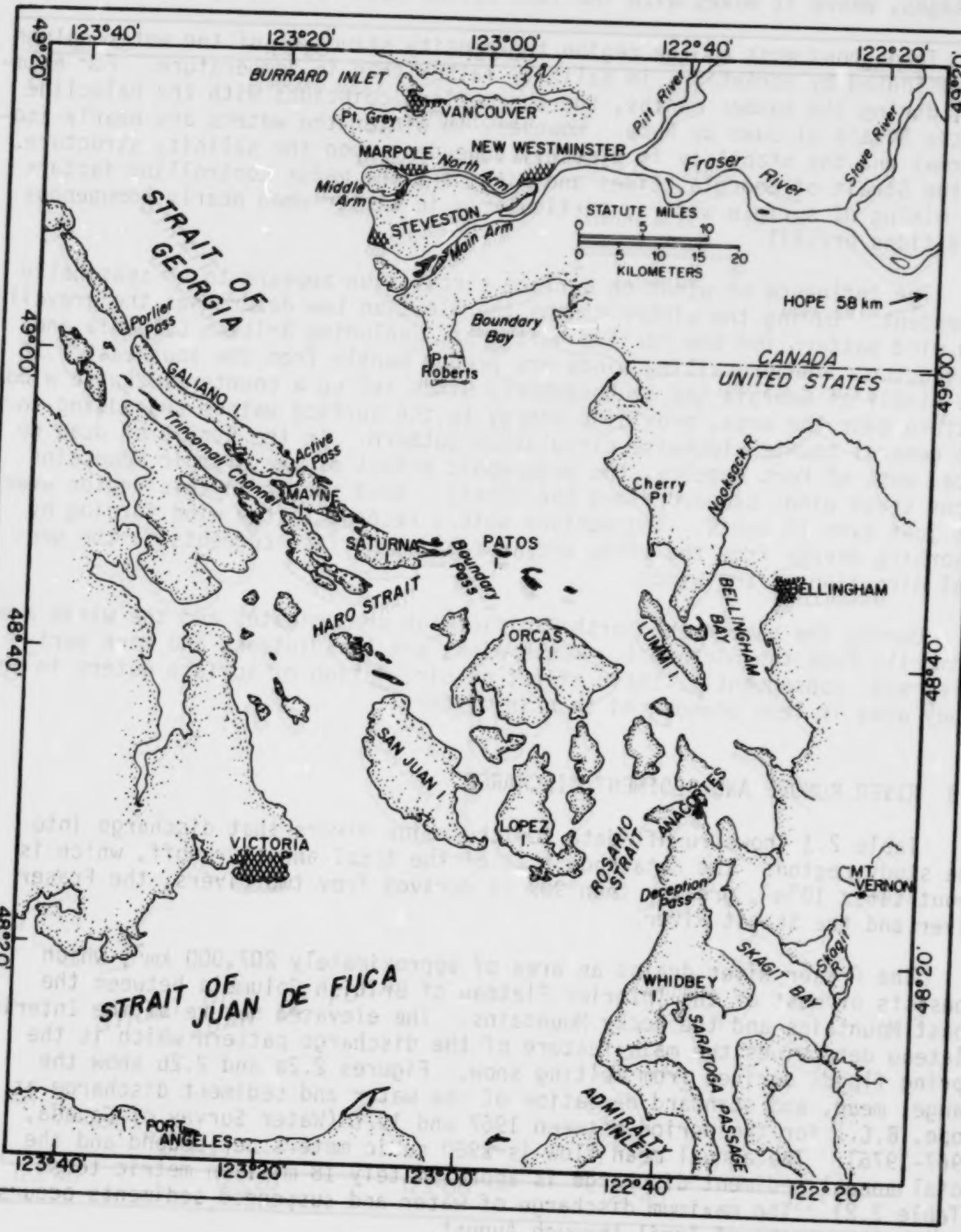
49°20'
123°40'
123°20'
123°00'
122°40'
122°20'
49°20'
BURRARD INLET
VANCOUVER
Pt. Grey
Pitt River
Stave River
MARPOLE
NEW WESTMINSTER
North Arm
Fraser River
Middle Arm
STRAIT OF GEORGIA
STEVESTON
Main Arm
STATUTE MILES
0 5 10
0 5 10 15 20
KILOMETERS
HOPE 58 km
Porlier Pass
Boundary Bay
49°00'
Pt. Roberts
CANADA
UNITED STATES
49°00'
GALIANO I.
Trincomali Channel
Active Pass
MAYNE
Cherry Pt
Nooksack R.
SATURNA I.
Boundary Pass
PATOS I.
HARO STRAIT
BELLINGHAM
BELLINGHAM BAY
LUMMI I.
ORCAS I.
48°40'
48°40'
SAN JUAN I.
ANACORTES
ROSARIO STRAIT
LOPEZ I.
VICTORIA
Deception Pass
MT. VERNON
48°20'
SKAGIT BAY
Skagit R.
48°20'
WHIDBEY
STRAIT OF JUAN DE FUCA
SARATOGA PASSAGE
ADMIRALTY INLET
PORT ANGELES
123°40'
123°20'
123°00'
122°40'
122°20'

Figure 2.1 Physical setting of the study region

moves eastward through the strait, then northward through the San Juan passages, where it mixes with the less saline water of the Strait of Georgia.

Throughout most of the region the density structure of the water column is dominated by variations in salinity rather than in temperature. For example, during the summer months, the thermocline coincides with the halocline in the Strait of Juan de Fuca. However, in winter the waters are nearly isothermal and the stability is directly dependent upon the salinity structure. In the Strait of Georgia, tides and winds are the major controlling factors for mixing of surface waters, particularly in winter when nearly homogenous conditions prevail.

The influence of winds on surface circulation appears to be seasonally dependent. During the winter months the Aleutian Low determines the prevailing wind pattern for the Pacific Northwest, including British Columbia and Washington. The prevailing winds are predominantly from the southeast. In the Strait of Georgia the southeasterly winds set up a counterclockwise wind pattern over the area, providing energy to the surface waters and adding to the general counterclockwise circulation pattern. In the Strait of Juan de Fuca, west of Port Angeles, the orographic effect of the Olympic Mountains turns these winds seaward along the Strait. Wind speeds in this region average just over 20 knots. The surface waters respond to the wind forcing by absorbing energy from the winds and increasing surface currents in the general direction of the winds.

During the summer the North Pacific High predominates and the winds are primarily from the northwest. These winds are less intense and more variable; and, consequently, their effect on circulation of surface waters in the study area is less pronounced than in winter.

2.3 RIVER RUNOFF AND SEDIMENT DISCHARGE

Table 2.1 shows runoff data for the major rivers that discharge into the study region. The data show that of the total annual runoff, which is about 116 x $10^9 m^3$, greater than 90% is derived from two rivers, the Fraser River and the Skagit River.

The Fraser River drains an area of approximately 207,000 km^2, which consists of most of the Interior Plateau of British Columbia between the Coast Mountains and the Rocky Mountains. The elevated nature of the Interior Plateau determines the main feature of the discharge pattern which is the spring floods derived from melting snow. Figures 2.2a and 2.2b show the range, mean, and standard deviation of the water and sediment discharge at Hope, B.C., for the period between 1967 and 1976 (Water Survey of Canada, 1967-1976). The annual mean flow is 2960 cubic meters per second and the total annual sediment discharge is approximately 18 million metric tons (Table 2.2). The maximum discharge of water and suspended sediments occurs during the months of April through August.

TABLE 2.1 Average annual runoff from the major rivers discharging into the study region

River	Area of Drainage Basin (km^2)	Average Annual Runoff ($m^3 \times 10^9$)
Fraser*	207,000	93.4
Skagit**	8,040	14.2
Nooksack**	3,270	4.6
Stillaguamish**	1,790	3.6

*Water Survey of Canada, Water Data, Canadian Rivers, Inland Waters Directorate, Ottawa, Canada, 1967-1976.

**Pacific Northwest River Basins Commission. Puget Sound Task Force. Comprehensive Study of Water and Related Land Resources, Puget Sound and Adjacent Waters, State of Washington, Appendix III, Hydrology and Natural Environment, March 1970.

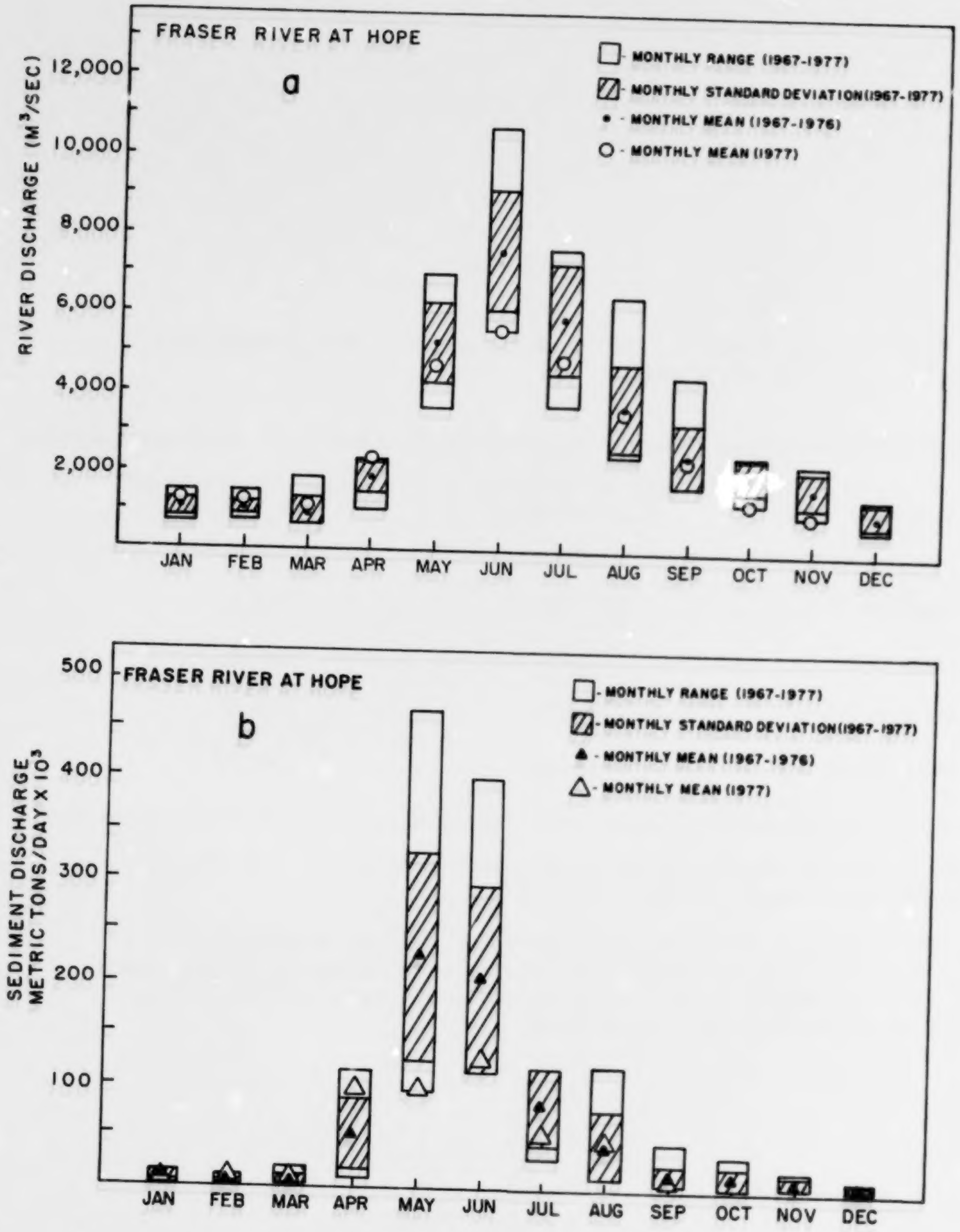

Figure 2.2 Monthly range, mean, and standard deviation of: a. water discharge and b. suspended sediment discharge for the Fraser River at Hope, B.C. for the period from Jan. 1967 through Sept. 1977 (Water Survey of Canada, Sediment Data, Canadian Rivers, Inland Waters Directorate, Ottawa, Canada, 1967-1976).

TABLE 2.2 Comparison of water and sediment discharge for the Fraser and Skagit Rivers during period of record (1967-1976)

Discharge Year	Fraser River**		Skagit River***	
	River Discharge (m^3/sec)	Sediment Discharge (metric tons/day)	River Discharge (m^3/sec)	Sediment Discharge (metric tons/day)
1976	3674	86560	497	2429*
1975	2649	32683	561	2184
1974	3172	63428	596	3075
1973	2492	44043	379	-
1972	3398	79424	625	-
1971	2832	44544	551	-
1970	2166	32846	379	-
1969	2753	36032	414	-
1968	3313	64362	583	-
1967	3172	64139	464	-
Mean	2962	63581	505	2563
Std. Dev.	462	27983	92	460

*January thru October.
**Water Survey of Canada (1967-1976).
***Water Resources Data for Washington, 1976.

At Hope, the Fraser River emerges from the Coast Mountains and flows through an alluvial valley to the Strait of Georgia. Near New Westminister (see Fig. 2.1), the Fraser bifurcates into a major channel or the Main Arm, which accounts for approximately 90% of the flow, and a minor channel, known as North Arm, which branches off at Marpole forming Middle Arm. Main Arm discharges into the Strait of Georgia at Stevenston and North Arm enters the Strait at Point Grey.

The Skagit River and its tributaries drain an area of approximately 8,040 km^2. The major tributaries of the Skagit River are the Baker, Cascade, and Sauk Rivers. The headwaters of the Skagit River and its tributaries are located in the North Cascade Range, where flow is partially derived from melting snow. Near Marblemount, Washington, the Skagit River is joined by the Cascade River, where it flows through broad flood plains and lowland areas until it reaches the coast. At a location about 12 km from the coast, the river splits into three distributaries which flow into Skagit Bay. Figure 2.3 shows water and sediment discharge data for the Skagit River at Mt. Vernon, Washington for 1975.* The data show a bimodal distribution for both water and suspended sediments. The major peaks occur in two periods: October through December and May through July. The October-December peak is associated with excessive rainfall in the lowland areas. The May-July peak corresponds with spring runoff due to melting snow near the headwaters.

---

*While water discharge records for the Skagit River are fairly complete from 1930 to the present, very few records for suspended sediments are available. Therefore, the records for 1975 were used to show the salient features of the Skagit River discharge pattern.

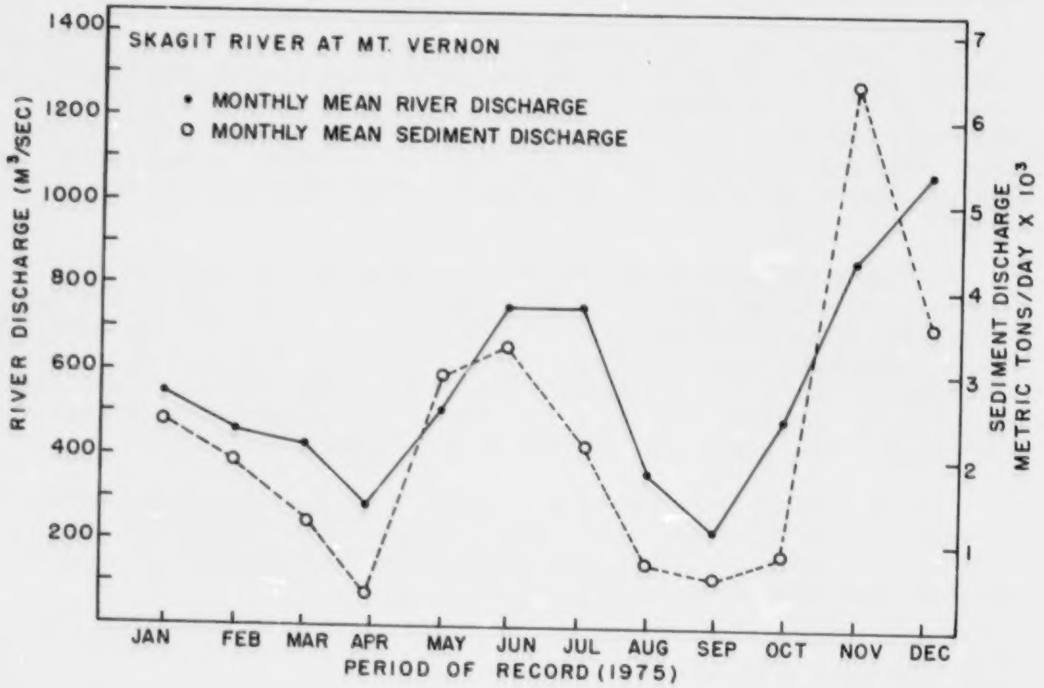

Figure 2.3 Monthly mean discharge of water and suspended sediments of the Skagit River at Mt. Vernon during 1975 (Water Resources Data for Washington, 1976).

3. CONCLUSIONS

3.1 SUSPENDED MATTER DISTRIBUTIONS

Typical values of the concentration of total suspended solids in the waters of the study area between November 1976 and August 1977 were 0.5-2 mg/ℓ. Significant local modification of this concentration level in surface waters occurred north of the San Juan Archipelago, within the influence of the Fraser River plume, where concentrations were as high as 8 mg/ℓ, and immediately seaward of Deception Pass, where concentrations were 2-3 mg/ℓ. Concentration values in the mid-depth and bottom waters showed little influence from riverine sediment sources.

The typical vertical distribution of SPM throughout the area tended towards relatively high values in the surface and bottom waters and relatively lower values in the mid-depth regions. This distribution is presumably due to different agents of particle production in different layers of the water column: high phytoplankton growth and fresh water runoff in the surface waters, and substantial additions of resuspended bottom sediment into the bottom waters.

Temporal variability of the SPM distributions was examined both on a seasonal and diurnal basis. Seasonal variability over most of the region, except for those areas directly influenced by river runoff, was negligible; overall SPM concentrations were 1.8 ± 2.4 mg/ℓ for MESA I, 1.4 ± 0.8 mg/ℓ for MESA II, and 1.2 ± 1.0 mg/ℓ for MESA III. The somewhat higher mean value and standard deviation for MESA I is the result of very high SPM values near the Fraser River and Deception Pass during November 1977.

Diurnal variability was most pronounced at locations where strong tidal currents and/or major sediment sources (Fraser River, Deception Pass) were present. At other locations the vertical SPM distribution was relatively uniform over short time scales.

3.2 SUSPENDED HYDROCARBONS

A systematic survey of suspended hydrocarbons was initiated in the waters of the eastern Strait of Juan de Fuca, San Juan Island Passages, and the southern Strait of Georgia. A total of five locations were selected for detailed study. Hydrocarbons extracted from suspended matter ranged from 0.2 mg/g dry weight to 1.4 mg/g dry weight. The range was largely due to variations in biological hydrocarbons and no correlations were apparent with probable sources of petroleum hydrocarbons (i.e., Fraser River). Both the amounts of hydrocarbons extracted and their compositional character suggest minimal impact with petroleum hydrocarbons, although weathered petroleum residues in a few samples may have been present. One exception was a sample taken near the Fraser River in which heavy motor oil components may have been present. Within the limits of these few data and the small sample weight of material, we conclude that suspended matter in the northern waters of Puget Sound is not obviously contaminated with petroleum hydrocarbons, but incipient levels may be present. More extensive analysis of larger samples, with attention to specific marker compounds, is required.

3.3 OIL-SEDIMENT INTERACTION STUDIES

Laboratory experiments were performed under simulated natural conditions to investigate the short-term interaction between Prudhoe Bay crude oil and two locally-derived riverine sediments. Suspended sediment obtained from the Fraser and Skagit Rivers was mixed with varying quantities of crude oil in sea water at 10°C and 15°C. Cursory attention was given to the influence of dissolved organic carbon in the interaction.

These experiments showed that significant concentrations of crude oil may be accommodated on suspended matter under optimal conditions. The mean particle size of Skagit River sediments was somewhat larger than the material collected from the Fraser River and accommodated up to 100% of its weight in oil at 10°C. An extrapolated value at the same loading (T = 15°C) would have been less than 40%. When smaller particles (Fraser River) were subjected to the same experimental conditions, considerably less oil was sedimented (up to 17%), but much of the clay fraction was retained in a surface slick. If weathering of the oil had been allowed to occur, the surface oil and sediment particles would have reached sufficient density to overcome surface tension and buoyancy and subsequently settled.

Our preliminary conclusions are that when coarse-grained material (i.e., silt) is added to oil, the oil coats the particles and settles rapidly. If the particles are finer (i.e., clay), the oil appears to inhibit normal flocculation of the clay-size material and the sediment is retained in a surface oil layer. Experiments show that significant concentrations of oil may be accommodated in suspended sediments, but the quantity retained in such a fashion will depend on the isoelectric point of the oil and sediment particles, particle size, temperature, and the concentration of oil relative to that of the sediment. Kinetic factors are also important if the oil and sediment are both present in low abundance.

3.4 LANDSAT IMAGERY

A set of LANDSAT images, obtained during the period between 1972 and 1977, have been utilized to study the surface trajectories of sediment plumes originating from the Fraser and Skagit Rivers. These plumes are natural tracers of the flow patterns of river water that are discharged into northern Puget Sound from these rivers.

Three separate plumes can be observed emanating from the mouths of the distributaries of the Fraser River. The plumes from Main Arm and Middle Arm join together to form a well-defined jet which can be traced across the Strait of Georgia and through Porlier, Active, and Boundary Passes. During ebb tide the plume is directed to the southeast from a point about midway between Steveston and Porlier Pass. The flood tide drives the plume across the Strait and to the northwest along the northern coast of Galiano Island.

The plum from North Arm moves to the northwest past Point Grey where it bifurcates, with some material flowing to the northwest during ebb tide and the remaining material moving into Burrard Inlet.

The existence of a number of separate plumes in some of the images suggests that the plumes are probably capable of maintaining their identity for periods longer than a single cycle. This implies that a dynamic balance exists between the inertial and pressure forces associated with the plumes and the coriolis and tidal forces associated with circulation patterns in the Strait.

The plumes from the distributaries of the Skagit River are most pronounced in early summer, during the peak runoff. During this period suspended sediments from the Skagit River can be traced as far south as the middle of Saratoga Passage and as far north as Deception Pass. During ebb tide, suspended solids from the Skagit River flow into Rosario Strait. During the period of low discharge, the Skagit River plume is confined to the nearshore regions of Skagit Bay.

4. RECOMMENDATIONS

4.1 SUSPENDED MATTER DISTRIBUTIONS

Results of this investigation describe the typical concentration of total suspended particulate matter to be expected during various seasons within the study area. Areas of high vertical and horizontal gradients in suspended matter also have been delineated. In addition, a few measurements at selected stations have indicated the magnitude of diurnal variability to be expected in the suspended matter distributions.

A logical extension of this work, although not proposed under this study, is to proceed with a detailed investigation of sediment transport processes. Given the likelihood that pollutants such as oil will be associated with the suspended matter, knowledge of the transport paths of the sediment, its residence time, and final depositional sites would be of immense value in assessing possible impacts. Such a study should include optical measuring devices (nephelometers or transmissometers) together with continuous recording current meters. Emphasis should be placed on the near-surface and near-bottom waters.

Our studies have shown that particle composition and size are critical parameters in assessing the adsorptive characteristics of suspended matter. Future studies should emphasize the sources of these sediments, including biological, fluvial, and resuspended bottom material. Detailed mineralogies of the detrital terrigenous fraction and particle size would be most useful in assessing its adsorptive behavior toward crude oil.

4.2 CHARACTERIZATION OF SUSPENDED HYDROCARBONS

The preliminary studies conducted in the eastern Strait of Juan de Fuca, San Juan Island passages, and the southern Strait of Georgia have suggested the presence of petroleum hydrocarbons, although the source of these hydrocarbons was not unequivocal. Small amounts of suspended matter (< 1 g to 5 g dry weight) severely hampered detailed analysis of the hydrocarbon fractions, in particular the aromatic compounds which are ubiquitous in petroleum and refined products. New procedures should be implemented in future work by which larger amounts of suspended matter (10-20 g) may be recovered for detailed HC analysis.

These studies also pointed to the inadequacies of the present analytical procedures used to distinguish petroleum-related hydrocarbons from the ever-present biological components. More intensive laboratory efforts are required to identify petroleum marker compounds that are persistent and can be readily assayed. Because petroleum may impact organisms via several pathways, suitable identification procedures should be developed for biota, suspended sediments, bottom sediments, and water.

4.3 OIL-SEDIMENT INTERACTION STUDIES

The studies performed in the work were preliminary in scope and served to identify major factors relating to the accommodation of oil by locally-derived riverine sediments. These investigations have shown the importance of surface chemistry in the adsorption process as well as the effect of particle size, mineralogy, associated organics, and temperature. All of these factors, to a greater or lesser degree, play an important role in governing the surface interaction between suspended oil and particles. Without a better understanding of the physical-chemical nature of interface reactions involving natural particles and oil, predictive behavior of the system will be left to a never-ending series of empirical experiments.

We recommend that specific studies be implemented by which the mineralogy and surface coating of particles are examined in terms of their interactions with oil droplets. Emphasis should be placed on the importance of surfactants, either in the oil or in the associated organic matter, and their importance toward interfacial reactions. The formation of colloidal electrolytes needs to be examined as a possible mechanism for oil accommodation as well as other interaction involving complex organics that may be present in oil or in suspended matter. Effects of salt (ionic medium) and temperature are easily incorporated once the fundamental mechanimsm describing the adsorption process is understood.

4.4 LANDSAT STUDIES

Results of the present study indicate that the LANDSAT images are extremely useful for studying surface trajectories of sediment plumes originating from the Fraser and Skagit Rivers. These data allow for synoptic observations of variations in plume trajectories which can be related to differences in tidal stages. In future studies of this kind, LANDSAT observations should be correlated with corresponding sea-truth data. If the resulting correlations are consistent in space and time, the data may be used to develop suspended matter distribution maps based upon the LANDSAT data. The reconstructed distribution maps may then be compared with historical records of river discharge to provide a realistic picture of the relationship between annual and seasonal variations of river discharge and suspended matter distributions.

5. SUSPENDED MATTER DISTRIBUTIONS

5.1 STATION LOCATIONS AND SAMPLING RATIONALE

The study area of this project included the eastern portion of the Strait of Juan de Fuca, the San Juan passages, and the southern Strait of Georgia. Thirty-five station locations (Fig. 5.1) were designated for seasonal sampling coverage on three cruises: MESA I (Nov. 16-24, 1976), MESA II (March 10-16, 1977), and MESA III (Aug. 7-14, 1977). These times were chosen on the basis of the local climate and runoff pattern. The dominant runoff source in this area is the Fraser River, whose flow peaks sharply between early May and late July (Fig. 2.2). The November and March cruises thus sampled the area during the relatively low runoff autumn and spring periods, while the August cruise occurred immediately after the midsummer runoff peak.

The station locations were chosen to form transects across the major passages of the survey region where horizontal and vertical gradients of the distribution of suspended particulate matter (SPM) were expected to be the greatest. Admiralty Inlet, the principal passage into Puget Sound, was covered by stations 1-3. Two transects across the Strait of Juan de Fuca, stations 4-7 and 8-10, covered the area between the inland waters and the entrance to the Pacific Ocean. SPM distributions around the San Juan Archipelago were measured across two east-west transects north (stations 17-21) and south (stations 11-15) of the islands. Stations were also occupied within Haro and Rosario Straits. Three transects, stations 21-30, monitored the Fraser River plume.

Since a synoptic survey of such a large region is impossible, the possible effects of tides on the temporal variability of SPM were investigated in a series of 24-hr time series stations (Fig. 5.1). SPM measurements were repeated approximately every two hours at these stations. The locations of these stations were chosen to represent a wide range of tidal current velocities, to represent a variety of SPM sources (oceanic, riverine, etc.), to provide wide spatial coverage, and to be compatible with the suspended matter-hydrocarbon sampling program (Section 6).

Coverage of this sampling grid was never complete during any of the cruises. Poor weather conditions occasionally aborted stations or shortened time series measurements on each cruise, particularly in the Strait of Juan de Fuca. International clearance problems forced cancellation of all stations in the Canadian portion of the Strait of Georgia during MESA II. Technical problems with the CTD and nephelometer systems caused some intermittent loss of data. Nevertheless, the data base is extensive and so the gaps are not generally serious. Because of the large amount of data, detailed discussions in this report will be limited to the transects formed by the following stations: 4-7 (Transect A), 11-15 (Transect B), 17-21 (Transect C), and 24-27 (Transect D). These transects are representative of the entire area and include (or are adjacent to) the four principal time-series stations (9, 15, 17, and 26).

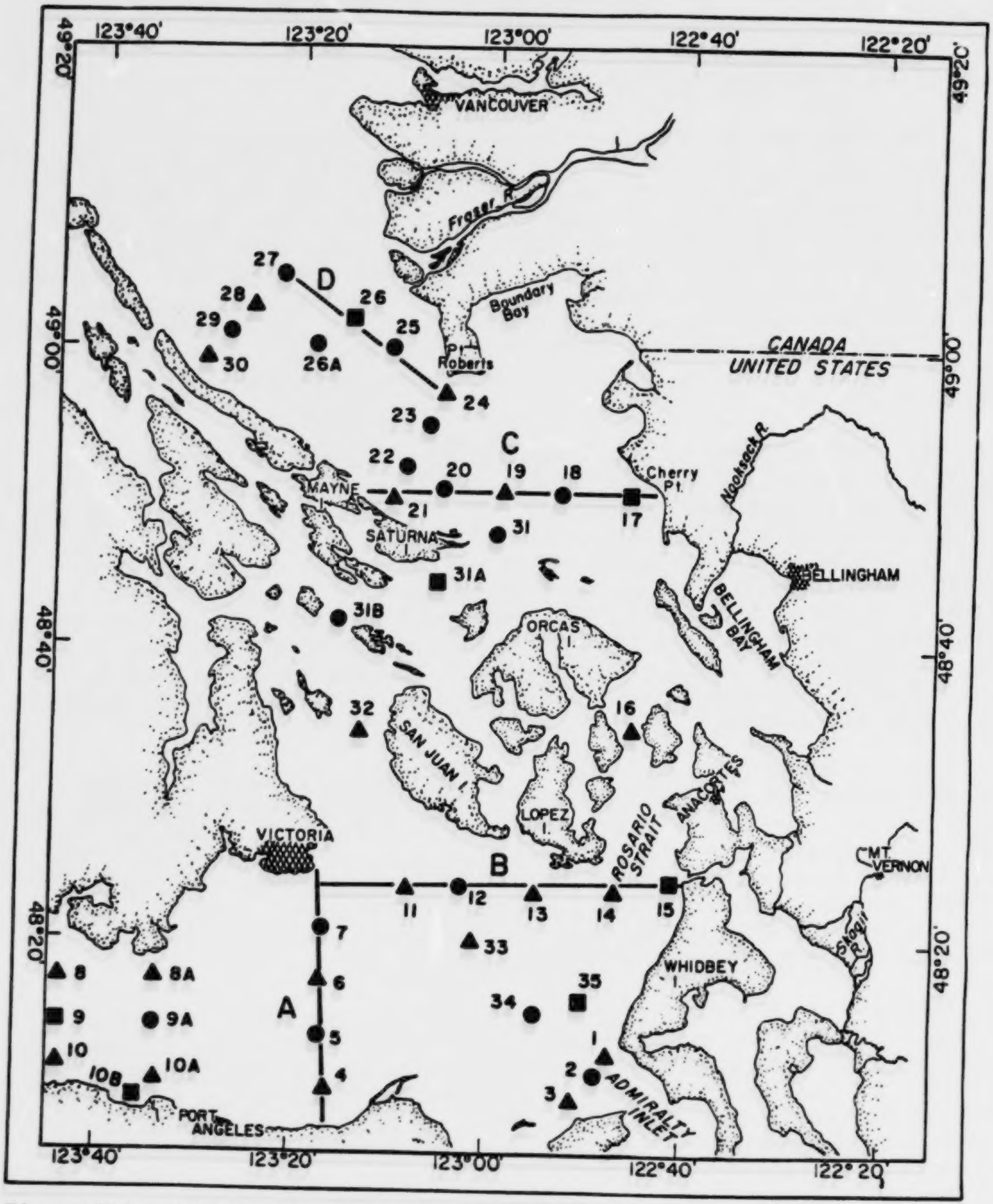

49°20'
123°40'
123°20'
123°00'
122°40'
122°20'
49°20'
VANCOUVER
Fraser R.
Boundary Bay
Pt. Roberts
CANADA
UNITED STATES
49°00'
49°00'
27
D
26
28
29
25
30
26A
24
23
C
22
20
19
18
Cherry Pt.
17
MAYNE
21
SATURNA
31
31A
Nooksack R.
BELLINGHAM
BELLINGHAM BAY
31B
ORCAS I.
48°40'
48°40'
32
16
SAN JUAN I.
LOPEZ I.
ROSARIO STRAIT
ANACORTES
VICTORIA
B
11
12
13
14
15
MT. VERNON
7
33
48°20'
48°20'
8
8A
6
WHIDBEY I.
Skagit R.
9
9A
A
35
34
5
10
10A
1
10B
4
2
3
ADMIRALTY INLET
PORT ANGELES
123°40'
123°20'
123°00'
122°40'
122°20'

Figure 5.1. Station locations for MESA I, II, and III. Light scattering measurements were made at all stations. Circles indicate stations where water samples also were collected. Squares indicate where time-series measurements were made and where large volume suspended particulate matter samples were collected by centrifuge.

5.2 OBSERVATIONAL PROCEDURES

The distribution of SPM within the study area was determined by continuous vertical profiles of light scattering intensity (nephelometer profiles) at each station. The nephelometer (Sternberg et al., 1974) consists of a flashing xenon light source, a scattered light detection system, a data transmission system, and Ni-Cd batteries mounted in a self-contained, easily portable, deep sea housing. During MESA I and MESA III, the nephelometer was interfaced with a Plessey 9400 CTD and a real-time surface-to-bottom profile of light scattering intensity was produced. Technical problems on MESA II required the use of the nephelometer's internal strip chart recorder.

Discrete water samples were collected at six (or less) depths at approximately half the stations (Fig. 5.1) by means of 6-liter PVC sampling bottles. Aliquots from each sample were vacuum filtered through a 47 mm diameter, 0.4 μm pore size Nuclepore polycarbonate filter. Filters were rinsed with three 10 mℓ aliquots of distilled, deionized, membrane filtered water, placed in individual plastic petri dishes, desiccated, sealed, and returned to the laboratory. The absolute concentrations of SPM obtained from gravimetric analysis of these samples were compared to the nephelometer measurements in an attempt to calibrate the relative nephelometer values in terms of SPM concentration. Unfortunately, the correlation between nephelometer values and absolute SPM concentration at the same station was poor (Fig. 5.2). Because no rosette sampling system was available, nephelometer/CTD casts and bottle casts were performed on successive lowerings rather than simultaneously. Consequently, the actual depth of each water sample could only be estimated from the meter wheel and wire angle. In a dynamic and patchy estuarine environment, with steep horizontal and vertical SPM gradients, it proved impossible to sample the same water parcel with both nephelometer and sampling bottle with the available sampling procedures. Even if the sampling procedure was ideal, optical measures of SPM concentrations would be difficult due to the particle inhomogeneities in the study area (i.e., high phytoplankton concentrations in the surface waters, largely inorganic particles at depth). Although scattering intensity depends to a large degree on the concentration of material in the water, it is also affected by changes in the particle size distribution, the index of refraction, and the particle morphology.

As an example of the utility of nephelometer profiles in a program of this type, Figure 5.3 illustrates the accuracy of calibration which may be achieved if water samples can be collected simultaneously with the light scattering readings. Thus, although absolute determination of the SPM concentration from the nephelometer data in the present study is difficult, the nephelometer profiles are nevertheless very useful and informative. Rather than yielding instantaneous values of the SPM concentrations of a particular water parcel, they reveal the gradients and overall magnitude of SPM throughout the entire water column. As discussed below, the transects of nephelometer values are internally consistent and the gradients often parallel gradients in the temperature distribution. Typical values for the absolute concentration of SPM are given by the water samples, and the details of the gradients are furnished by the nephelometer profiles.

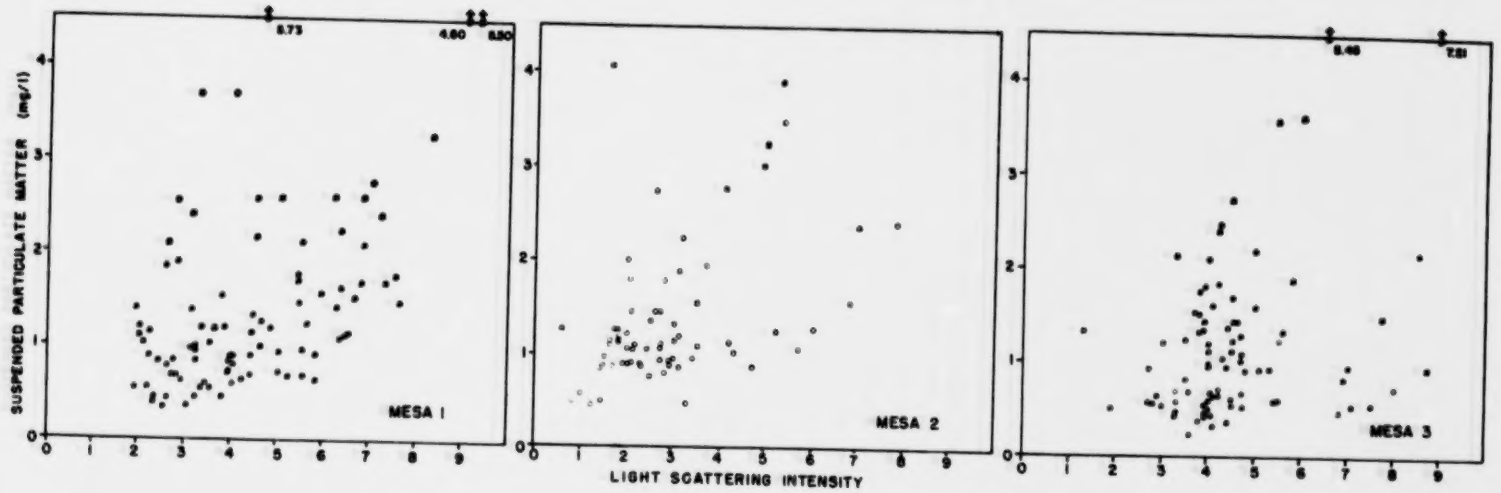

Figure 5.2. Scatter plot of nephelometer data versus particulate concentration in the study area. Reasons for the poor correlation are discussed in the text. Compare these plots with Figure 5.3.

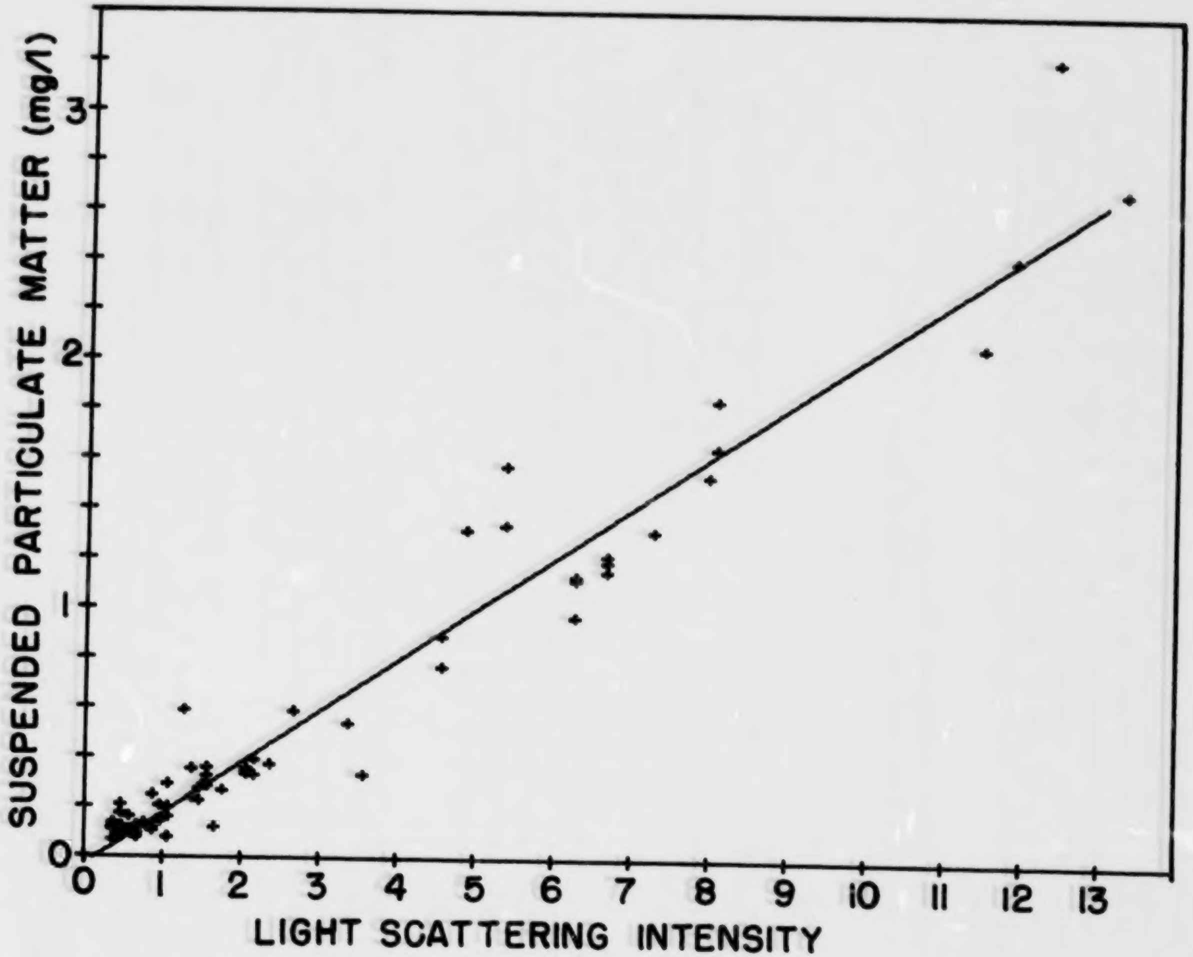

Figure 5.3. Scatter plot of nephelometer data versus particulate concentration for some Gulf of Mexico samples collected simultaneously with the light scattering measurements. This calibration curve is an example and cannot be directly used to interpret the present data.

Water samples were also used to obtain samples for x-ray diffraction mineralogy. The stations and depths of samples examined for mineralogy are given in Table 5.1. In order to obtain enough material, samples often had to be combined. In the laboratory, selected filters were treated with 15% H_2O_2 to remove the oxidizable organic matter, and the remaining inorganic sediment load was removed from the Nuclepore filter ultrasonically. Oriented mounts for x-ray diffraction analysis were prepared by filtering the resuspended particles through silver membrane filters (0.45 μm mean pore size). Since the SPM collected on the filters included silt-size particles as well as clay-size, quantitative estimates of mineral abundances could not be determined. Instead, relative ratios of chlorite:illite, quartz:illite, and feldspar:illite were computed as indicators of these minerals' distribution patterns. Montmorillonite was present only in trace amounts and kaolinite was not detected.

A few samples were collected for particle size analysis in conjunction with the in-situ pump sampling for suspended hydrocarbons.

5.3 RESULTS AND DISCUSSION

5.3.1 Suspended Particulate Matter Concentrations - Areal Distributions

5.3.1.1 Seasonal surface values. SPM concentrations as measured by bottle sampling were relatively uniform throughout the year in the eastern Strait of Juan de Fuca and the San Juan passages, varying between 0.5 and 2 mg/ℓ (Figs. 5.4a, 5.5a, 5.6a). The influence of the Fraser River plume is obvious in the Strait of Georgia, with concentrations as great as 8 mg/ℓ near the river mouth in November and August. Although areal sampling was restricted in March, samples taken as far north as the Canadian border yielded concentrations of < 1 mg/ℓ (compared with > 3 mg/ℓ in November and August). These low concentrations correspond to the very low spring runoff typical of the Fraser River (Fig. 2.2).

5.3.1.2 Seasonal near-bottom values. Figures 5.4b, 5.5b, and 5.6b show the distribution of SPM values 5 m above the seabed. These values tend to possess somewhat more variability than the surface values because their actual depth below the sea surface varies widely and resuspension of bottom sediments may be an important process in controlling the observed concentration values.

The absolute value of near-bottom SPM concentrations throughout the entire region is between 0.5 and 3 mg/ℓ - almost identical to the surface values. Furthermore, there is no Fraser River influence detectable in the bottom waters of the Strait of Georgia at any time of year.

5.3.2 Suspended Particulate Matter Distribution - Seasonal Nephelometer Transects

The locations of the four representative nephelometer transects to be discussed in detail in this report are shown in Figure 5.1. The sea bottom profile for a particular cross-section sometimes changes slightly from cruise to cruise due to small errors in reoccupying a particular station.

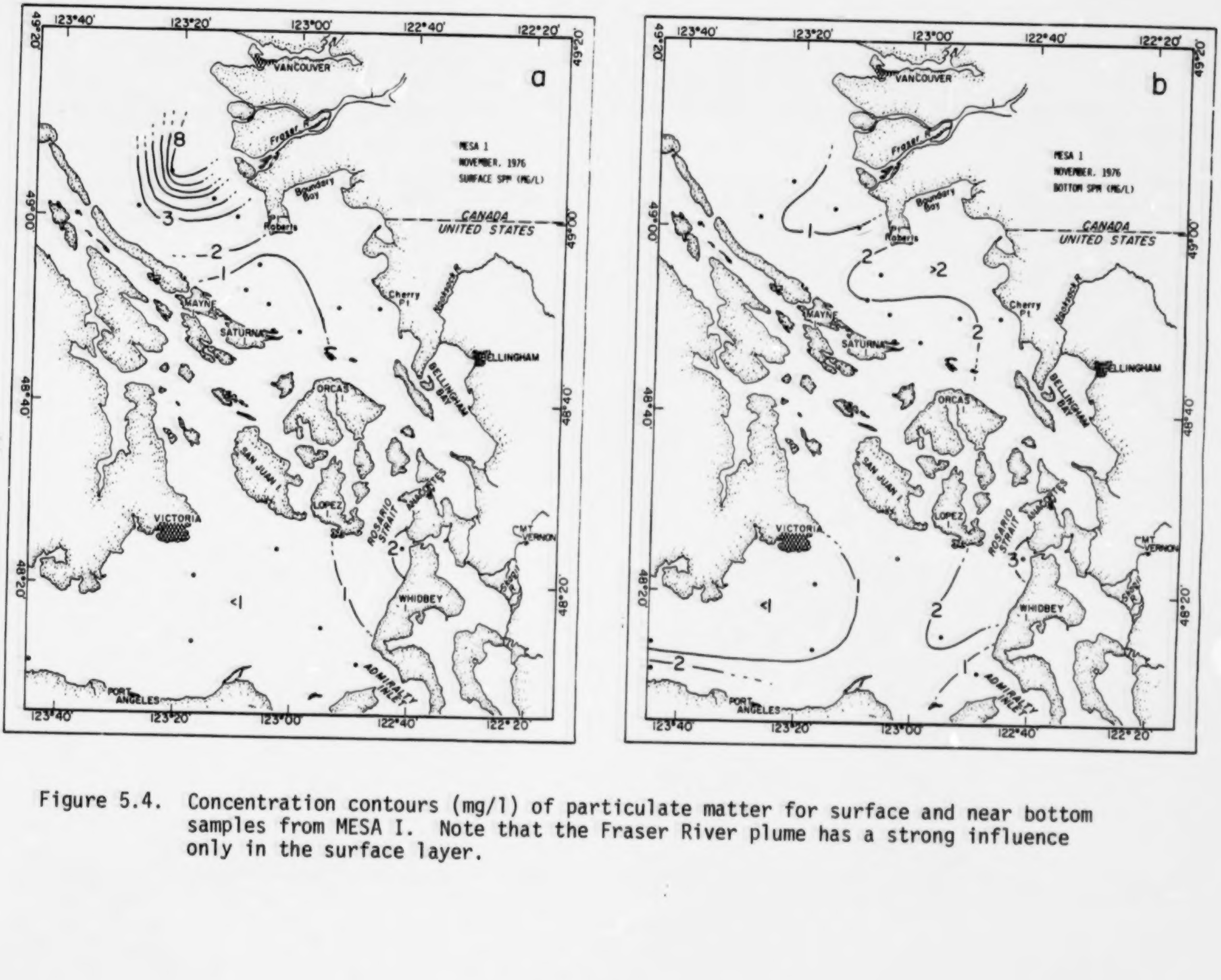
a
MESA 1
NOVEMBER, 1976
SURFACE SPM (MG/L)
b
MESA 1
NOVEMBER, 1976
BOTTOM SPM (MG/L)
CANADA
UNITED STATES
VANCOUVER
Fraser R.
Boundary Bay
Pt. Roberts
Cherry Pt.
Nooksack R.
BELLINGHAM
BELLINGHAM BAY
MAYNE
SATURNA
ORCAS I.
SAN JUAN I.
LOPEZ I.
ROSARIO STRAIT
VICTORIA
WHIDBEY
MT. VERNON
ADMIRALTY INLET
PORT ANGELES
8
3
2
1
<1
>2
123°40'
123°20'
123°00'
122°40'
122°20'
49°20'
49°00'
48°40'
48°20'

Figure 5.4. Concentration contours (mg/l) of particulate matter for surface and near bottom samples from MESA I. Note that the Fraser River plume has a strong influence only in the surface layer.

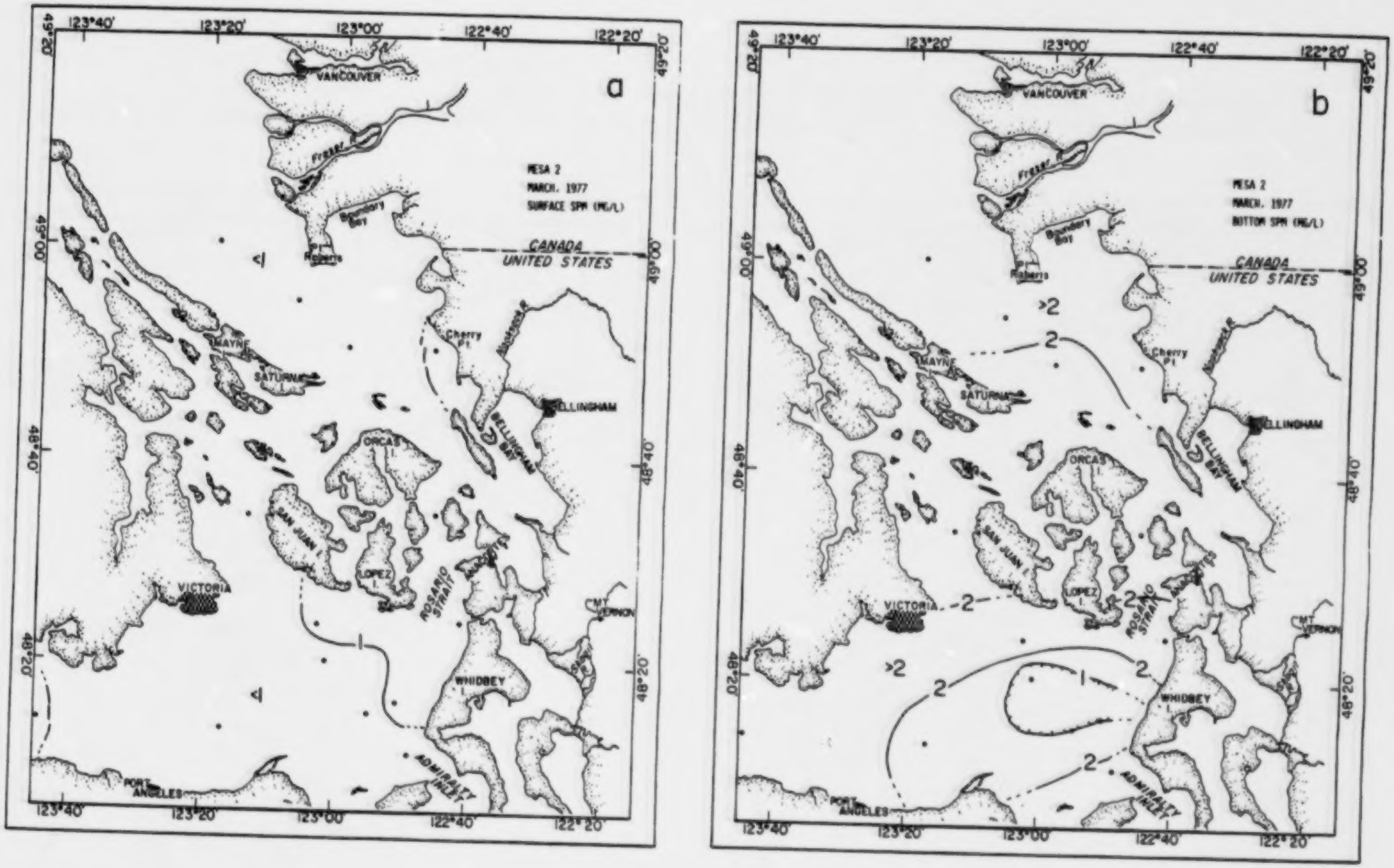
a
MESA 2
MARCH, 1977
SURFACE SPM (MG/L)
b
MESA 2
MARCH, 1977
BOTTOM SPM (MG/L)
CANADA
UNITED STATES
VANCOUVER
Fraser
Boundary Bay
Pt. Roberts
Cherry Pt.
Nooksack R.
BELLINGHAM
BELLINGHAM BAY
MAYNE
SATURNA
ORCAS
SAN JUAN I.
LOPEZ I.
ROSARIO STRAIT
VICTORIA
MT. VERNON
WHIDBEY I.
ADMIRALTY INLET
PORT ANGELES
<1
1
>2
2
1
123°40'
123°20'
123°00'
122°40'
122°20'
49°20'
49°00'
48°40'
48°20'

Figure 5.5. Concentration contours (mg/l) of particulate matter for surface and near bottom samples from MESA II. Note the low spring-time values near both the Fraser River and Deception Pass (at the north end of Whidbey Island).

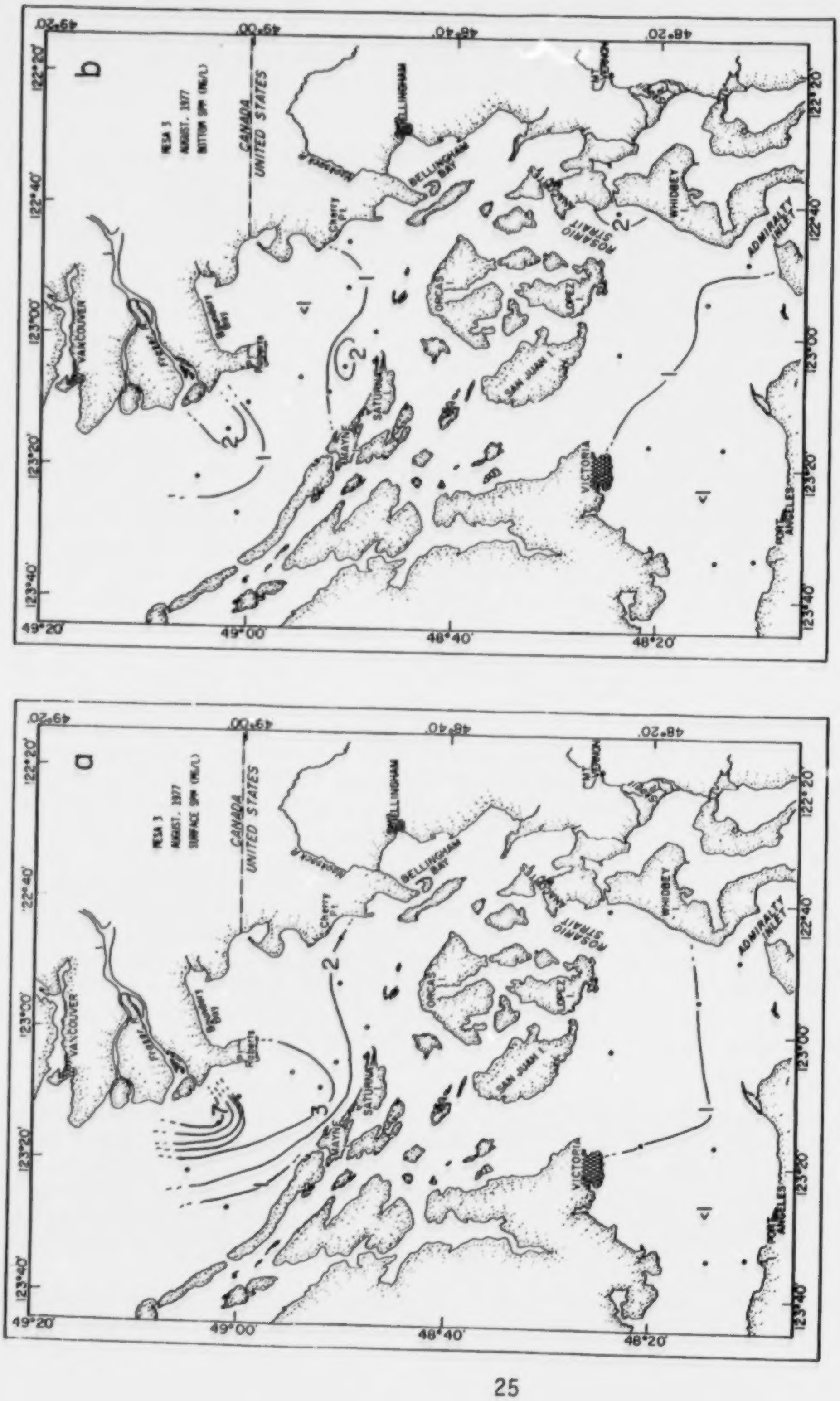

a
MESA 3
AUGUST, 1977
SURFACE SPM (MG/L)
b
MESA 3
AUGUST, 1977
BOTTOM SPM (MG/L)
CANADA
UNITED STATES
VANCOUVER
FRASER
BOUNDARY BAY
BELLINGHAM
BELLINGHAM BAY
CHERRY PT.
ROSARIO STRAIT
ORCAS
LOPEZ
SAN JUAN I.
SATURNA
MAYNE
VICTORIA
PORT ANGELES
WHIDBEY
ADMIRALTY INLET
MT. VERNON
2
3
1
<1
49°20'
49°00'
48°40'
48°20'
123°40'
123°20'
123°00'
122°40'
122°20'

Figure 5.6 Concentration contours (mg/l) of particulate matter for surface and near bottom samples from MESA III. Note the prominence of the Fraser River plume due to the summer runoff.

Cross-sections of the temperature distribution are also presented for these transects in order to compare the SPM distributions with the hydrography. Because of difficulties with the magnetic tape recorder on the CTD system, density and salinity values were not available for all three cruises.

5.3.2.1 Transect A (sta. 4-7). Scattering contours in these cross-sections (Fig. 5.7) show very weak horizontal gradients except for an apparent discontinuity below 40 m at the south end of the transect during the August cruise. Scattering contours during March showed lower scattering and weaker gradients than either November or August. In general, inferred SPM concentrations in the deep water on the south side of the Strait of Juan de Fuca (sta. 5) were less than in the shallower water on the north side. This generalization agrees with the observation of Herlinveaux and Tully (1961) that inward transport of (presumably less turbid) oceanic water dominates on the south side, while seaward transport of Puget Sound and Strait of Georgia water dominates on the north side.

The temperature cross-sections (Fig. 5.8) possess far more variability than the nephelometer profiles. There was a distinct front across the middle of the Strait in November, with warmer water on the southern side of the Strait. In March, when the scattering gradients were lowest, the water column was nearly isothermal. The strongest vertical gradients were, of course, found in August. The vertical scattering gradients were also strongest at this time.

5.3.2.2 Transect B (sta. 11-15). This cross-section south of the San Juan Archipelago reveals the influence of the Deception Pass SPM source during all three seasons (Fig. 5.9), although the extent of its influence was markedly reduced during the March cruise (see also Figs. 5.5, 8.2, and 8.3). The typical mid-depth scattering minimum was less well developed south of Rosario Strait than south of Haro Strait, apparently because of the Deception Pass SPM supply.

The temperature cross-sections (Fig. 5.10) agree particularly well with the nephelometer profiles. During November, slightly warmer Deception Pass water occupied the upper 40 m of the eastern half of the cross-section, corresponding to the location of high scattering levels. Gradients were much weaker in March, but a temperature front still separated the eastern and western halves of the cross-section. Horizontal gradients in temperature and light scattering were superseded by the vertical structure in August.

5.3.2.3 Transect C (sta. 17-21). SPM distributions along Transect C (Fig. 5.11) north of the San Juan Archipelago were rather stable except for the shallow water off Cherry Point. During November and August there was a well-developed, although thin, mid-depth minimum off Cherry Point which may or may not have been continuous with the broader minimum found further offshore. Below this minimum, scattering values increased steadily with depth.

During November, the scattering structure off Cherry Point was probably closely related to the salinity structure, since a prominent halocline was

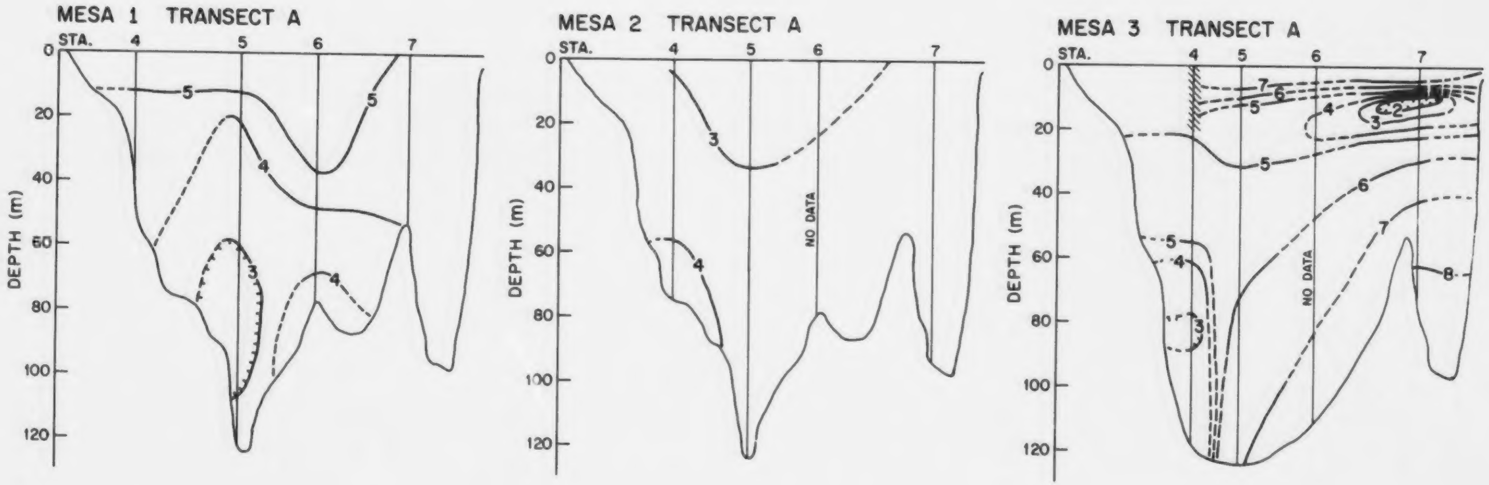

Figure 5.7. Light scattering values, Transect A. Cross-hatching at a station location indicates the depth of daylight interference with the nephelometer. Vertical exaggeration = 250x.

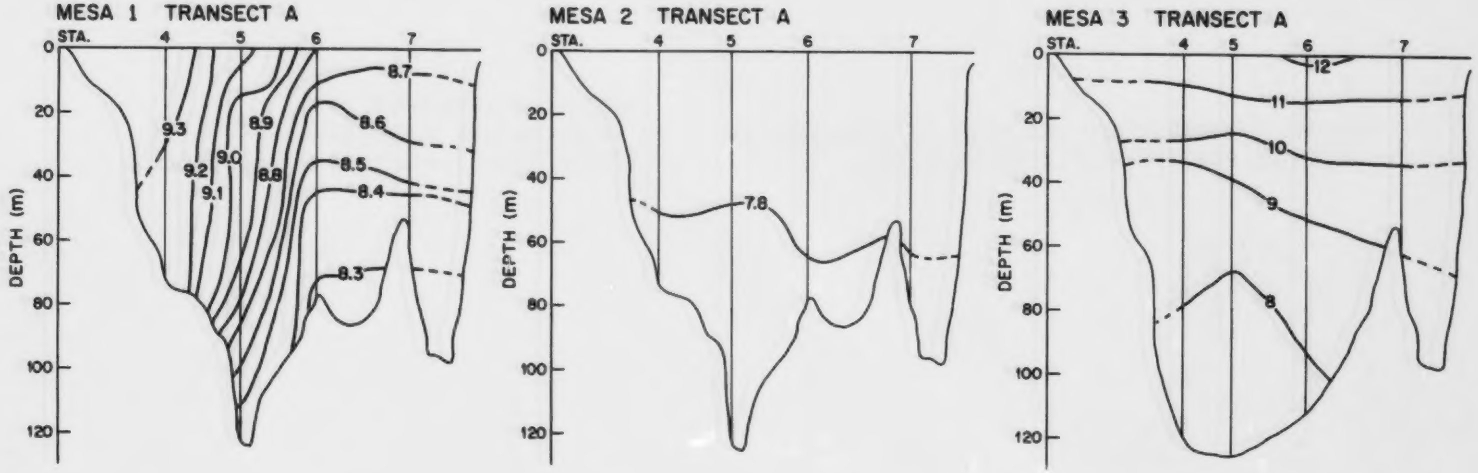

Figure 5.8. Temperature values (°C), Transect A. Contour interval is 0.1°C for MESA I and II, 1°C for MESA III. Vertical exaggeration = 250x. Note the nearly isothermal structure during MESA II.

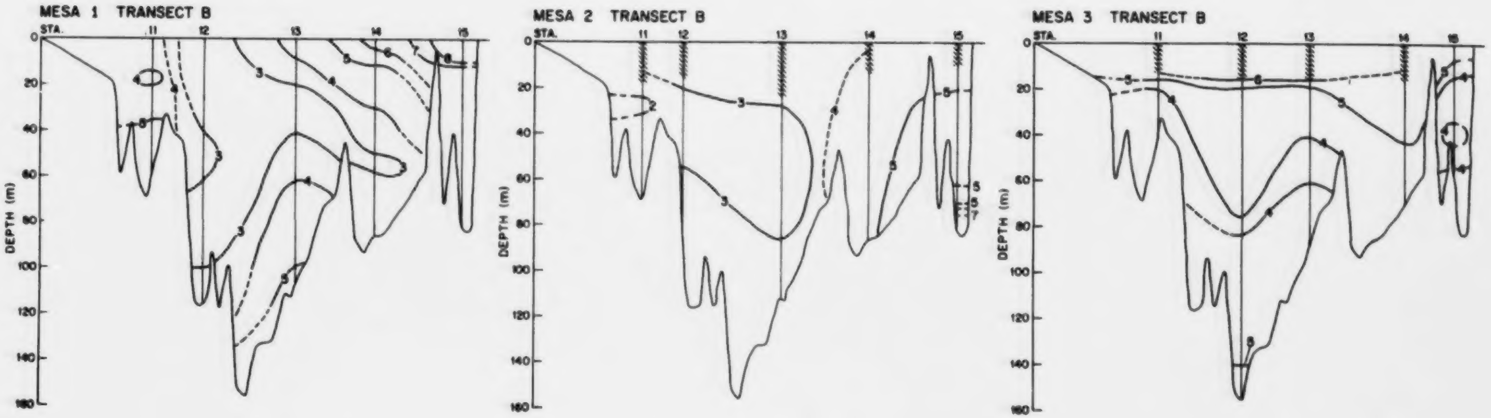

Figure 5.9. Light scattering values, Transect B. Cross-hatching at a station location indicates the depth of daylight interference with the nephelometer. Vertical exaggeration = 250x. This transect is a good example of the mid-depth light scattering minimum found throughout most of the study area.

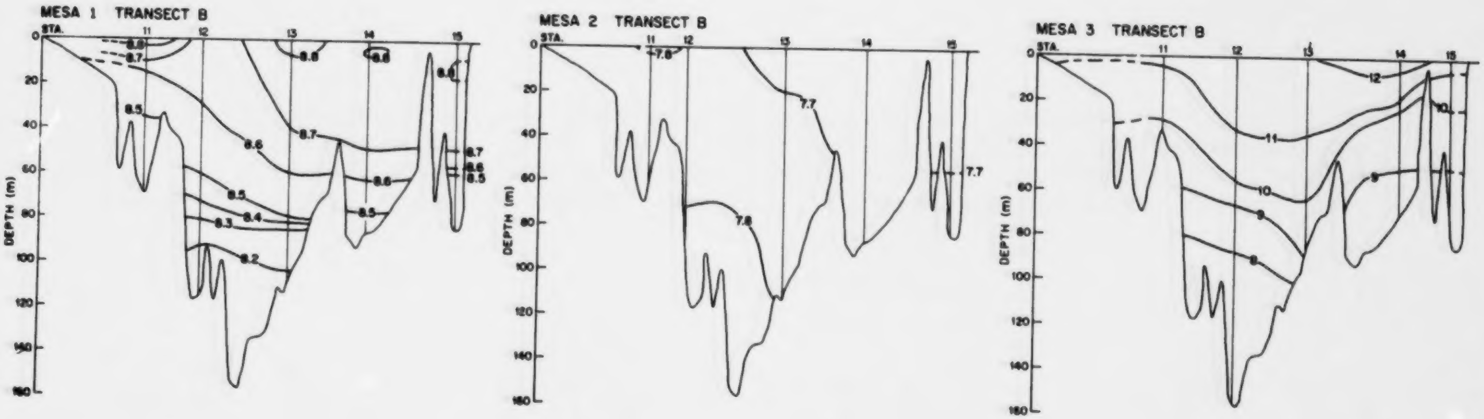

Figure 5.10. Temperature values (°C), Transect B. Contour interval is 0.1°C for MESA I and II, 1°C for MESA III, Vertical exaggeration = 250x.

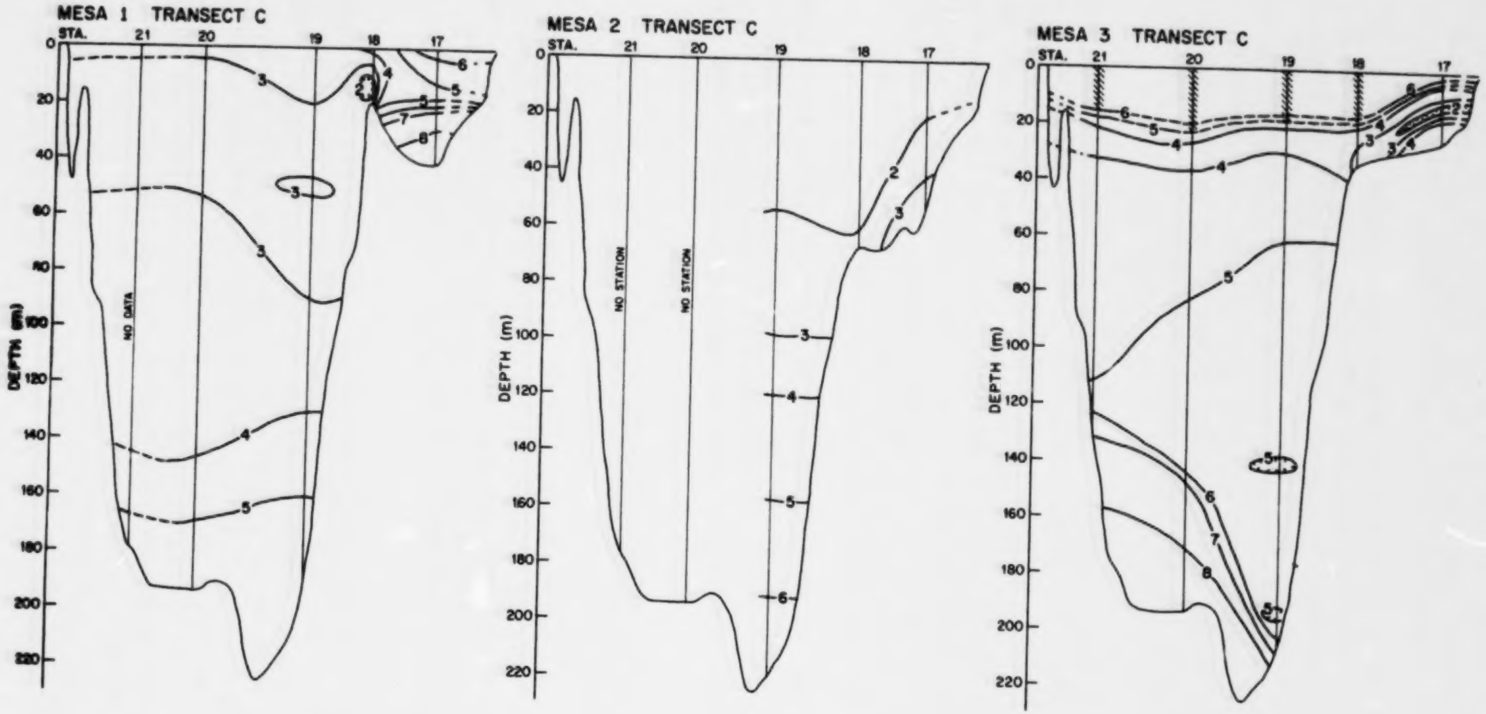

Figure 5.11. Light scattering values, Transect C. Cross-hatching at a station location indicates the depth of daylight interference with the nephelometer. Vertical exaggeration = 250x.

observed at ~20 m and vertical temperature gradients (Fig. 5.12) were almost nonexistent. The prominent discontinuity in the scattering contours at station 18, however, was associated with a strong thermal front.

Although the scattering structure in August was similar to that of November, the hydrography was considerably different. The halocline at station 17 weakened considerably in August, whereas the vertical temperature stratification became strong due to the warm summer runoff water. The hydrography in March was somewhat intermediate of these extremes - vertical salinity and temperature stratification were both present but moderate. The lack of a prominent scattering structure was probably due to the abnormally low runoff and consequently low sediment supply available during the spring of 1977.

5.3.2.4 Transect C (sta. 24-27). These cross-sections off the mouth of the Fraser River illustrate the steep scattering (Fig. 5.13) and temperature (Fig. 5.14) gradients in both vertical and horizontal directions typical of river plumes. Most of the river derived SPM near the river mouth was evidently confined to the upper 5 m during November and August (no data available from March). Below the fresh water river plume at station 27, scattering was relatively uniform or increased slowly with depth. South of the river mouth lensing of turbid layers was quite common in November and August, but largely absent during the low runoff period around March.

Because of the Fraser River influence, the vertical temperature gradients were far more steep than any horizontal ones. The prominent lensing of SPM observed at stations 24 and 25 during November can be correlated with the weakening of the vertical temperature gradient moving southward from the river mouth.

5.3.3 Suspended Particulate Matter Distribution - Time Series Measurements

The 24-hr time series measurements made at selected stations (Fig. 5.1) on each cruise are particularly valuable because they give the instantaneous data from the transects a temporal perspective. The various stations reveal differing degrees of variability which are in general related to their proximity to major suspended sediment sources (i.e., Fraser River, Deception Pass).

5.3.3.1 Strait of Juan de Fuca (sta. 9/10). Generalizations about this locality are difficult, since poor weather aborted this station during November and forced a station change to close inshore during August. The time series at station 9 in March showed a persistent mid-depth minimum centered between 40 and 60 m (Fig. 5.15). Station 10A, in much shallower water, showed simply a steady decrease in scattering with depth and uniform scattering levels for the duration of the observations. This locality was thus relatively free of marked short-term variability during the observation period in March and August.

5.3.3.2 Deception Pass (sta. 15). Station 15 was located in relatively shallow water, near an important source of SPM, and within a strong and

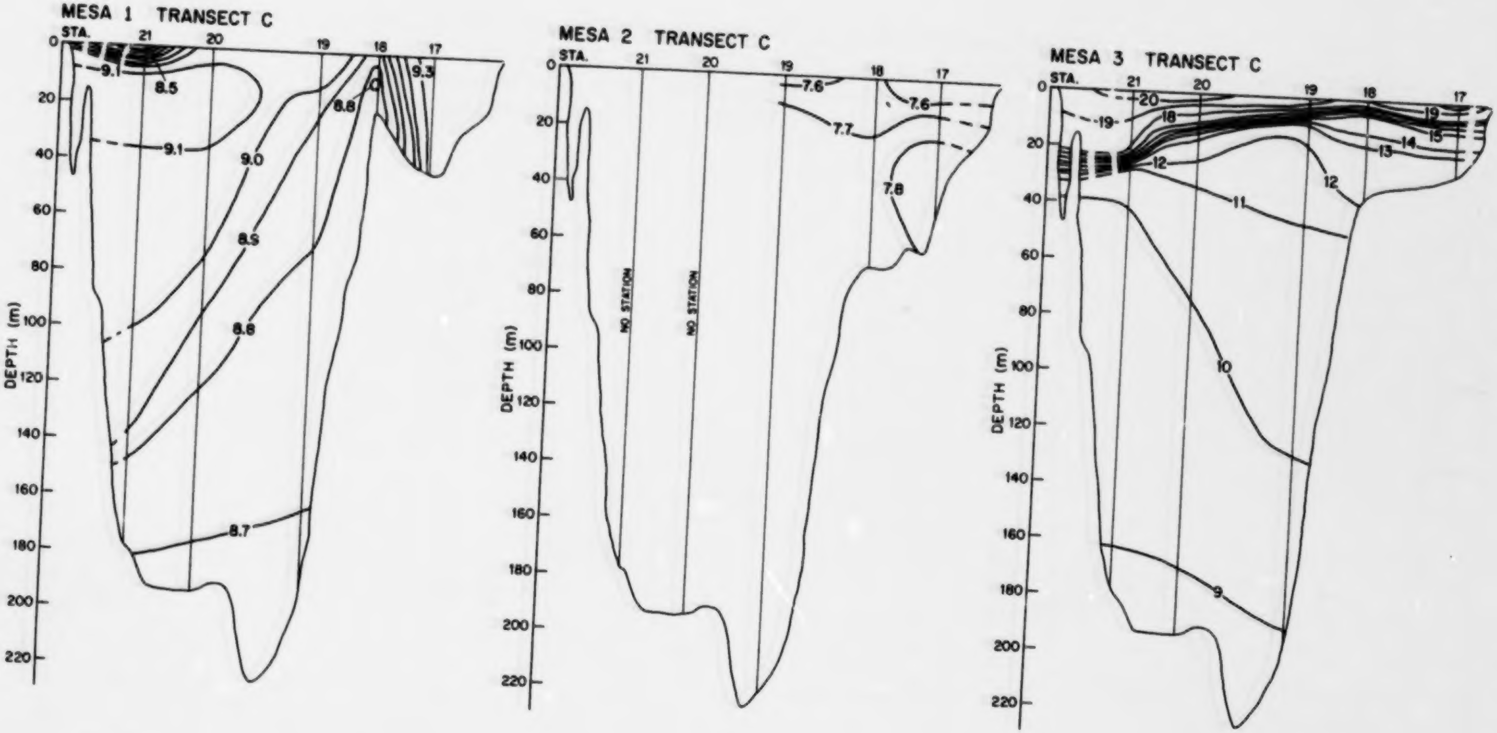

Figure 5.12. Temperature values (°C), Transect C. Contour interval is 0.1°C for MESA I and II, 1°C for MESA III. Vertical exaggeration = 250x.

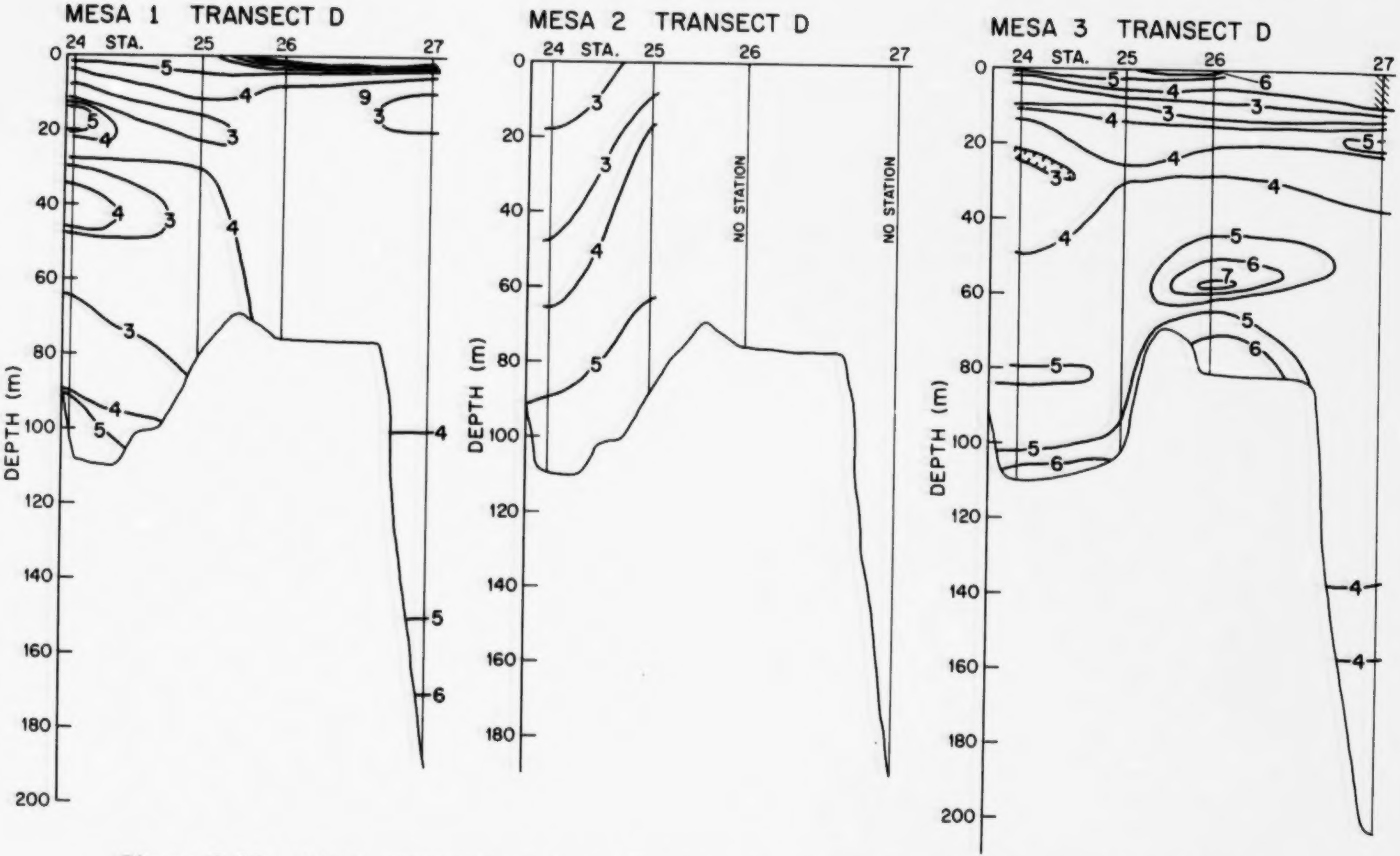

Figure 5.13. Light scattering values, Transect D. Cross-hatching at a station location indicates the depth of daylight interference with the nephelometer. Vertical exaggeration = 250x. Note the high light scattering intensities and complex layering due to suspended sediments from the Fraser River.

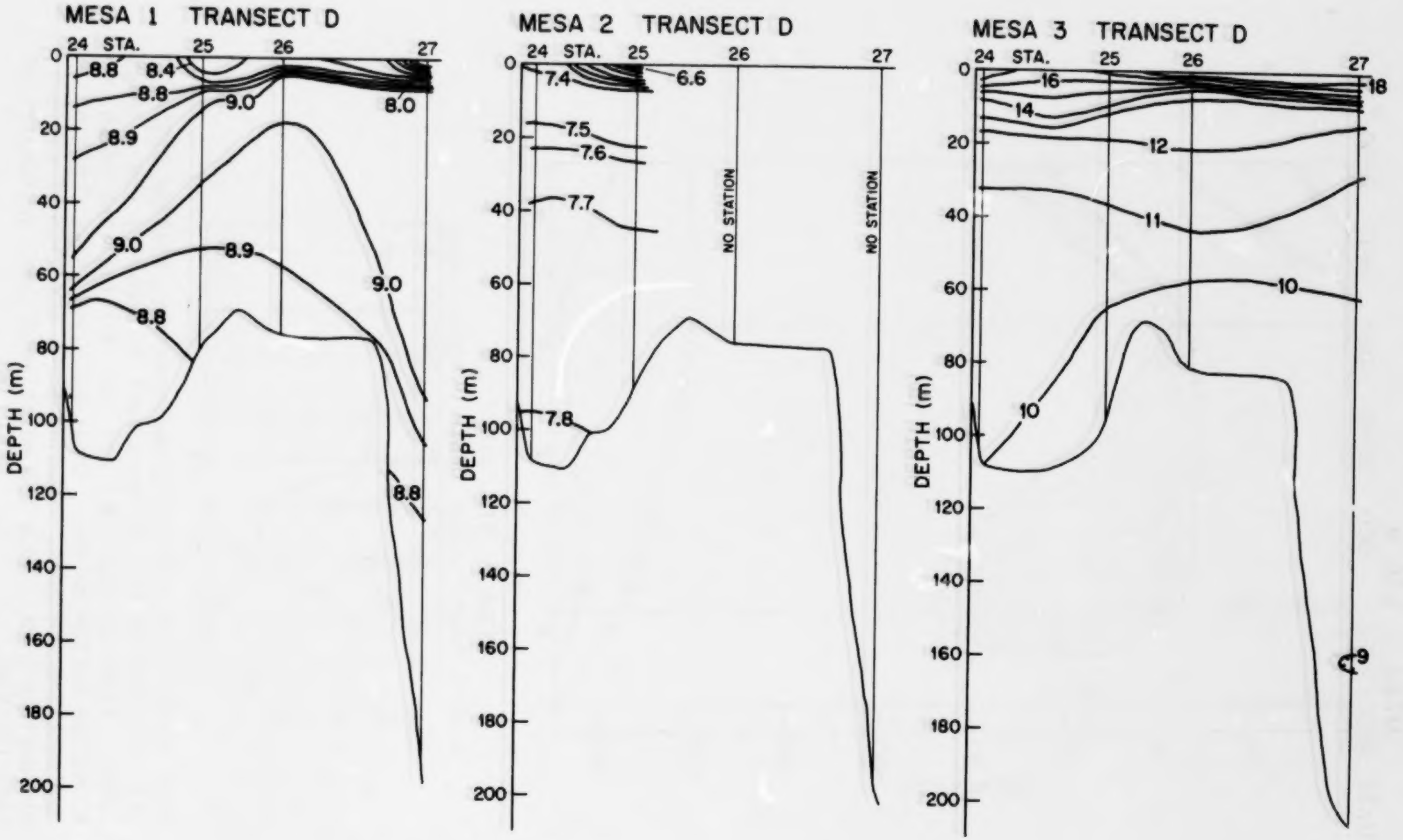

Figure 5.14. Temperature values (°C), Transect C. Contour interval is 0.1°C for MESA I and II, 1°C for MESA III. Vertical exaggeration = 250x.

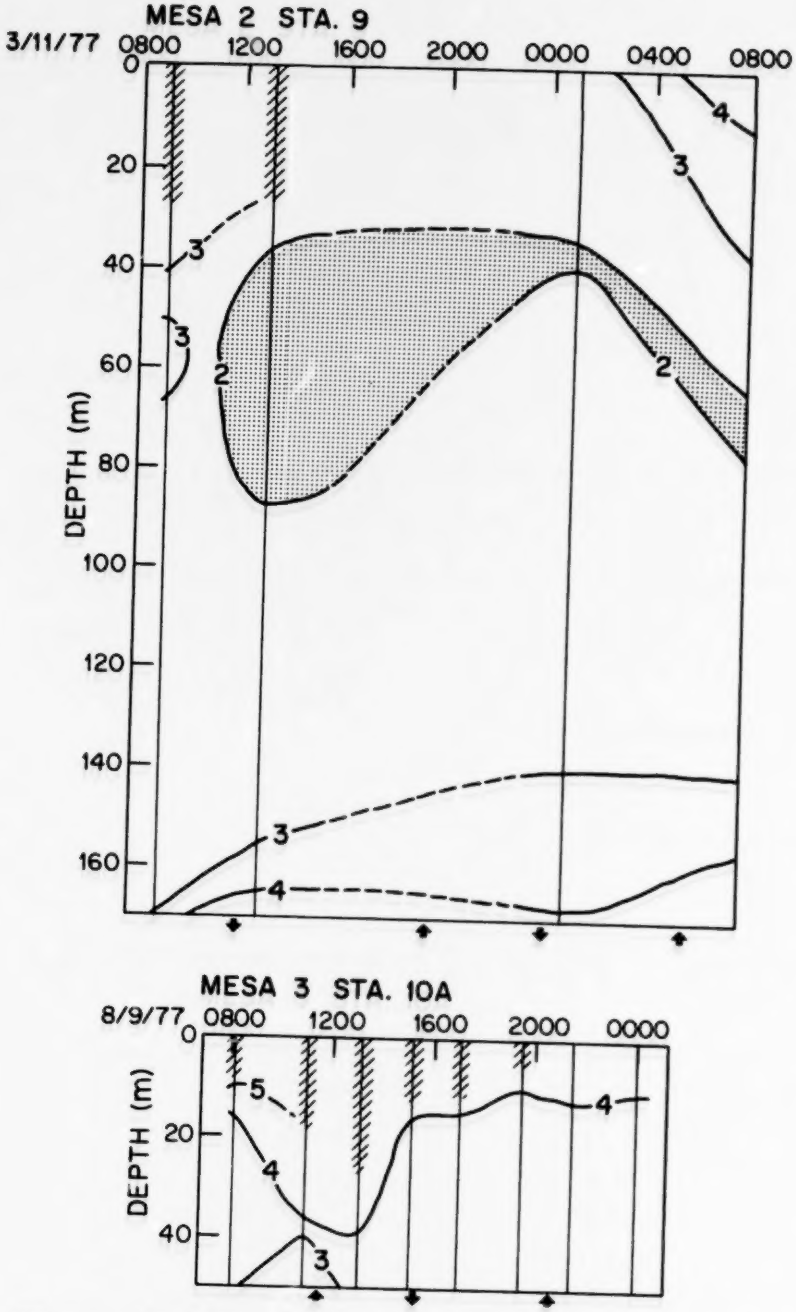

Figure 5.15. Time series line scattering measurements, station 9/10A. The time (PST or PDT) of each cast is shown by the vertical lines. Times of high (🡅) and low (🡇) tide are shown along the bottom border. Cross-hatching shows depth of daylight interference. Shading shows position of various mid-depth minima. Note the relative diurnal uniformity of this location.

variable current regime. These factors combined to produce rapid changes of both concentration and structure in the observed SPM distributions (Fig. 5.16). During the November cruise, the nephelometer profiles were stable during the first 12 hrs with a well-defined mid-depth minimum. Very substantial changes occurred during the following 12 hrs, including a pulse of very turbid water which coincided with the ebb tide (Fig. 5.16). During March, surface scattering dropped considerably, whereas near-bottom values remained variable and high. A mid-depth minimum was apparent during the last half of the time series. Surface values were still low in August, a mid-depth minimum was present throughout the time-series, and near-bottom scattering was again highly variable. Surface water SPM concentrations at this locality, although high compared to other regions in the study area, are still somewhat seasonally variable due to changes in runoff volume. Bottom water SPM concentrations evidently remain high throughout the year, probably due to resuspension of bottom sediments by the strong tidal currents.

5.3.3.3 Cherry Point (sta. 17). During November, suspended matter concentration was moderately stable for the first 12 hrs of observation and developed a very intense mid-depth minimum (Fig. 5.17). Both surface and near-bottom scattering values were relatively high and generally more uniform than at station 15. Incomplete data from March do not indicate a mid-depth minimum, and overall scattering values are low. The SPM distribution during August was remarkably uniform, showing high surface values, moderate and uniform bottom values, and a very stable mid-depth minimum centered at ~15 m.

5.3.3.4 Fraser River (sta. 26). Station 26 (Fig. 5.18) shares many of the characteristics of station 15, except that tidal currents are not nearly as influential. During November, scattering was very high in the upper 5 m due to the Fraser River plume. Below the plume the SPM distribution was uniform, with the development of a slight mid-depth minimum. Surface scattering was the same in August, but the underlying water column had taken on an entirely different character. The SPM distribution was extremely variable, presumably due to sinking and entrainment of the surface plume. The lenses of turbid water between about 10 and 25 m seemed relatively stable over the 24 hr time series, whereas the deeper lenses were more transitory, usually being observed only on 2 to 3 successive casts.

5.3.4 Suspended Particulate Matter - X-ray Mineralogy

Mineralogic data from selected filter samples are given in Table 5.1. Although the data are highly variable, some area-wide trends do emerge. Stations within the influence of the Fraser River plume (20, 23, 26, 29, 31, and 31A) tend to have lower values of chlorite/illite, quartz/illite, and feldspar/illite ratios than stations within the San Juan passages and Strait of Juan de Fuca. Low values of all these ratios imply a relatively smaller average grain size in the suspension. Samples collected from the Fraser River (Dec. 1977) and the Skagit River (Nov. 1977) reinforce this areal distinction in mineralogy (see also Table 6.2). The Fraser River samples are substantially lower in all three ratios than the Skagit River samples, although it should be noted that these rivers were sampled only once during the study period and the values obtained are not necessarily typical of the three seasons sampled in the marine waters.

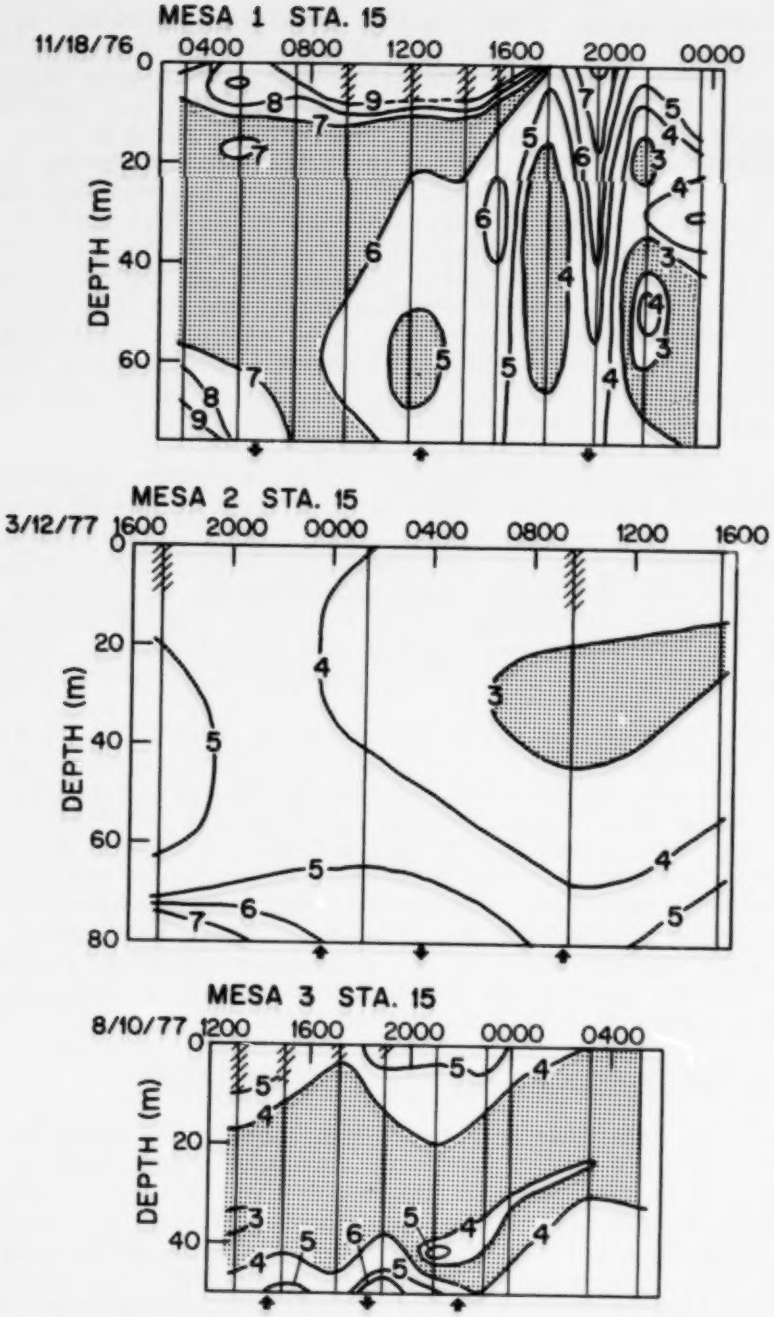

Figure 5.16. Time series light scattering measurements, station 15. Symbols as in Figure 5.15. Note the higher variability and scattering levels relative to the Strait of Juan de Fuca location (Fig. 5.15).

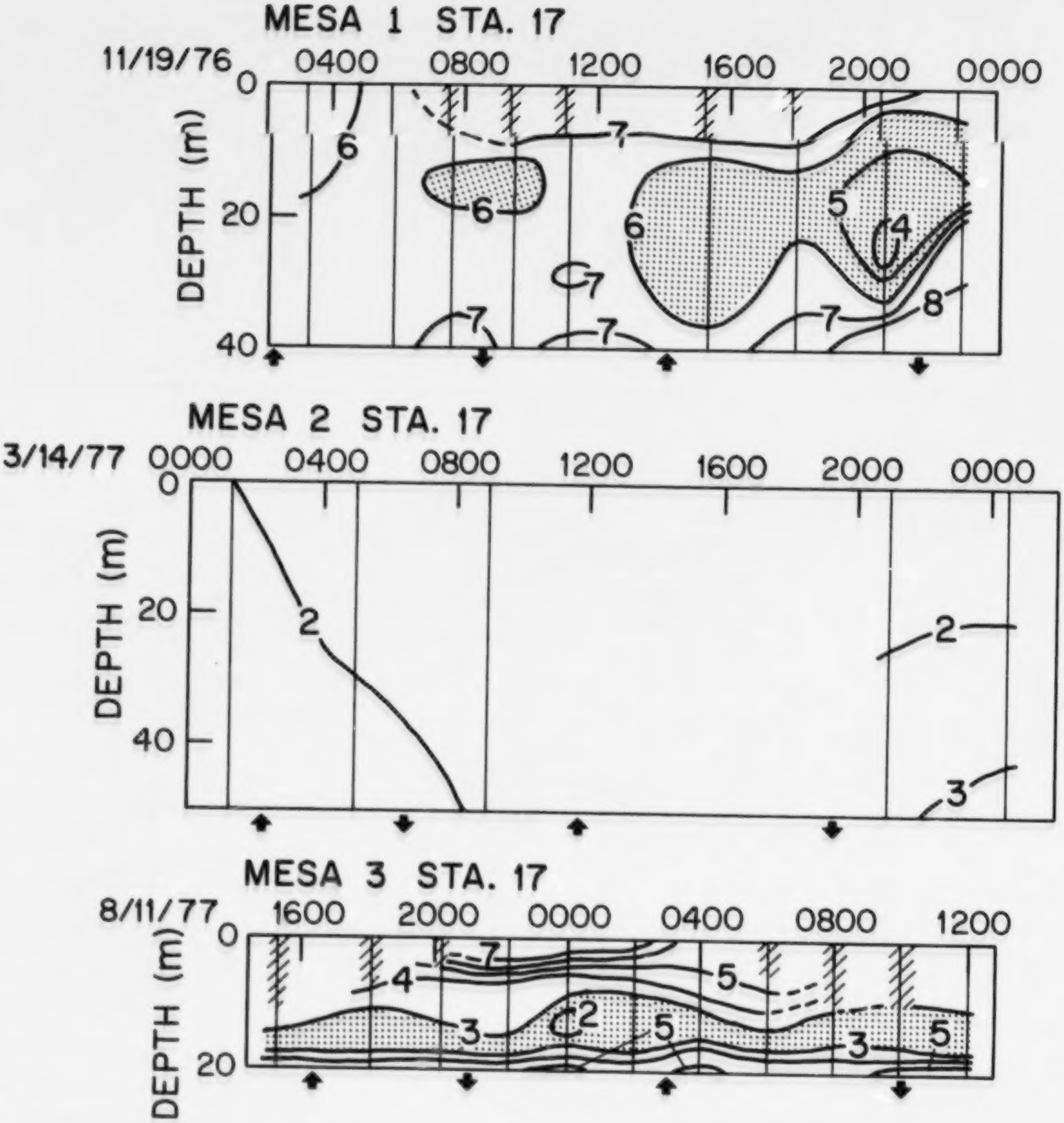

Figure 5.17. Time series light scattering measurements, station 17. Symbols as in Figure 5.15. Note the very weak structure during MESA II compared with conditions during MESA I and III.

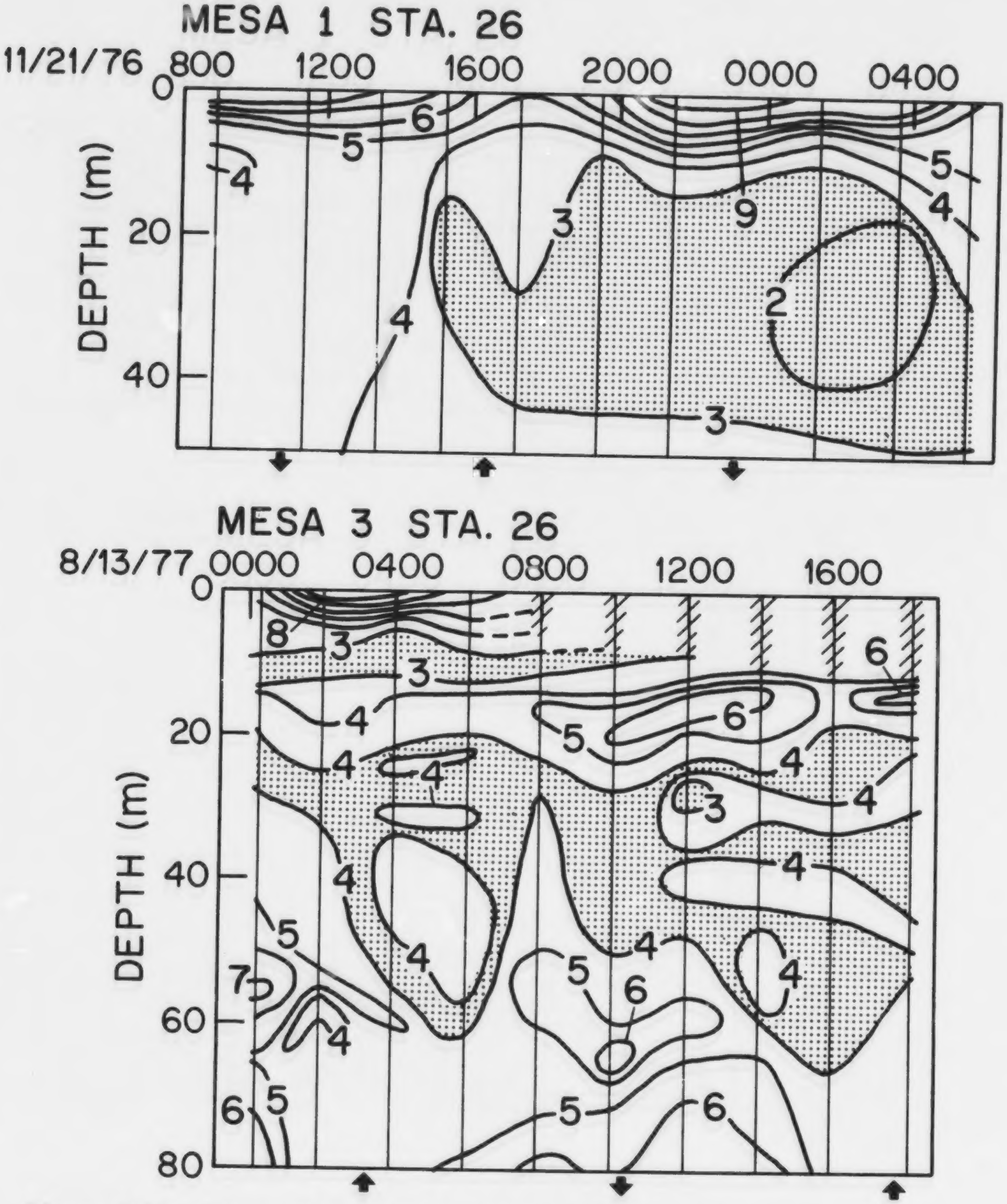

Figure 5.18. Time series light scattering measurements, station 26. Symbols as in Figure 5.15. Note that the river plume is confined to the upper 5 m. Subsurface structure was very complex during the high-runoff period during MESA III.

TABLE 5.1 X-ray mineralogy ratios of selected water samples and centrifuge samples

Station	Depth (m)	Chlorite Illite	Quartz Illite	Feldspar Illite
		MESA I		
10	98	2.22	2.89	7.33/6.89[1]
15	(0,10)[2]	2.89	3.11	4.44
	8	3.44	2.89	4.33/4.67
	(71,70)	2.08	3.25	4.17
	72	2.86	4.29	6.86
	8	2.83	1.92	5.33
	Centrifuge	2.64	1.36	4.79
		2.06	1.06	1.81
17	(0,10)	2.45	2.55	3.00
	22	1.93	1.71	2.29
	35	2.00	3.80	6.10/5.80
	37	3.29	4.57	4.86
	Centrifuge	1.79	1.37	1.74
26	0	1.79	1.50	1.82
	0	1.45	1.55	1.36
	42	1.27	0.95	3.77
	51	1.19	1.09	0.94
	Centrifuge	0.97	0.73	1.04/0.96
29	(0,10)	1.15	0.47	0.79
31	Centrifuge	1.81	1.38	2.31
31A	(0,10)	1.92	1.62	2.62
34	(0,10)	2.33	3.00	3.56/3.89
	125	2.13	12.25	7.00
		MESA II		
9	(0,10)	3.10	2.80	2.90
	(150,170)	2.00	4.67	4.56

(Contd.)

TABLE 5.1 (Contd.)

Station	Depth (m)	Chlorite Illite	Quartz Illite	Feldspar Illite
9	(150,165)	1.80	1.53	1.93
	Centrifuge	2.31	1.92	1.92
15	(0,10)	2.50	3.40	5.60
	(0,10)	2.80	1.93	3.53
	73	2.50	2.33	4.50
	(60,73)	3.20	3.20	4.50
	Centrifuge	1.71	2.00	2.57
17	(0,10)	2.08	3.00	2.31
	(0,10)	1.89	1.22	1.78
	44	2.08	2.77	2.69
	46	2.45	3.82	5.00
	Centrifuge	2.46	2.54	4.46
23	(0,10)	1.55	0.80	1.10
	119	1.81	2.31	2.63
26A	(0,10)	1.07	0.36	0.71
	188	2.13	2.19	2.56
35	(0,10)	1.80	0.50	1.30/1.40
	Centrifuge	2.52	2.35	2.96/3.04
		MESA III		
2	(0,10)	2.71	2.00	2.00
	47	2.30	1.30	2.90
10A	50	2.09	1.36	1.91
	Centrifuge	2.10	1.70	1.80
15	(0,10)	2.60	2.10	3.40
	60	2.64	2.55	2.91/3.18
	(0,10)	3.37	2.32	4.11
	45	1.95	1.00	1.32
	Centrifuge	2.50	1.50	2.90

(Contd.)

TABLE 5.1 (Contd.)

Station	Depth (m)	Chlorite Illite	Quartz Illite	Feldspar Illite
17	(0,10)	2.44	2.44	3.33
	(0,10)	2.43	3.43	3.29
	20	1.85	1.77	2.85
	20	2.00	1.46	2.23
	Centrifuge	2.50	2.69	3.85
20	(0,8.7)	1.13	0.78	0.78
	163	1.77	1.54	2.08
26	0	1.39	1.91	1.91
	0	1.04	0.96	0.81
	0	1.56	1.19	1.13
	77	0.98	0.50	0.50
	79	1.21	1.83	1.81
	Centrifuge	1.27	2.41	1.91
31	(0,10,20)	2.06	1.19	1.53
	200	1.60	1.20	1.70
River Samples				
Fraser River (Nov. 1977)		1.71	0.45	0.92
Skagit River (Oct. 1977)		4.00	1.05	35.05

[1] Indicates two principal feldspar peaks.

[2] Indicates pooling of samples from different depths.

5.3.5 Particle Size Distributions

Particle size analyses (Fig. 5.19) were performed by Coulter Counter techniques on six samples collected by centrifugation for analysis of suspended hydrocarbons. Samples suitable for analysis were collected during MESA I at stations 15 and 26, during MESA II at stations 9 and 17, and during MESA III at stations 17 and 26. Although the median diameters of all but one of the samples are similar at 5-6 μm (sta. 17, MESA III, is higher at ~11 μm), stations 15, MESA I, and 17, MESA III, possess prominent peaks in the 50-70 μm diameter range. This peak may be due to biogenic fragments (such as diatoms) and/or rock fragments of quartz and feldspar.

5.4 SUMMARY

Typical values of the concentration of total suspended solids in the waters of the study area between November 1976 and August 1977 were 0.5-2 mg/ℓ. Significant local modification of this concentration level in surface waters occurred north of the San Juan Archipelago, within the influence of the Fraser River plume, where concentrations were as high as 8 mg/ℓ, and immediately seaward of Deception Pass, where concentrations were ~2-3 mg/ℓ. Concentration values in the mid-depth and bottom waters showed little influence from riverine sediment sources.

The total particulate load in the study area, based on an estimated water volume of ~250 km^3 (estimated from calculations of the Strait of Georgia volume made by Waldichuk, 1957) and an overall SPM concentration average of 1.5 mg/ℓ is approximately 4×10^{11} g. Because of the unusual climatological year during the study period, which resulted in a substantial decrease in fresh water runoff (Fig. 2.2) compared to a normal year, the relationship of this estimated total SPM load to other years is uncertain.

The typical vertical distribution of SPM throughout the area tended towards relatively high values in the surface and bottom waters and relatively lower values in the mid-depth regions. This distribution is presumably due to different agents of particle production in different layers of the water column: high phytoplankton growth and fresh water runoff in the surface waters, and substantial contribution from resuspended bottom sediment into the bottom waters. Confirmation of this hypothesis - particularly the nature of the SPM increase in the bottom water - would require chemical analyses which were not undertaken in the present study.

Temporal variability of the SPM distributions was examined both on a seasonal and diurnal basis. Seasonal variability over most of the region was negligible: overall SPM concentrations were 1.8 ± 2.4 mg/ℓ for MESA I, 1.4 ± 0.8 mg/ℓ for MESA II, and 1.2 ± 1.0 mg/ℓ for MESA III. The somewhat higher mean value and standard deviation for MESA I is the result of very high SPM values near the Fraser River and Deception Pass during November 1977.

Diurnal variability was most pronounced at locations where strong tidal currents and/or major sediment sources (Fraser River, Deception Pass) were present. At other locations the vertical SPM distribution was relatively uniform over short time scales.

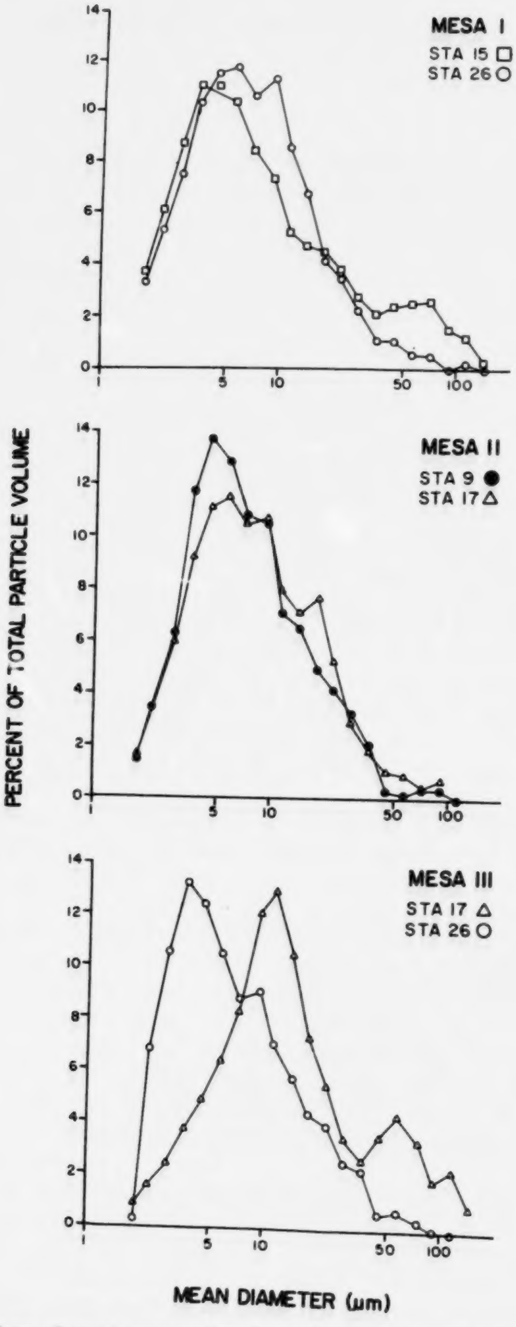

Figure 5.19. Coulter Counter particle size distributions from six centrifuge samples. Note the peak in the coarse silt-fine sand range (50-70 µm) for stations 15, MESA I, and 17, MESA II.

6. OIL-SEDIMENT INTERACTIONS

6.1 GENERAL STATEMENT

Oil spilled onto the surface of the ocean is acted upon by several physical processes including evaporation, emulsification, solution, and the injection of oil particles into the atmosphere during bubble formation (Kreider, 1971; McAuliffe, 1966, 1969; Baier, 1970). Except for solution of the soluble fraction, these processes represent a physical transfer of petroleum from the aquatic environment, thus reducing its potential impact on marine organisms. In contrast, petroleum adsorbed onto particles becomes entrained in the water column and ultimately deposited on the bottom.

There is very little published information about the processes by which oil is transported in association with suspended particles or the quantities of oil that can be adsorbed onto the particles. Early investigators have shown that flocculation of oil bears an inverse relationship to salinity (Chipman and Galtsoff, 1949; Hartung and Klinger, 1968). Later investigations indicate that sedimentation of oil involves a two-step process (Bassin and Ichiye, 1977). This process begins with the adsorption of oil onto the suspended particles and is followed by the flocculation of these oil-sediment emulsions by electrostatic interactions. The amount of oil that can be sedimented by a specific quantity of suspended matter appears to be dependent upon the physical and chemical nature of the suspended particles as well as the amount of naturally-occurring organic matter that is associated with the particles (Poirier and Thiel, 1941; Meyers and Quinn, 1973).

Oil adsorbed onto the surface of particles is one of the principal mechanisms by which petroleum contaminants may be ingested by marine organisms (NAS, 1975). Of particular concern is the effect on planktonic and benthic detrital feeders. Conover (1971) observed following the wreck of the tanker Arrow in Chedabucto Bay that zooplankton could graze as much as 20% of the oil particles less than 1 mm in diameter and sediment them as fecal material. Parker (1970) also found that copepods and barnacle larvae could encapsulate oil as fecal material. Because fecal material is an important food source for other members of the food chain, oil transmitted to the bottom in this form becomes an important mechanism by which benthic detrital feeders may be impacted by oil. Many of these species, including shrimp, clams, oysters, and crabs, are of economic interest.

In most previous studies, the adsorption of petroleum components from solution by various clay mineral phases has been investigated. The results, as typified in the report by Meyers and Quinn (1973), show that approximately 6% of a fuel oil solution was taken up by Narragansett Bay sediments, but the amount increased to 51% when bentonite clay was substituted. Temperature, salinity and concentration of organic matter play important roles in determining the quantities of oil in solution adsorbed. These results are not surprising in view of the low solubility of petroleum hydrocarbons, particularly the long chain aliphatics.

The purpose of this study was not to clarify the adsorption phenomenon from true solution, but rather to investigate the agglutination process associated with natural suspended material and surface or emulsified oil. In spill situations, excess oil is present on the surface of the water and may be readily accommodated by suspended particles that come in contact with the surface layer. The first step in characterizing the agglutination process is to establish the capacity of natural material for oil as a function of selected environmental parameters. This approach avoids the question of kinetics, but does establish a fundamental criterion for assessing the loading characteristics of the sediment.

6.2 LABORATORY STUDY

In the preliminary design of the experiment, various quantities of oil were mixed with known amounts of riverine-derived suspended matter under controlled laboratory conditions. Suspended matter was retrieved from both the Skagit and Fraser Rivers with a continuous flow centrifuge, the efficiency of which will be discussed in greater detail below. The amount of sediment chosen for the experiment was nominally 50 mg, resuspended in 600 mℓ of Puget Sound sea water. This concentration of sediment is high and not representative of the concentrations actually observed in the waters of "Northern Puget Sound," except possibly in the river estuaries, but represented a convenient amount with which to effectively carry out the preliminary measurements. The quantities of oil added were adjusted to give oil:sediment loadings of 0.2 to 3, or 20 mg to 150 mg of added oil.

The procedure was as follows: Approximately 50 mg of riverine suspended matter was added to 600 mℓ of sea water in a separatory funnel and placed in a controlled temperature bath. After thermal equilibration, the desired quantity of oil was added to the system, tightly stoppered, and the mixture shaken gently for 1 hour. The intensity of shaking was controlled to avoid overdevelopment of oil-water emulsion. After 1 hour, the mixtures were allowed to stand in the water bath until the sediment/oil flocs had settled, at which time settled material was carefully removed with a long pipette and extracted with methylene chloride. The remaining mixture (unsettled sediment, oil, and water) was back extracted with methylene chloride to recover the remaining oil. Organics associated with the sea water and the sediments were estimated in separate experiments. The amount of sediment recovered from the lower layer is used as the basis for computing the loading (i.e., mg oil/mg sediment). The total quantities of oil recovered from each step was determined by gravimetry on a Cahn^{R} microbalance. Most of the experiments were conducted in triplicate and repeated if either the oil recovery or sediment recovery was judged to be low.

6.3 METHODOLOGY

6.3.1 Petroleum Hydrocarbon Analysis

Qualitative analysis of the alkane fraction was carried out to evaluate gross compositional variations that might occur during the agglutinization process. Extracts from the settled oil/sediment flocs were subdivided into two fractions (alkanes and aromatics) by silica gel chromatography. The resulting alkane fraction was analyzed by glass capillary gas chromatography according to the procedures established by Macleod et al. (1976). Because the quantities of sediment being extracted were less than 1 g, the solvent extraction volumes were reduced to 1/10th those recommended by the above procedure.

6.3.2 Oil Recovery Efficiency

Preparatory to the study, it was necessary to establish the reliability of various experimental procedures related to the recoveries of oil. The first of these dealt with determining the reliability of weighing crude oil quantitatively on a Cahn^R microbalance. The results of this experiment are shown in Figure 6.1, where approximately 25 μℓ of Prudhoe Bay crude oil was pipetted into a tared aluminum pan at room temperature and its weight determined as a function of time. The largest change in weight occurred during the first 10 mins., after which time the rate slowed appreciably. Ten minutes was chosen as a convenient time at which to weigh the oil residue. Extrapolation of the curves in Figure 6.1 show that less than 5% of the total oil was lost during the first 10 mins. The observed loss in weight presumably reflects the volatilization of the low molecular weight aliphatics and aromatics.

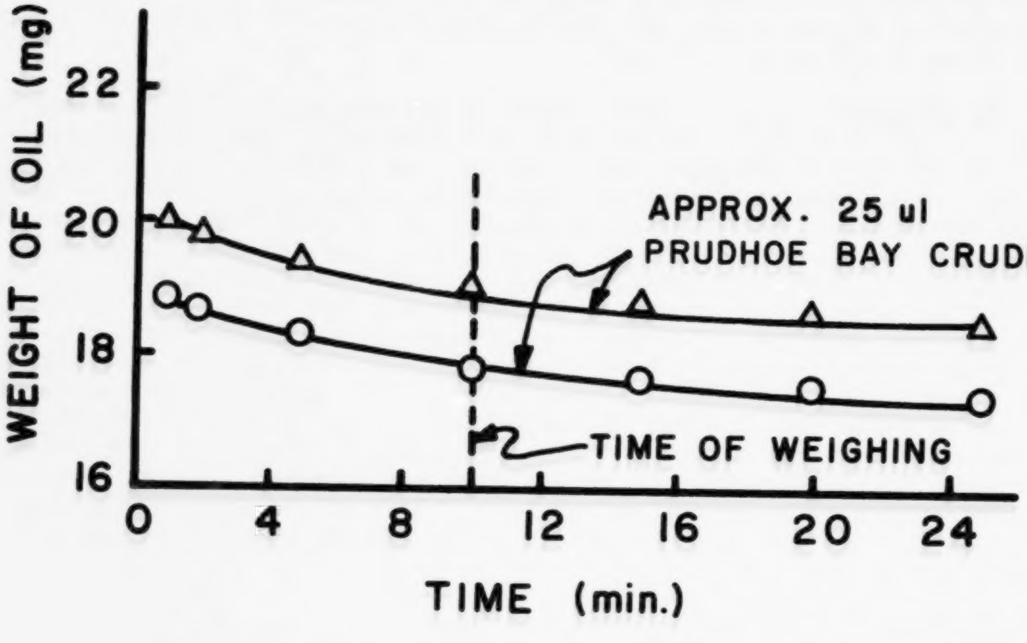

Figure 6.1. Evaporative weight loss of Prudhoe Bay crude oil. Two curves shown are replicate experiments.

The extraction and concentration efficiencies were also investigated (Table 6.1). In the first case various amounts of Prudhoe Bay crude oil were added to 60 mℓ of methylene chloride, reduced to 2 mℓ in a concentrator tube, solvent exchanged for hexane, and the volume again reduced to 2 mℓ. A 50 mℓ aliquot of this solution was evaporated on a tared pan at room temperature and weighed on a Cahn^R microbalance. The corrected concentrations of oil recovered are shown in column A. The average for three concentrations of oil was 82%. The material lost (approx. 18%) presumably represents the light fraction of the oil.

TABLE 6.1 Extraction and concentration step efficiencies. (A) Various amounts of Prudhoe Bay crude oil were added to 60 mℓ $CH_2 Cl_2$ and reduced to 2 mℓ volume in hexane. (B) Various amounts of oil were added to 600 mℓ of Puget Sound sea water and backextracted with 3-20 mℓ aliquots of $CH_2 Cl_2$. Average percent recoveries and standard deviations are shown together with the number of replicate experiments in parentheses.

Amount Oil Added mg	A	B
	% Recovery	
8.45	83 ± 6 (6)	57 ± (1)
16.90	86 ± 6 (6)	67 ± 4 (2)
25.35	77 ± 13 (5)	62 ± 4 (2)
42.25	--	73 ± 9 (5)
84.45	--	75 ± 10 (6)

6.3.3 Sediment-Sea Water Organic Matter Corrections

During the extraction process, a portion of the organics associated with the aqueous phase (i.e., DOC) and the solid phase (i.e., organic matter) was coextracted with the oil. In order to correct for this effect, which results in an overestimation of the quantity of oil recovered from each phase, sediment (50 mg) and water (600 mℓ) were extracted separately with 3-20 mℓ aliquots of methylene chloride. The amount of organics so extracted were determined gravimetrically on a Cahn^R microbalance. Our results show that the concentration of extractable organics in the sea water medium was approximately .002 mg/mℓ sea water; the concentration of extractable organics from the sediment was approximately .006 mg/mg sediment. Organics coextracted in the sediment and water layers were calculated based on water volumes and sediment recoveries in each fraction.

The above correction represents a rather crude estimate of the partitioning of the organics between the various phases. The mixing of sea water-oil-sediment represents initially a three-phase system. Organics will be redistributed among the various phases depending on their solubility in water and oil and their relative adsorption affinity for the solid phases present. No attempt was made to characterize the actual distribution of the organics present in the various phases.

In column B is shown a measure of the extraction efficiency. Various quantities of oil were added to 600 mℓ of Puget Sound sea water and back-extracted with 3-20 mℓ aliquots of methylene chloride. The volume was reduced to 2 mℓ in a concentrator tube and the solvent exchanged for hexane as before.

There appears to be a systematic increase in the extraction efficiency as the concentration of oil increases. The reason for this has not been explored further, but may be a function of the solubility of the oil and the quality and amount of dissolved organic carbon (DOC) present. In a separate experiment, we determined that the extraction procedure outlined above removed approximately 2.3 mg/ℓ of organic matter present in the sea water used. Results shown in column B have been corrected for extractable organics. The difference in recoveries noted between the concentration and extraction steps presumably reflects the relative extraction efficiency as a function of the oil concentration and serves as a basis for interpreting total oil recoveries to be discussed below.

6.3.4 Sediment Morphology and Compositional Characteristics

The matrix for the oil agglutinization studies was suspended material from the Skagit and Fraser Rivers. Sampling was conducted in the lower reaches of the rivers, but above the salt wedge, in order to obtain representative material actually entering the estuary.

Sediment recovery was effected with a Sorvall^{R} model SS-3 high speed continuous flow centrifuge operated nominally at 15,000 rpm and a fluid flow rate of 400-500 mℓ min^{-1}. At this orbital velocity, particles are subjected to approximately 30,000 G's of acceleration. Because the sedimentation efficiency of individual particles is a function of both the density difference between particles and the fluid and their size, organic matter, having a density near that of water, is not recovered as efficiently as mineral matter.

Water was pumped to the centrifuge through a sampling manifold consisting of two prefilters, the smallest of which was 100 μm. This procedure effectively rejected larger pieces of vegetable matter that would have heavily biased the compositional analysis. Flow rate and accumulated volume through the centrifuge were monitored electronically.

The centrifuge, intake manifold, and flow monitoring system is shown in Figure 6.2. For shipboard operations in the Straits of Juan de Fuca and Georgia, it was necessary to gimbal the centrifuge to reduce accelerations due to the pitch and roll of the ship.

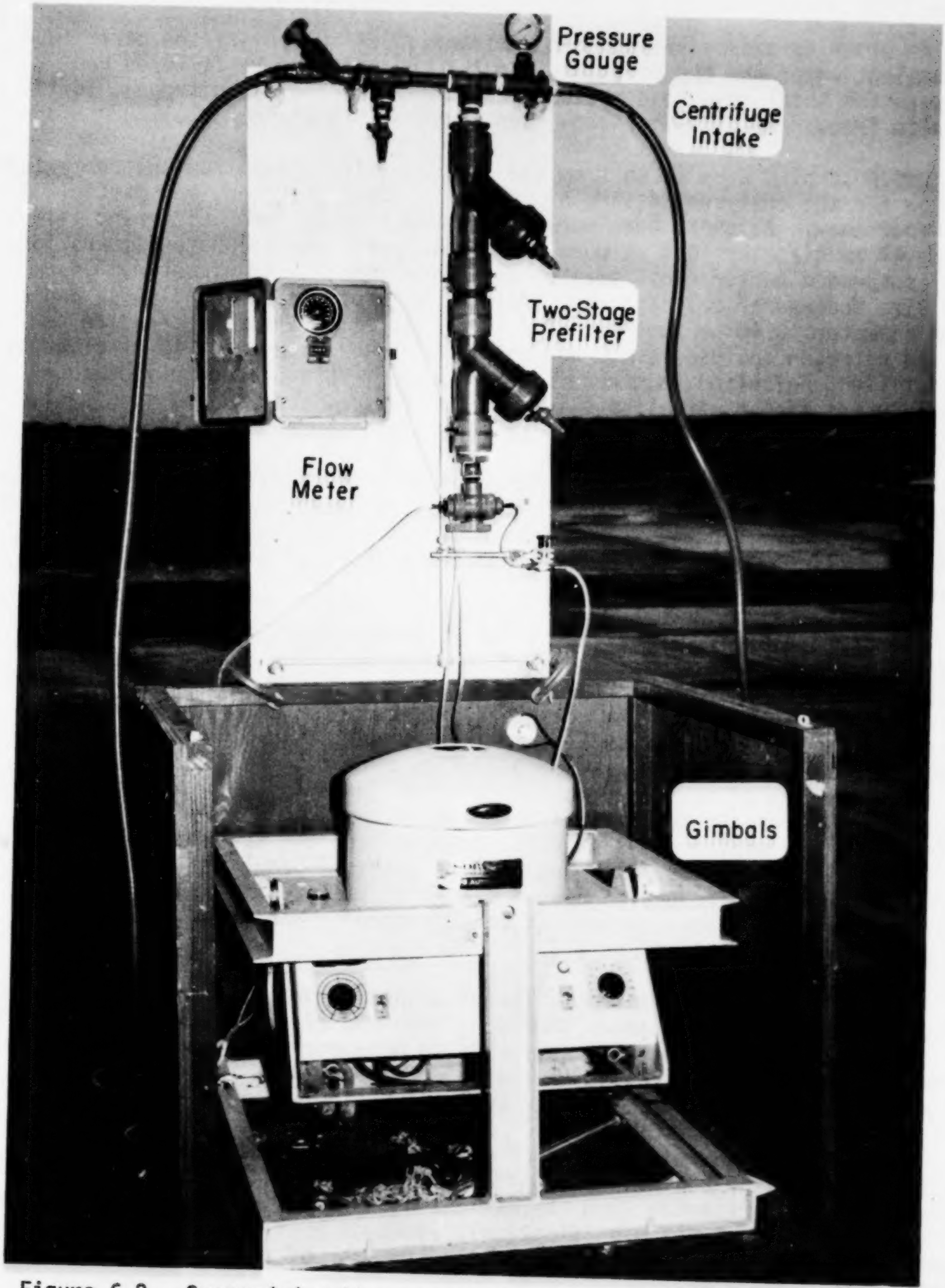
Pressure Gauge
Centrifuge Intake
Two-Stage Prefilter
Flow Meter
Gimbals

Figure 6.2. Suspended matter recovery system. Suspended solids are pumped to the intake manifold and passed through a two-stage prefilter (dia. < 100 μm). Flow rate and accumulated volume through the centrifuge are monitored electronically. Centrifuge is shown mounted in gimbal for use at sea.

In order to assess the sediment extraction efficiency of the centrifuge, the ambient water and the effluent from the centrifuge were filtered and analyzed for total suspended matter (TSM), total carbon and nitrogen, particle size frequency, and mineralogy (see sections 5.3.4 and 5.3.5).

Water samples were taken from the intake manifold and from the centrifuge outflow for the analyses of TSM, organic carbon and nitrogen, and particle size frequency. Aliquots were vacuum filtered through three different filters: 47 mm diameter, 0.4 μm pore size Nuclepore^R polycarbonate filters for total suspended matter concentration determinations; 25 mm diameter, 0.4 μm pore size Nuclepore^R polycarbonate filters for particle size analysis; and 25 mm diameter, 0.45 μm pore size Selas^R silver filters for particulate carbon and nitrogen analyses. All samples were rinsed with three 10 mℓ aliquots of distilled, deionized, membrane filtered water, then placed in individual plastic petri dishes with lids slightly ajar for desiccation and then sealed and stored (silver filters frozen) for subsequent laboratory analysis.

The Nuclepore^R filters were weighed on a Cahn^R Model 4700 electrobalance before and after sample filtration with the suspended masses being determined by difference. Particulate carbon and nitrogen were analyzed by the micro-Dumas combustion method, employing a Hewlett Packard 185B C-H-N analyzer (Sharp, 1974).

The compositional parameters of the river-derived suspended matter is shown in Table 6.2, together with the mineralogies. The Skagit River was visited in May and November of 1977, representing two widely differing hydrologic conditions. In May, the river was extremely low and suspended loads averaged only 5.5 mg/ℓ. In 1975, the mean concentration of suspended matter in May for the Skagit River was approximately 60 mg/ℓ (see Fig. 2.3). The low concentration of suspended matter observed in May of 1977 reflects the anomalously low precipitation that occurred in the Skagit River drainage basin during the winter of 1976-1977. In contrast, the November sampling was carried out at a time following several weeks of heavy rain. The suspended loads were extremely high as a result of soil erosion in the lower alluvial basin. The mean concentration of suspended matter was 134 mg/ℓ; its organic carbon content was 2.3%.

A comparison of the concentration of suspended matter in the effluent to that in the ambient water shows that more than 92% of the filterable material was removed by centrifugation in May; 98% in November. The higher figure in November reflects the increased abundance of larger, more dense particles, and a lower concentration of organic matter (see Table 6.2).

Scanning electron micrographs of filtered material derived from the Skagit River and the centrifuge of effluent are depicted in Figure 6.3a,b (November 1977). Material from the ambient water (Fig. 6.3a) shows particles as large as 20 μm (1000 X magnification), although most of the material appears to be less than 5 μm. A statistical number of these particles were counted with a Zeiss Particle Size Analyzer and the results are shown in Table 6.3. Of the particles counted, 37% were less than 2 μm in diameter, whereas 97% of the particles were less than 10 μm.

TABLE 6.2 Comparison of the concentrations of total suspended matter (TSM) in the ambient water with that in the centrifuge effluent. Also shown are the concentrations of total carbon in the suspended material, its carbon: nitrogen ratio (C:N), and the chlorite:illite, quartz:illite, and feldspar: illite ratios.

Location Date	Volume Centrifuged (liters)	TSM (mg/ℓ)		Total Carbon (μg/ℓ)		C:N	Mineralogy		
		Ambient	Effluent	Ambient	Effluent	(mg/mg)	Chl/Ill	Qtz/Ill	Feld/Ill
Skagit River (Sedro Woolley) May 10-11, 1977	1178	5.5 ± 1.2 (n = 5)	0.4 ± 0.2	177 ± 39	5 ± 5	3.9 ± 21	-	-	-
Skagit River (Sedro Woolley) Nov. 29, 1977	220	134 ± 3 (n = 2)	3.0 ± 0.1	3140 ± 460	ND	-	4.00	1.05	35.05
Fraser River (Port Mann) Dec. 2, 1977	512	29 ± 6 (n = 4)	2.9 ± 0.6	406 ± 216	ND	-	1.71	0.45	0.92

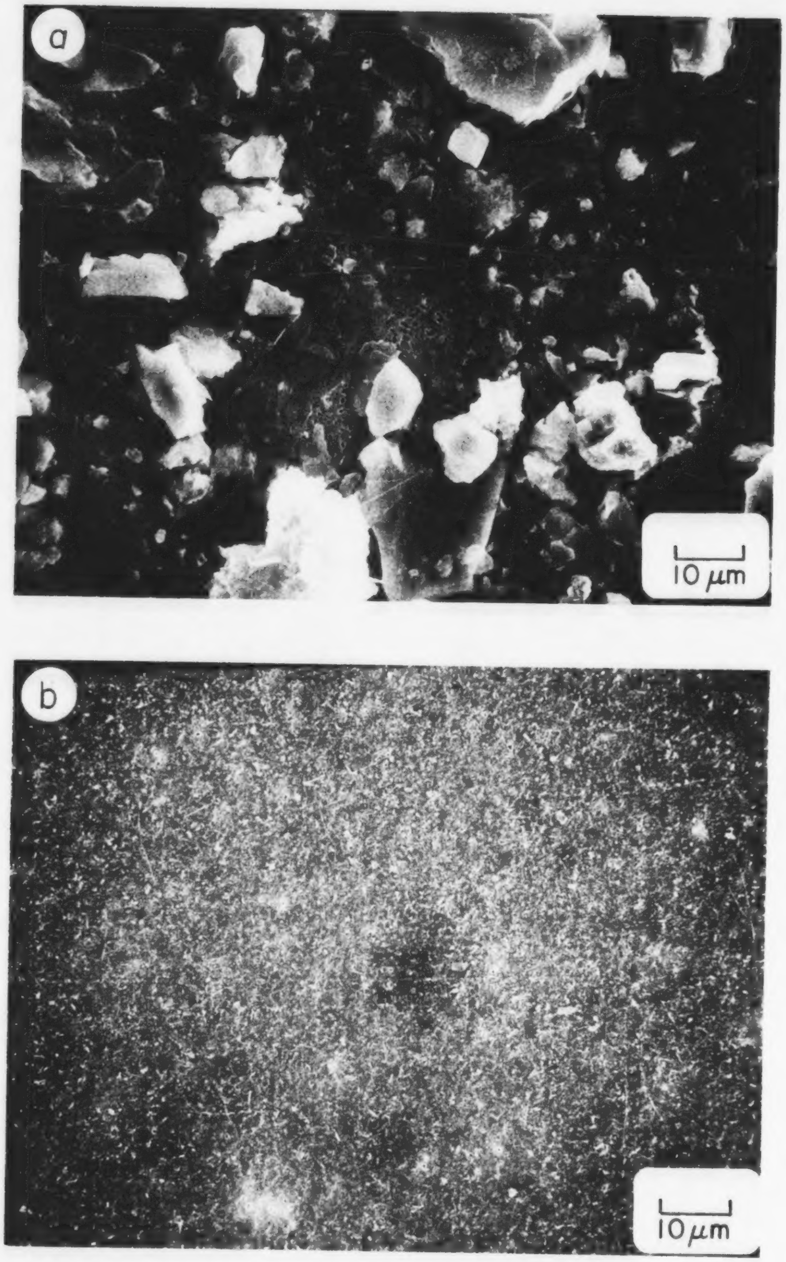

Figure 6.3. Scanning electron micrographs of Skagit River suspended matter showing particles recovered in the ambient water (a) and in the effluent from the centrifuge (b). Note the pores in the Nuclepore® 0.4 μm membrane filter used in the recovery efficient test. Particles are shown 1000x actual size.

Table 6.3 Representative particle size distributions from the Skagit and Fraser Rivers. Values are expressed in terms of cumulative percent within a size classification

Sample Location	Cumulative Percent <2 μm	<5 μm	<10 μm
Skagit River November 1977	37	83	97
Fraser River December 1977	55	94	99

Figure 6.3b shows a similar scanning electron micrograph of the material filtered from the centrifuge effluent. When subjected to higher magnification (10,000 X, not shown), the morphology of the particles was poorly defined as they appeared to be coated with an organic gel-like material. It is this material that results in the clogging of the pores of the filter, resulting in the retention of many particles less than 0.4 μm, the nominal pore size. Most of the particles shown in Figure 6.3b are $\leq$ 0.4 μm. Analyses for organic carbon and nitrogen were negative as sufficient material was not present on the filter to obtain a measurable chromatographic response (Table 6.2).

The scanning electron micrographs of suspended sediment derived from the Fraser River are shown in Figures 6.4a,b. In contrast with Figure 6.3a the filterable material from the Fraser River is, on the average, smaller in size than that obtained from the Skagit. Approximately 94% of the retained material was less than 5 μm in diameter as compared to 83% for the Skagit River (Table 6.3). This is not surprising, since the turbulent energy was much higher in the Skagit River at the time of sampling, relative to conditions in the Fraser. Figure 6.4b depicts the material passing through the centrifuge and is similar in morphology to that obtained in the Skagit (see Fig. 6.3b).

Particle size determination of the riverine suspended matter was calculated using photomicrographs taken on an ISI^R Super Mini SEM-II scanning electron microscope. The particles were then sized (assumed to be spheres) on a Zeiss^R TGZ-3 particle size analyzer. In section 5.3.5, the particle sizes were determined with a Coulter Counter, which measures the effective volume of the particle, rather than the nominal diameter as done here. If the particles analyzed by both methods were perfect solid spheres, the calculated median diameters would be nearly the same; but, of course, the morphology of the particles is not uniform as is vividly shown in Figures 6.3 and 6.4. No intercalibration of the two procedures was carried out, but a systematic difference in the calculated median diameters is expected.

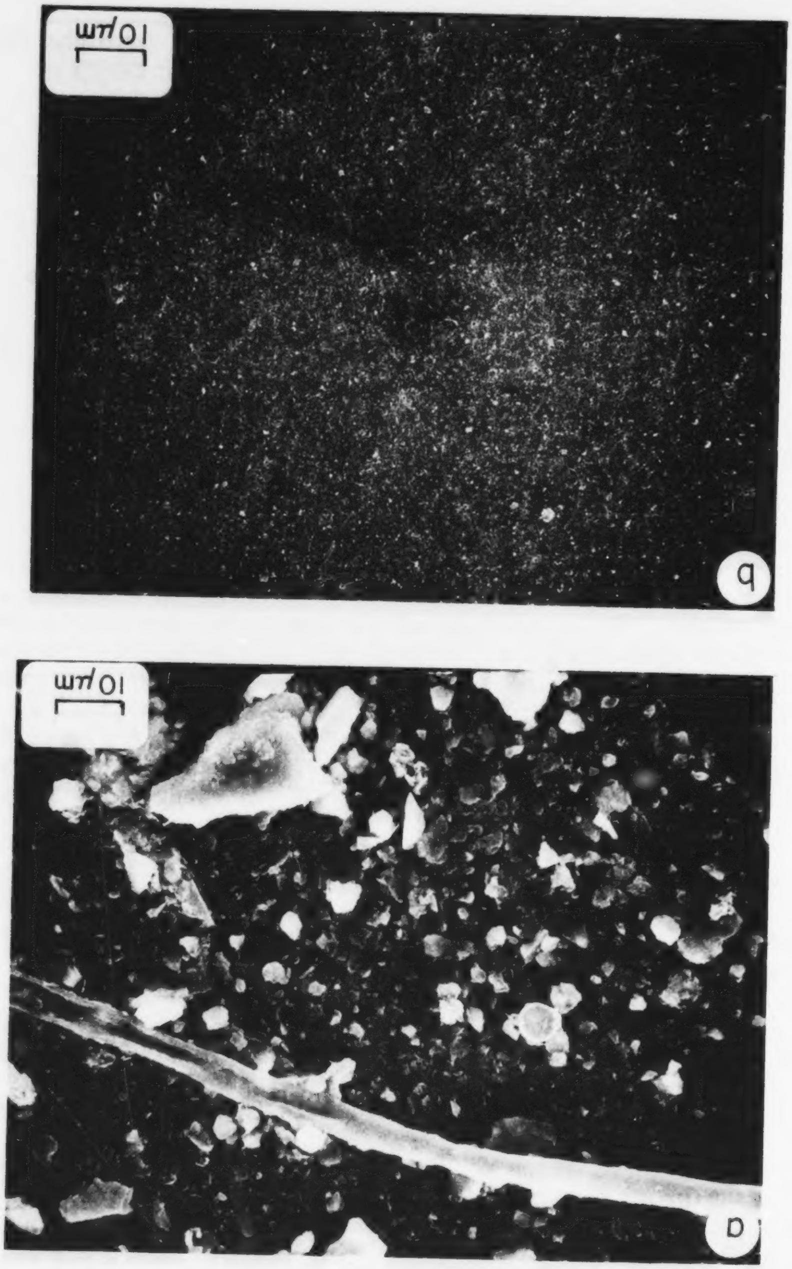

Figure 6.4. Scanning electron micrographs of Fraser River suspended matter showing particles recovered in the ambient water (a) and in the effluent from the centrifuge (b). Particles are shown 1000x actual size.

In summary, it appears that the continuous flow centrifuge collects representative samples of suspended matter from the rivers studied, but may bias the composition of the material in favor of the detrital inorganic fraction. This is particularly true if the organic particles are less than 1 μm in diameter.

6.4 RESULTS

6.4.1 Skagit River Sediments

The oil agglutinization studies, using Skagit River suspended material, is summarized in Table 6.4. In each experiment, approximately 50 mg of sediment was added to the quantities of oil shown in column 1 of Table 6.4. Temperature was maintained at 10° and 15°C, respectively, for each suite of experiments.

Table 6.4 The concentration of sediment-accommodated Prudhoe Bay crude oil for various initial oil loadings. All experiments were carried out in 1 ℓ separatory funnels to which was added 600 mℓ of sea water (S = 32°/oo) and 50 mg of Skagit River suspended sediment. Sediment recovery in the lower layer and total oil recovery are also shown in columns 2 and 4. Number of replicate experiments is shown in parentheses in column 1.

Amount of Oil Added (mg)	Sed. Recovered Lower Layer %	Oil Recovered Lower Layer %	Total Oil Recovered %	Loading (La) mg oil/mg sed.
		Temperature 10°C		
8.9 (7)	73 ± 19	20 ± 10	43 ± 18	.07 ± .02
17.7 (5)	76 ± 4	30 ± 7	54 ± 9	0.14 ± .04
26.6 (6)	78 ± 5	22 ± 6	72 ± 5	0.15 ± .04
44.4 (11)	83 ± 4	28 ± 6	86 ± 5	0.30 ± .05
133.0 (3)	86 ± 2	31 ± 2	93 ± 4	0.96 ± .02
		Temperature 15°C		
17.7 (3)	73 ± 2	18 ± 4	58 ± 1	.08 ± .02
44.4 (3)	73 ± 2	12 ± 2	85 ± 6	0.15 ± .03

Sediment recovery, as reflected in column 2, shows that more than 70% of the total sediment added was removed in the lower layer, although the recovery efficiency increased systematically with the amount of oil added. Presumably, the large flocs of oil and sediment formed at higher concentrations of oil were effective in sieving the finer particles from suspension.

In the experiment conducted at 10°C, the oil loading (mg oil/mg sed.) increased monotonically from .07 mg/mg to 0.96 mg/mg as the amount of oil was increased from 9 mg to 133 mg. This situation is graphically displayed for both 10°C and 15°C in Figure 6.5. Ignoring for the moment the apparent plateau in the curve, which may be an experimental artifact, the linear regression line for all points was $L_a = 0.36 L_o - .01$, where L_a is the loading or the amount of associated oil per unit weight of sediment recovered and L_o is the initial oil/sediment weight ratio. At 15°C, the quantity of oil recovered per weight of sediment recovered (L_a) decreased by approximately 50%, implying a large temperature effect.

Although the curve in Figure 6.5 shows a linear relationship up to $L_a = 1$, it is unlikely that this trend would continue. If we assume a density for the adsorbed oil of 0.89 g cm^{-3} and that for the suspended matter of 2.5 g cm^{-3}, the mean density of the flocs would be 1.7 g cm ^{3}. At $L_a = 10$, an unlikely situation, the mean density would be 1.04 g cm^{-3}, and the particles would be almost neutrally buoyant in sea water ($p = 1.026$ g cm^{-3}).

Also shown in Table 6.4 (column 4) is the systematic increase in the total recovery of oil as the concentration increases. As stated previously, the reason for this is not understood, since methylene chloride has been used by several investigators to extract petroleum hydrocarbons from sea water (Gordon and Keizer, 1974; Hites and Biemann, 1972). Experiments in our laboratory have shown that quantitative recovery of oil from distilled water can be achieved but apparently not in sea water containing suspended sediments. The reason for this may be due to a complex interaction between the oil and organic phases present in the sediments and water. This aspect of the study needs clarification.

During the agglutinization process, various components of crude oil may partition themselves between the adsorbed phase and the emulsified fraction. To investigate this possibility, sedimented oil was extracted from the mineral phases and analyzed for its paraffin composition. The results of this analysis are shown in Figure 6.6. For comparison, a similar amount of Prudhoe Bay crude oil was fractionated into its saturated and unsaturated fractions; the paraffin fraction was analyzed as stated above. These results are reflected in Figure 6.7. Both chromatograms show the predominance of the C_{15}-C_{18} normal paraffins, and if any fractionation has occurred, it resides with the light fraction. Because of their volatility, quantitative recoveries are not reliable. It is also important to note the absence of an unresolved complex mixture, even with fresh crude oil. The numerous small peaks present are due to branched alkanes and cycloparaffins (Clark and MacLeod, 1977).

Under the short-term conditions of this experiment, little fractionation of the oil was observed (i.e., closed systems, 10°C, flocculation time: 1 hour). Exceptions include the vaporization and solution of the more volatile

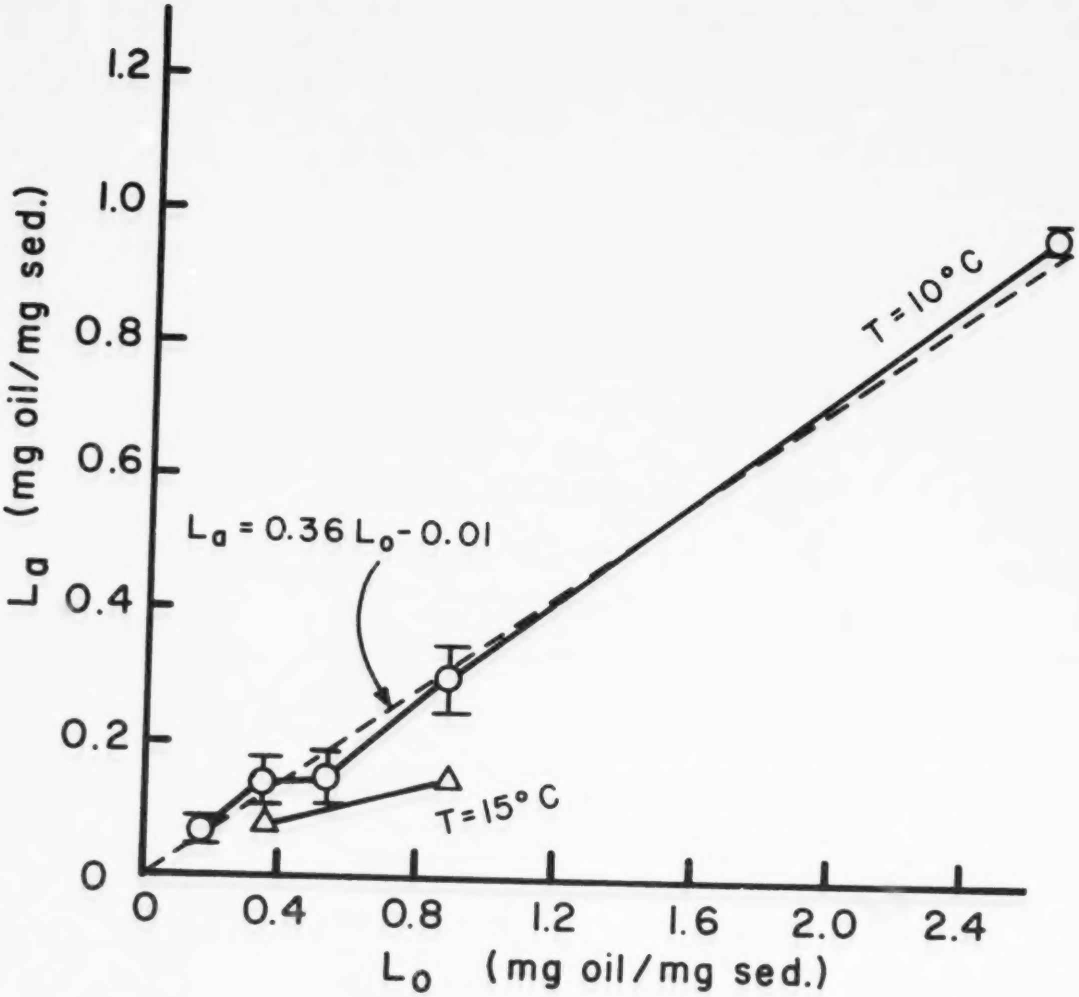

Figure 6.5. Concentration of accommodated Prudhoe Bay crude oil (La) on Skagit River suspended sediments as a function of the initial oil loading (Lo). Experiments were performed at 10°C (○) and 15°C (△) in normal Puget Sound sea water (S = 32°/oo). Concentration of suspended sediments was 83 mg/ℓ in each experiment.

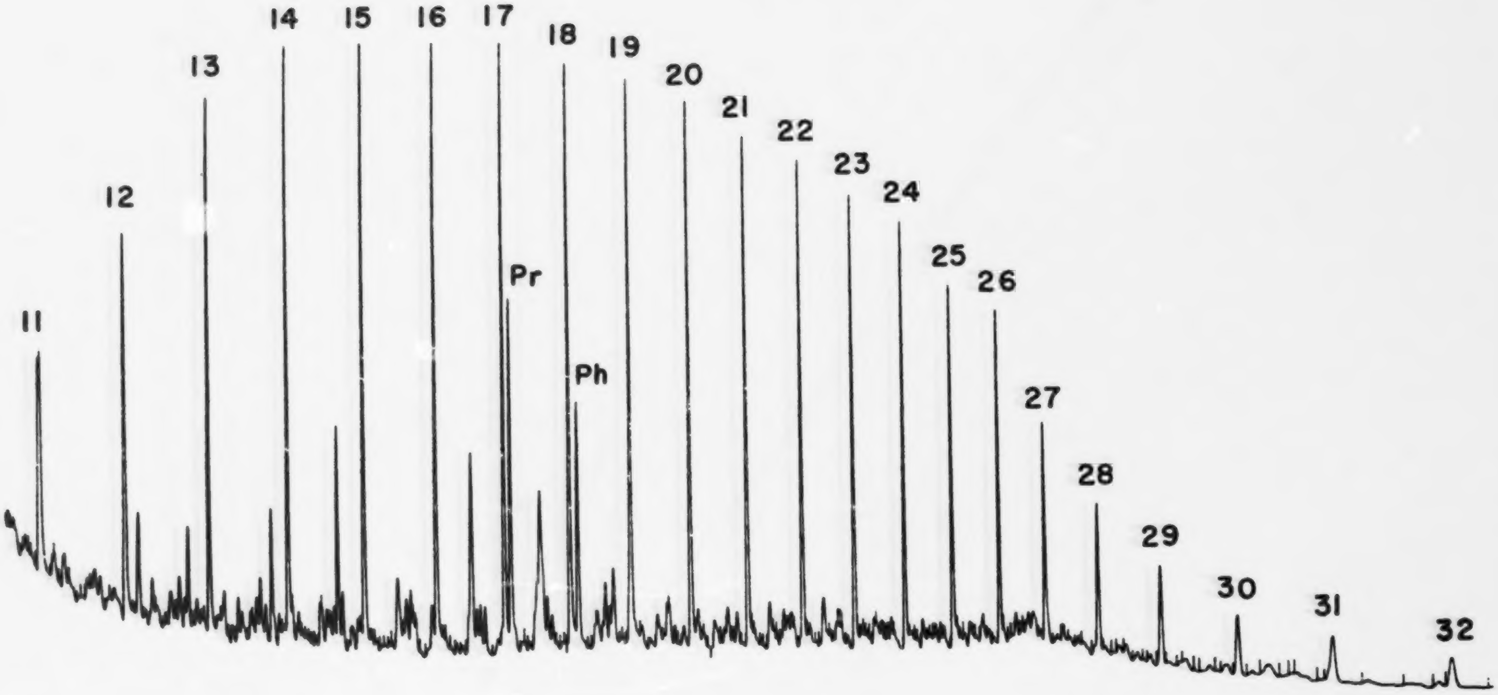

Figure 6.6. Gas chromatogram of the extracted aliphatic fraction taken from oil flocculated sediments. The amount of oil added was 44.4 mg; the temperature 10°C.

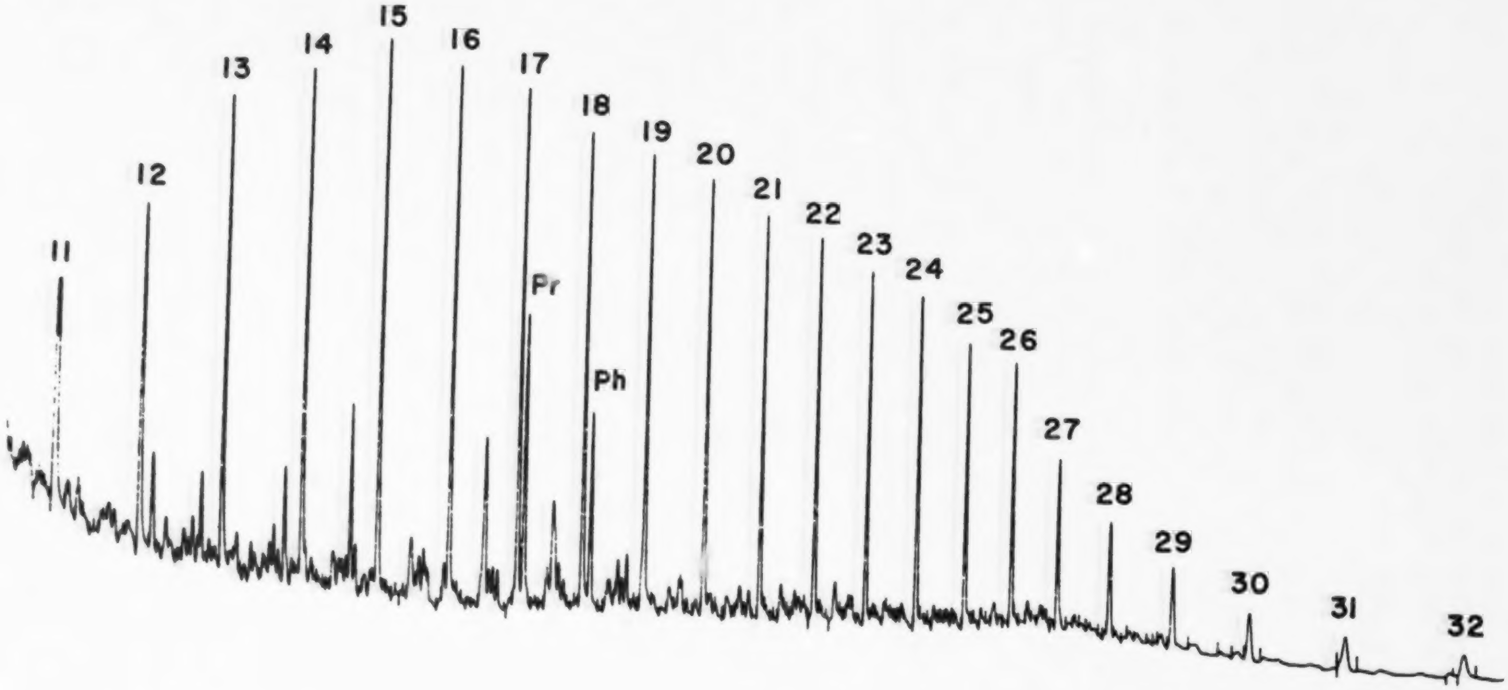

Figure 6.7. Gas chromatogram of the aliphatic fraction of Prudhoe Bay crude oil. The amount of oil was adjusted to give a response similar to that shown in Figure 6.6.

components (< C_{12}). In a natural circumstance where physical, chemical, and biochemical weathering of the oil would occur, the composition of sedimented oil would change significantly with time.

6.4.2 Fraser River Sediments

The oil agglutinization studies conducted with Fraser River suspended matter are summarized in Table 6.5 and Figure 6.8. Both normal sea water and water free of dissolved organic carbon were used in the study. Salinity and temperature in all experiments was 32°/oo and 10°C, respectively. The initial amounts of oil added were varied from 18 to 89 mg, resulting in loading ratios of 0.36 to 1.78 (L_0). Number of replicate experiments is shown in parentheses under column 1 of Table 6.5.

Sedimentation of oil by Fraser River sediments was not linearly proportional to quantity of oil as shown with Skagit River sediments. The maximum loading of 12% was observed at $L_0 = 0.36$ (Fig. 6.8), and decreased uniformly to 7% at higher concentrations of oil. Quantities of sediment recovered also decreased slightly from 67% to 51% of the total added. It was observed visually that much of the oil sediment was floating on the surface of the water and did not settle during the course of the experiment. As more oil was added, the surface slick became larger and accommodated a greater number of the particles.

Suspended sediments derived from the Fraser River were smaller in size (Table 6.3) and mineralogically distinct from sediments taken from the Skagit River (Table 6.2). The median diameter of the Fraser River material was 1.8 μm compared to 2.6 μm in the Skagit River sediment. Mineralogically, Fraser River suspended sediments were relatively rich in clay minerals, with lesser amounts of clastics (i.e., rock fragments, quartz, feldspar) than observed in the Skagit River material (Table 6.2). Thus, the smaller amount of oil sedimented with fine-grained material is provisionally ascribed to mineralogical differences and particle size. A more thorough discussion of these effects and others will be presented below.

Dissolved organic carbon was removed from the sea water to assess its effect on the interaction between oil and sediment. Dissolved organic carbon was removed from sea water by passage through activated charcoal according to a modified procedure of Jeffrey and Hood (1958). Subsequent extraction of the water with methylene chloride indicated that approximately 1.6 mg/ℓ of organic carbon was removed, or about 70% of the original amount. Although present in small amounts, relative to the concentrations of oil used, DOC may be rich in surfactants and thus appreciably influence the behavior of oil with sediments.

The removal of dissolved organic carbon appears to have had little effect, except at the highest initial oil loading (89 mg oil added), on the amount of oil retained on the settled sediments. With an initial oil loading of 1.78, approximately 17% of the sediment weight aggultinated oil. This represents approximately 25% of the oil that was sedimented by Skagit River sediments under the same conditions (Fig. 6.5). Effect of particle size is again clearly evident as approximately 50% of the sediment was recovered in

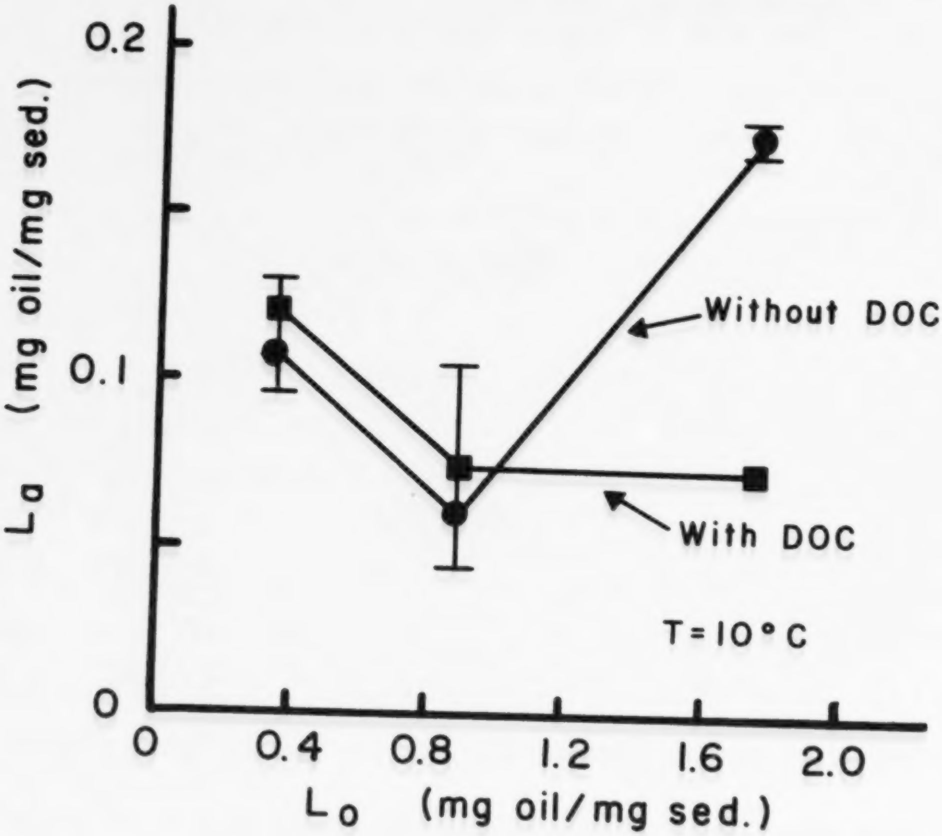

Figure 6.8. Concentration of accommodated Prudhoe Bay crude oil (La) on Fraser River suspended sediments as a function of the initial oil loading (Lo). Experiments were performed in normal Puget Sound sea water (S = $32^{o}/oo$) and in sea water which had 70% of its extractable DOC removed. In each experiment, the concentration of suspended sediments was 83 mg/ℓ.

Table 6.5 Accommodation of Prudhoe Bay crude oil on Fraser River suspended sediments at 10°C and 32°/oo. Comparisons are made between normal sea water and DOC-free sea water. Number of replicate experiments is shown in parentheses under column 1.

Amount Oil Added (mg)	Sediment Recovered Lower Layer (%)	Oil Recovered Lower Layer (%)	Total Oil Recovered (%)	Loading (L_a) $\frac{\text{mg oil}}{\text{mg sed.}}$
		NORMAL SEA WATER		
17.7 (3)	67 ± 4	21 ± 3	46 ± 12	0.12 ± .01
44.4 (3)	60 ± 4	5 ± 2	92 ± 8	.07 ± .03
88.7 (2)	51 ± 10	2 ± 0	92 ± 5	.07 ± .00
		DOC ABSENT		
17.7 (4)	52 ± 1	16 ± 2	57 ± 3	0.11 ± .01
44.4 (1)	56	4	84	.06
88.7 (2)	47 ± 1	5 ± 1	86 ± 13	0.17 ± .00

all three experiments (Table 6.5) compared to more than 80% in the aforementioned experiments (Table 6.4).

The relationship shown between the quantity of oil added and the amount sedimented is subject to further interpretation (Table 6.5). If the single value at L_0 - 0.88 is low, then the provisional interpretation of the plot is that the removal of DOC has the apparent effect of increasing the accommodation of oil on sediment. It appears that the effect is not great, however. An explanation of this phenomenon would be that surfactant compounds present in the DOC fraction have diminished the interfacial energy between mineral particles and oil droplets. Because an oil-in-water emulsion is unstable, the coated particles rapidly coalesce into flocs. These few data only suggest this mechanism.

6.5 DISCUSSION

Clay minerals and quartz sols (presumably other rock forming minerals as well) usually possess a net electrical charge, brought about by charge dislocation or imperfections within the crystal lattice, or "broken bond" surfaces created by the fracture of mineral grains (Van Olphen, 1963). In the latter case, cations or unions may be adsorbed or chemisorbed to the surface to satisfy the electrical imbalance. The net effect is that the mineral grains repulse each other due to their like charges. Counteracting this force is Van der Waal's force which tends to minimize the surface-free energy of the individual particles through particle agglomeration or growth (Castellan, 1964). In an ionic medium, such as sea water, the electrical double layer is compressed, and the particles are said to flocculate under the effect of Van der Waal's forces.

When oil is added to an ionic clay sol, complex behavior of the system is observed and not readily predictable by theory. How the system behaves depends on the specific interactions between the oil and water, oil and particles, and water and particles. In turn, these relationships depend on the composition of the aqueous medium, size and mineralogy of the particles, presence of surfactants, and the composition of the oil.

In an early study by Poirier and Thiel (1941), numerous natural materials (e.g., shale, silt, bentonite, humus soil, etc., to name a few) were selected and evaluated as to their adsorptive behavior toward a typical Mid-Continent crude oil. Selecting deflocculation times of 30 minutes (1 hour in this study), their results show that the oil loadings ranged from 0.6 to 2.2 g oil sedimented for each gram of solid phase added. Kaolin accommodated the largest amount of oil (not at low flocculation times, however), oil shale the least. Fine-grained material (< 125 μ) entrained more oil than coarser material (> 125 μ). This latter result is not necessarily at variance with our own, since the two riverine sediments examined in this report were considerably smaller than 125 μ (see Table 6.3). Entrainment of up to 1 mg oil/mg sediment in our experiments is within the above range, even though amounts of oil (2.2 g) and sediment (1.0 g) used in the aforementioned studies were much larger than in ours.

Poirier and Thiel (1941) also observed that oil shale accommodated oil poorly and attributed this to the presence of organic acids and the larger particle size of the shale. If amphipolar molecules were present in the oil shale, as suggested by Poirier and Thiel, the interfacial tension would have been reduced and the oil would, in effect, coat the surface of the clay particle and assume its shape. This was apparently observed, although the amounts of oil transported downward were less than with other substances tested ($L_a \doteq 0.8$). All of our experiments showed visually that the oil-sediment flocs consisted of attached plates forming a card-house structure. This would imply that surfactants in the oil, or possibly interfacially-active compounds in the oil, were important in the flocculation process.

Bassin and Ichiye (1977) proposed that oil forms colloidal electrolytes with cations in sea water (e.g., Na^+) and is subsequently bonded electrostatically to the surfaces of clay minerals. Although stated somewhat differently, Van Olphen (1963) describes the replacement of double layer cations (e.g., Na^+) with an organic cation, such as an amine salt, thus forming an adsorbed or chemisorbed film of oil. The differences between these two mechanisms appear to us to be subtle and lead to the same effect.

Because these particular mechanisms imply a thin-surface film of oil on the particle, rather than the trapping of oil by settling flocs, Bassin and Ichiye (1977) estimated the loading of oil expected on kaolinites and montmorillonites, assuming a film thickness of 20-50 Å. The amount thus entrained by sediment particles was 0.25 mg oil/mg sediment to 3 mg oil/mg sediment; the range of values agrees rather well with our data. The authors also point to the importance of trapped oil globules in the interstices of the flocs, which will increase the burden of accommodated oil. It remains to be shown that significant concentrations of colloidal electrolytes can be formed from oil in sea water and thus provide a basis for the suggested mechanism.

In a simple system composed of charged particles in an ionic medium, flocculation occurs when the attractive forces exceed the repulsive electrostatic interactions between particles (Van Olphen, 1963). Huang and Elliot (1977) investigated the electrophoretic mobility of several crude oils and inorganic particles (e.g., silica, kaolinite, Al_2O_3, etc.) and all but the aluminum oxide phases were found to be negatively charged at a pH typical of sea water (< 8.5). Zero-point charge of silica and kaolinitic solid phases occurred at pH = 2. Their studies show that the negatively charged particles were transported to the surface of the oil, in spite of the repulsive charges, but amounts of settled oil were apparently small relative to dispersed oil (Huang and Elliot, 1977). The amount of settled oil was only shown for the Cabosil (silica phase) system in which no more than 4% of the original oil was accommodated on the settled fraction. This was an unfortunate choice of solids for our purposes because the particle size of this material was .007 - .014 μm, at least two orders of magnitude smaller than our median particle size. Should no oil have been added to the system, it is unlikely that much of this material would have settled over the duration of the experiment. Cabosil was found to armor the oil particles against coalescence and thus increase the stability of the oil emulsion. We did not observe this predictable phenomenon, since concentrations of solids were not varied. It is interesting to note that in the Cabosil system, approximately 30% of the oil extracted was recovered from a surface slick, to which was presumably attached some of the particles. This was the case with Fraser River sediments in which the finer-grained material was observed attached to the surface slick.

Increasing the concentration of the solids resulted in a destabilization of the emulsion and greater quantities of oil were transported downward with the settling particles. Unfortunately, these quantities were not tabulated, except in the case cited above, and cannot be compared with our observations.

The study of Huang and Elliott (1977) makes a very crucial point. That fact is that negatively charged particles are wet by similarly charged oil droplets, thus the electrostatic repulsive forces are weak relative to other interactions, such as adsorption or chemisorption of surface active compounds. The authors stress the ability of certain solids to collect at the oil-water interface of emulsified droplets and thus inhibit flocculation. However, our results show that natural sediment assemblages rapidly accommodate large amounts of oil (see Table 6.4). When natural sediments of smaller particle size were studied, larger fractions of the sediment were retained in a surface film (Table 6.5).

These studies and many other more specialized reports not included here graphically point to our fundamental lack of understanding concerning the behavior of oil toward natural suspended solids. Further work should stress the specific interactions of components of oil toward natural materials and the mechanics of the adsorption and flocculation processes. Special emphasis is needed on the presence of surfactants in the oil, in the DOC, or in organic matter associated with the solid phases.

6.6 SUMMARY

Laboratory studies were performed to investigate the amounts of oil that might be accommodated by suspended matter from the Skagit and Fraser Rivers. Experiments were conducted in sea water ($S = 32^{\circ}/_{oo}$) at 10° and 15°C with varying amounts of Prudhoe Bay crude oil (9-133 mg) added to 50 mg of sediment. These sediment concentrations are unrealistically high, except for the river estuaries, but represented levels that are analytically tractable and at the same time provide insight into the accommodation levels that might be achieved under ideal conditions.

Skagit River suspended sediments, with a median diameter of 2.6 μm, were the most efficient scavengers of crude oil. At the highest loading of oil attempted (L_o = 2.7 mg oil added/mg sediment added), the loading of accommodated oil was near 1 mg oil/mg sediment, and decreased linearly as the amount of oil was systematically decreased. Increasing the temperature to 15°C resulted in a marked decrease in the amount of oil coprecipitated with the sediment particles. Highest loadings observed at 15°C were 15% of the sediment weight, down from 30% at 10°C.

Fraser River sediments were finer-grained (d_{media} = 1.6 μm) and mineralogically distinct from the Skagit River suspended sediments. The proportion of clay minerals was higher in the former sediments relative to the latter. The highest loading observed was 17%, in the absence of dissolved organic carbon ($T = 10^{\circ}C$), but was more typically 5-10%. The differences between the amounts of oil recovered from the different sediment types are provisionally assigned to differences in particle size and mineralogy. Associated organics may have played a role, but we were not able to assess their significance at this time.

Oil spilled onto the surface of the ocean is immediately affected by several physical, chemical, and biological processes. One of them is the coating of suspended particles and their subsequent suspension in the water column or transport to the bottom where benthic detrital feeders may assimilate them. Our experiments have shown that locally-derived riverine sediments possess the capacity to accommodate up to their own weight in oil under controlled laboratory conditions. What is desired ultimately, however, is an evaluation of the kinetic factors responsible for the coflocculation of oil and suspended matter under natural environmental conditions, such as waves, wind, and suspended matter concentrations. At the same time, a better understanding of the specific interactions between particles of diverse composition and equally complex oil is desired.

7. NATURAL DISTRIBUTIONS OF HYDROCARBONS ON SUSPENDED MATTER

7.1 GENERAL STATEMENT

The occurrence and distribution of petroleum hydrocarbons adsorbed to suspended matter have not been extensively investigated, although there are numerous inferences to the importance of particulate matter in the adsorption and subsequent transport of hydrophobic pollutants (see section 6.1). An excellent review of the literature on this topic is contained in an article by Clark and MacLeod (1977) and a report by the National Academy of Science (1975).

In a very recent study by Van Vleet and Quinn (1977), the importance of suspended solids in the transport of petroleum hydrocarbons discharged from a waste treatment plant was emphasized. Their study showed that approximately 95% of the hydrocarbons discharged were in the particulate form, the remainder as solubles. Because fulvic and humic materials are known to incorporate hydrocarbons, either through interlatice absorption or surface adsorption (Ogner and Schnitzer, 1970), the aforementioned authors found that only 20% of the suspended hydrocarbons were associated with these fractions.

The Strait of Juan de Fuca, San Juan Island passages, and the Strait of Georgia represent contiguous commercial waterways over which significant quantities of petroleum and refined products are transported. Puget Sound and, in particular, the San Juan Archipelago represent major recreational areas, enjoyed by many small boat enthusiasts. Moreover, these waters are in direct communication with the major ports of Washington and British Columbia and, consequently, receive discharged waste materials and pollutants. Sources of pollutants include transfer operations, wastewater discharge, spillage (accidental or otherwise), and riverine input.

Because of the likely sources of petroleum and related materials in the waters of Northern Puget Sound, a complementary study was formulated to investigate the character of hydrocarbons associated with suspended matter and thus elucidate their probable origin. This section focuses on the seasonal distribution of hydrocarbons adsorbed to suspended matter, compositional characteristics, and probable sources.

Suspended matter consists of both living and dead material. It is primarily composed of inorganic detrital mineral phases derived from river and stream runoff; terrestrial plant material; living planktonic organisms, including phytoplankton, zooplankton, and bacteria; and marine organic detritus such as fecal matter and the tests of dead organisms. These components are largely natural in origin and are supplemented by a wide compositional range of particles of anthropogenic origin. Some of these would include plastics, wood fibers, styrofoam, inorganic particles arising from industrial activities, and weathered petroleum residues (i.e., tar balls). Tar balls are a rather common artifact in waters used as major transportation routes and their occurrence in the Strait of Juan de Fuca would not be unexpected.

7.2 FIELD STUDIES

In an attempt to ascertain the distribution and abundance of adsorbed petroleum-related hydrocarbons, four stations were strategically located near probable or anomalous source areas; the fifth station, near Port Angeles (sta. 9) was chosen for control. The station near Admiralty Inlet (sta. 35) was occupied in order to characterize material derived from Puget Sound. Stations were also located near Deception Pass (sta. 15), Cherry Point (sta. 17), and the southern arm of the Fraser River (sta. 26) in order to characterize possible inputs from these sources. Waters passing through Deception Pass carry a portion of the suspended load derived from the Skagit River. Although this river is not heavily industrialized, modest levels of agriculture are carried out in the lower aluvial basin of the river. Cherry Point and nearby Ferndale are the loci of major oil refineries in Washington, and thus, represent sites for probable oil input. Lastly, the station near the Fraser River estuary was selected to assess hydrocarbon levels associated with a major industrialized river complex, although substantial agriculture also is carried out in the lower river basin.

Attempts were made to occupy each of these stations seasonally, although weather was sometimes a factor. This was particularly true for stations 9 and 35, located in the westerly fetch of the Strait of Juan de Fuca. Station 31A, occupied only once in Harrow Strait (MESA-I), was abandoned because of its close proximity to major shipping lanes and intense tidal currents which hampered anchoring of the vessel. In place of this location, station 35 in the eastern Strait of Juan de Fuca was chosen as an alternate (see above).

Suspended matter was retrieved from preselected depths at each station, depending on the location of the near-surface suspended matter concentration maximum. This was determined every four hours with a continuous profiling nephelometer (see section 5) and the depth of the pump head adjusted accordingly. The suspended material was pumped from depth and passed through a Sorvall^R SS-3 continuous flow centrifuge in a manner described earlier (see section 6.3.4).

7.3 METHODOLOGY

7.3.1 Sample Collection

Suspended matter was sedimented in a continuous flow centrifuge operated at approximately 15,000 r.p.m. or 30,000 G's. Flow rate was maintained between 400 and 500 mℓ min^{-1}. Filtration of the effluent through 0.4 μm Nuclepore^R membrane filters indicated that more than 90% of the mass of the material greater than 0.4 μm was recovered during centrifugation. As described earlier (section 6.3.4), small organic particles are probably lost due to their low specific gravity.

The centrifuge was operated continuously for the sampling period, except in the case of mechanical failure. Prior to actual sample collection, water was pumped (12 gal min^{-1}) through the hose and prefiltration manifold for one hour to reduce contamination arising from the pump, hose, manifold, and tubing.

Suspended matter was collected in eight stainless steel centrifuge tubes which, prior to use, were cleaned in methylene chloride and hexane. All centrifuge parts in contact with the sample were cleaned in a similar fashion.

At the termination of sampling, the contents of the sampling tubes were quantitatively transferred to precleaned jars fitted with an aluminum-foil lined cap. The sample was immediately frozen at -20°C until analysis.

7.3.2 Sample Preparation and Analysis

The sample, usually between 1 and 5 g dry weight, was placed in a 50 mℓ centrifuge tube and the hydrocarbons extracted according to the original procedure of MacLeod et al. (1976). In this procedure, a 35% methyl alcohol/methylene chloride mixture was used instead of diethyl ether to extract the lipid fraction. Extractions were carried out on a tumbler at room temperature for 18 hours, solvent decanted, and the extraction repeated for an additional 18 hours. The extracts were combined and the remaining sediment dried and weighed. Aliphatic and aromatic fractions were separated on silica gel as described in the aforementioned reference.

The component analyses of the aliphatic and arene fractions were carried out on wall-coated glass capillary columns (30 m x 0.25 mm i.d.) treated with SE-30. The G.C. analysis of the aromatic hydrocarbons was performed by NNAF under the supervision of Dr. William MacLeod. Also, both alkane and aromatic standards were provided to us by NNAF. Component composition of the aliphatic and aromatic standards is shown in Table 7.1 with typical chromatograms of the alkane standard (ALK-9) and the arene standard (PAH-6) presented in Figures 7.1a,b. Reagent and procedural blanks were determined for all runs.

The concentration of each component in the mixture is calculated from its response factor as determined from daily calibration and normalized to the response of the internal standard, hexamethylbenzene. Component identification is based on retention indices, again normalized to the internal standard.

Replicate injections of standards show component precision to be no better than ± 20%. However, errors associated with extraction efficiencies due to matrix effects may be much larger (Rohrbach and Reed, 1975). We have not performed an intercomparison of various extraction techniques on suspended matter, although because of its large compositional variability, matrix effects could be severe.

Table 7.1 Component listing and concentrations for aliphatic standard (ALK-9) and arene standard (PAH-6)

Alkane Standard (ALK-9)		Arene Standard (PAH-6)	
Component	Conc. ng/μℓ	Component	Conc. ng/μℓ
C_{12}	15.6	Indane	11.1
C_{13}	10.3	1,2,3,4-Tetramethybenzene (TMB)	10.6
C_{14}	11.3	Naphthalene (NPH)	10.3
Hexamethyl-benzene	9.8	Benzothiophene (BTP)	12.8
C_{15}	10.4	2-Methylnaphthalene (2MN)	13.1
C_{16}	30.0	1-Methylnaphthalene (1MN)	12.1
C_{17}	11.1	Triisopropylbenzene (TPB)	9.0
Pristane	10.2	Biphenyl (BPH)	13.8
C_{18}	9.5	2,6-Dimethylnaphthalene (DMN)	11.0
Phytane	8.8	Hexamethylbenzene (I.S.)	10.1
1-Cl-C_{16}	11.6	2,3,5-Trimethylnaphthalene (TMN)	10.0
C_{19}	10.4	Fluorene (FLU)	10.5
C_{20}	14.6	Dibenzothiothiophene (DBT)	14.8
C_{21}	10.4	Phenanthrene (PHN)	11.1
C_{22}	10.3	Anthracene (ANT)	9.4
C_{23}	10.6	1-Methylphenanthrene (MPH)	10.2
C_{24}	9.9	Fluoranthene (FLA)	11.8
C_{25}	21.4	Pyrene (PYR)	9.9
C_{26}	10.4	Benz[a]anthracene (BAA)	12.4
C_{27}	10.5	Chrysene (CHR)	9.5
C_{28}	10.6	Benz[e]pyrene (BEP)	10.0
C_{29}	10.2	Benz[a]pyrene (BAP)	12.1
C_{30}	10.0	Perylene (PER)	10.2
C_{31}	10.8		
C_{32}	9.9		

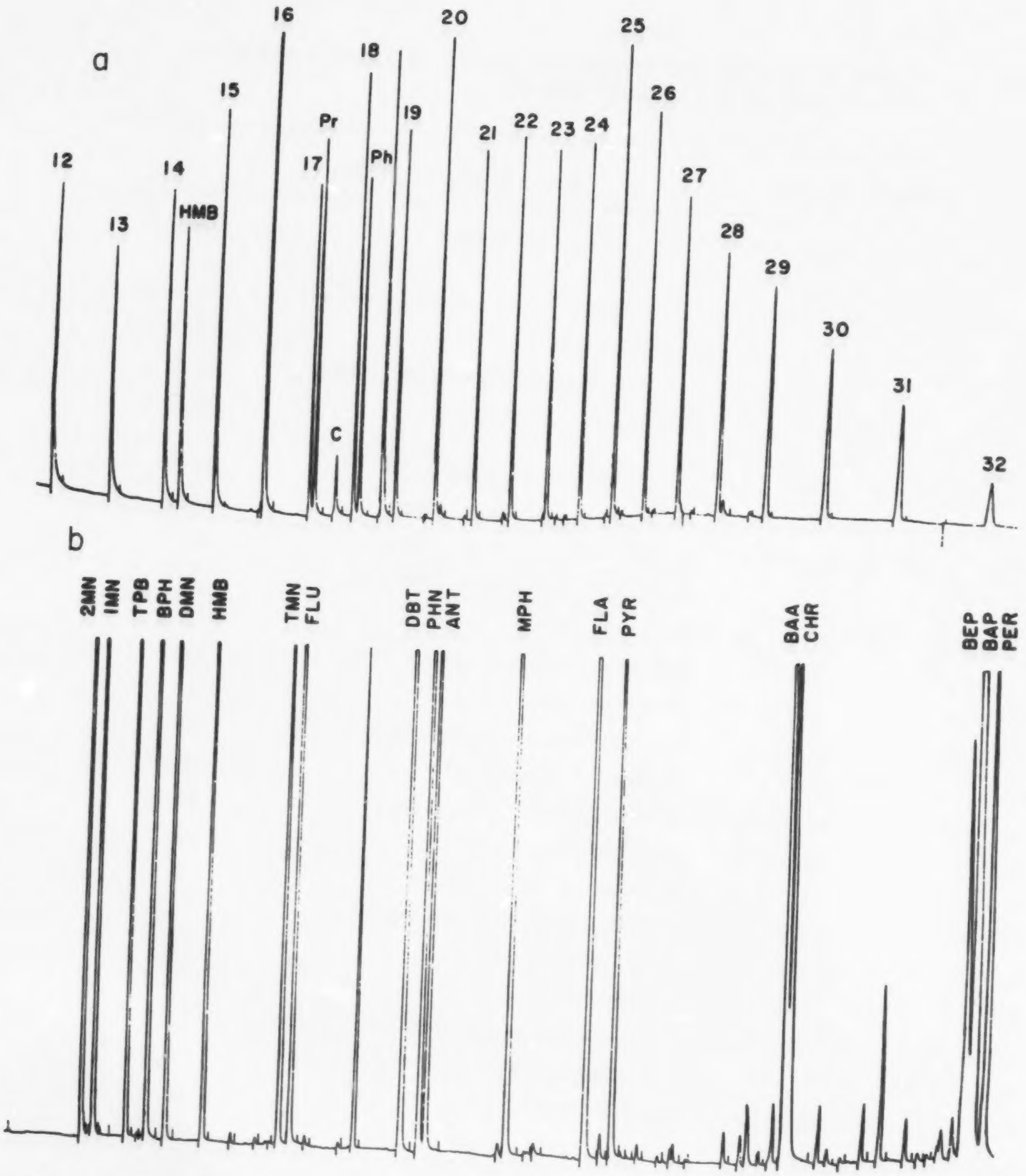

Figure 7.1 Chromatograms of the (a) alkane standard (ALK-9) and (b) the arene standard (PAH-6). Abbreviations for aromatic compounds are shown in Table 7.1. Hexamethylbenze (HMB) was used as the internal standard.

7.4 RESULTS

7.4.1 Field Sampling

A summary of the suspended matter samples collected for hydrocarbon analysis during the three MESA cruises is presented in Table 7.2. Of the five stations originally scheduled, one station was lost during each cruise. With the exception of station 26 during the MESA-II cruise, all others were lost due to inclement weather. During MESA-III, the normal time series at station 9 was moved into Freshwater Bay (sta. 10B), west of Port Angeles, because of poor sea conditions (see Fig. 5.1).

It is readily apparent from Table 7.2 that on the average only small amounts of suspended material were recovered in most instances. The low recovery of sediment resulted in reduced sensitivity; in fact, some chromatograms were not distinguishable from the solvent and procedural blanks. A case in point was station 10B, occupied during MESA-III, in which only .08 g of material was obtained (Table 7.2). Time spent on each station varied from 17 hours to 24 hours, resulting in 282 ℓ to over 700 ℓ of water passed through the centrifuge.

7.4.2 Suspended Hydrocarbons - MESA I

Four time series stations were successfully occupied during this cruise as depicted in Table 7.2. Station 9, located in the central strait, was not occupied because of high winds and seas. Dry weight recoveries of suspended material ranged from 0.90 g to 4.69 g, the latter amount recovered from station 26 near the mouth of the Fraser River.

Extractable hydrocarbons recovered from all the samples acquired during this cruise reflected unusual, but similar compositional patterns, not observed on subsequent cruises. All samples taken during this cruise were recovered and extracted in the same fashion as were other samples, except they were freeze dried. Subsequent check of our freeze drier indicated no interference at the levels suggested in the gas chromatograms.

Rather than treat each station individually, since the results may be a sampling or an analytical artifact, we will discuss the results obtained at station 15 as representative and for the sake of completeness.

The chromatographic signature of the aliphatic fraction is shown in Figure 7.2. The dominant characteristic of the chromatogram is the presence of an unresolved complex mixture centered near heneicosane, extending from C_{17} to C_{24}. Specific characteristics of the UCM include a slight dominance of odd-numbered n-alkanes, pristane/phytane ratio near 0.5, and a heptadecane/pristane ratio of 1.2. The most abundant straight chain paraffins, tentatively identified on the basis of retention times, were nonadecane and heneicosane, although isoprenoid hydrocarbons of similar carbon length also are likely candidates. Identification of individual contributions to the UCM was not undertaken, but it was suggested that the UCM may be composed of unsaturated hydrocarbons, presumably biological in origin (personal communication, Dr. D. Brown, NNAF).

TABLE 7.2 Sampling protocol for suspended hydrocarbons at each of the time series stations. Volume of water is the quantity passing through the centrifuge as determined by a cumulative flow meter. Amount of material recovered is expressed in grams dry weight.

MESA-I

	Stations				
	9	15	17	26	31A
Date	N.S.[1]	11/18/77	11/19/77	11/21/76	11/22/76
Time on Station, hours		17.5	20.0	17.5	23.6
Nominal Pump Depth, meters		8	25	2.5	3
Volume of Water, liters		568	600	525	708
Amount of Material, grams		2.26	0.90	4.69	1.65

MESA-II

	Stations				
	9	15	17	26	35
Date	3/11/77	3/12/77	3/14/77	N.S.[1]	3/15/77
Time on Station, hours	22.5	22.5	22.0		22.0
Nominal Pump Depth, meters	18	18	18		10
Volume of Water, liters	673	693	741		690
Amount of Material, grams	0.47	1.00	1.24		0.67

MESA-III

	Stations				
	10B	15	17	26	35
Date	8/9/77	8/10/77	8/11/17	8/13/77	N.S.[1]
Time on Station, hours	18.5	17.3	21	17.8	
Nominal Pump Depth, meters	10	10	12	15	
Volume of Water, liters	282	349	478	511	
Amount of Material, grams	.08	0.49	1.27	1.79	

[1] No sample taken.

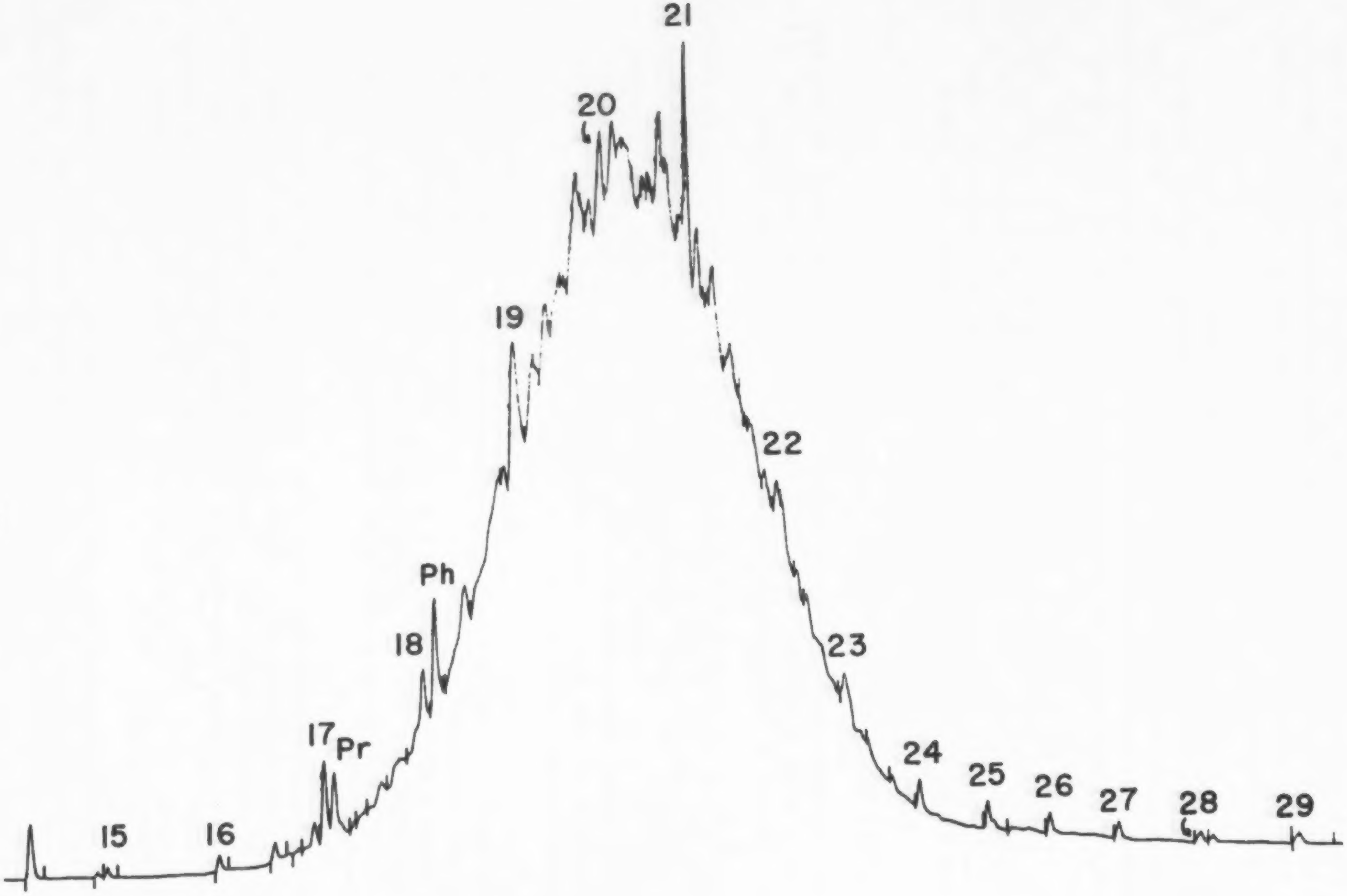

Figure 7.2 Gas chromatogram of the saturated hydrocarbon fraction from station 15. The numbers reflect the chain length of the normal alkanes.

A GC analysis of the aromatic fraction revealed few major compounds; none were identifiable on the basis of retention indices. A UCM was present, but not as large as that observed in the saturate fraction. When compared to standards, the bulk of the components were characterized by retention indices similar to that of 3- and 4-ring aromatics.

Without further corroborating evidence, these observations do not clearly identify the source of the hydrocarbons. However, several compositional features are evident. The abundance of n-alkanes in the carbon range C_{17}-C_{24}, modest odd-even dominance of normal paraffins, and the apparent presence of olefinic hydrocarbons, all suggest the hydrocarbons are of biogenic origin (Clark and Brown, 1977). Subsequent discussions with Dr. T. Reed of UCLA suggested that the complexity of compounds observed in this rather small carbon range indicate bacterial metabolism of the organic matter. While this may be a viable explanation, it remains unclear why samples from this cruise only show the unusual hydrocarbon pattern. The absence of paraffinic compounds in the range of C_{21}-C_{32} indicates no significant input from either plant waxes or weathered petroleum residues.

7.4.3 Suspended Hydrocarbons - MESA II

Stations occupied and amounts of suspended material recovered during the spring cruise are reflected in Table 7.3. Quantities of suspended matter retrieved were generally small, ranging from 0.47 g to 1.24 d dry weight.

The quantity of hydrocarbons recovered varied widely, depending on location and probable sources (Table 7.3). Hydrocarbon concentration was greatest at station 9 (nearly 790 μg/g) and a minimum at station 17 near Cherry Point (approximately 170 μg/g). Amounts of hydrocarbons obtained do not correlate with suspended matter concentrations, but appear to be regionally dependent. With the exception of station 15, the concentrations of saturates and unsaturates were nearly equal (Table 7.3).

Chromatographic analysis of the aliphatic fraction obtained from station 9 is shown in Figure 7.3a and the concentrations of individual normal alkanes are indicated in Table 7.4. Significant concentrations of normal paraffins were observed in the C_{27} to C_{32} range and may represent weathered petroleum residues or possibly terrestrial plant waxes. With the exception of pentadecane, no significant contribution of hydrocarbons from plankton were observed.

Minimum detection limits for individual hydrocarbons are indicated by concentration "less than" and were computed on the basis of sample blanks and quantity of sediment recovered. The average response factor for the normal alkanes (C_{12}-C_{32}) only decreases about 10% over the range; thus the minimum detection limits shown in Table 7.4 have been computed on the basis of a mean response factor, corrected for daily variation using the internal standard hexamethylbenzene.

As shown in both Figure 7.3a and Table 7.4, the most abundant alkanes were in the carbon range C_{25} to C_{32}. The most abundant paraffin was hentriacontane; its concentration was approximately 2 μg/g. Inspection of Table 7.4

TABLE 7.3 Concentrations of saturated and unsaturated hydrocarbons at stations sampled.

Cruise / Station	Sample Weight (g)	Saturates (μg/g)	Unsaturates (μg/g)
MESA I			
9	-	-	-
15	1.13	1858	371
17	0.90	4556	764
26	4.69	541	96
31A	1.65	5289	752
MESA II			
9	0.47	356	453
15	1.00	233	87
17	1.24	75	99
26	-	-	-
35	0.67	164	198
MESA III			
10B	.08	900	510
15	0.49	178	307
17	1.27	42	161
26	1.79	236	82
35	-	-	-

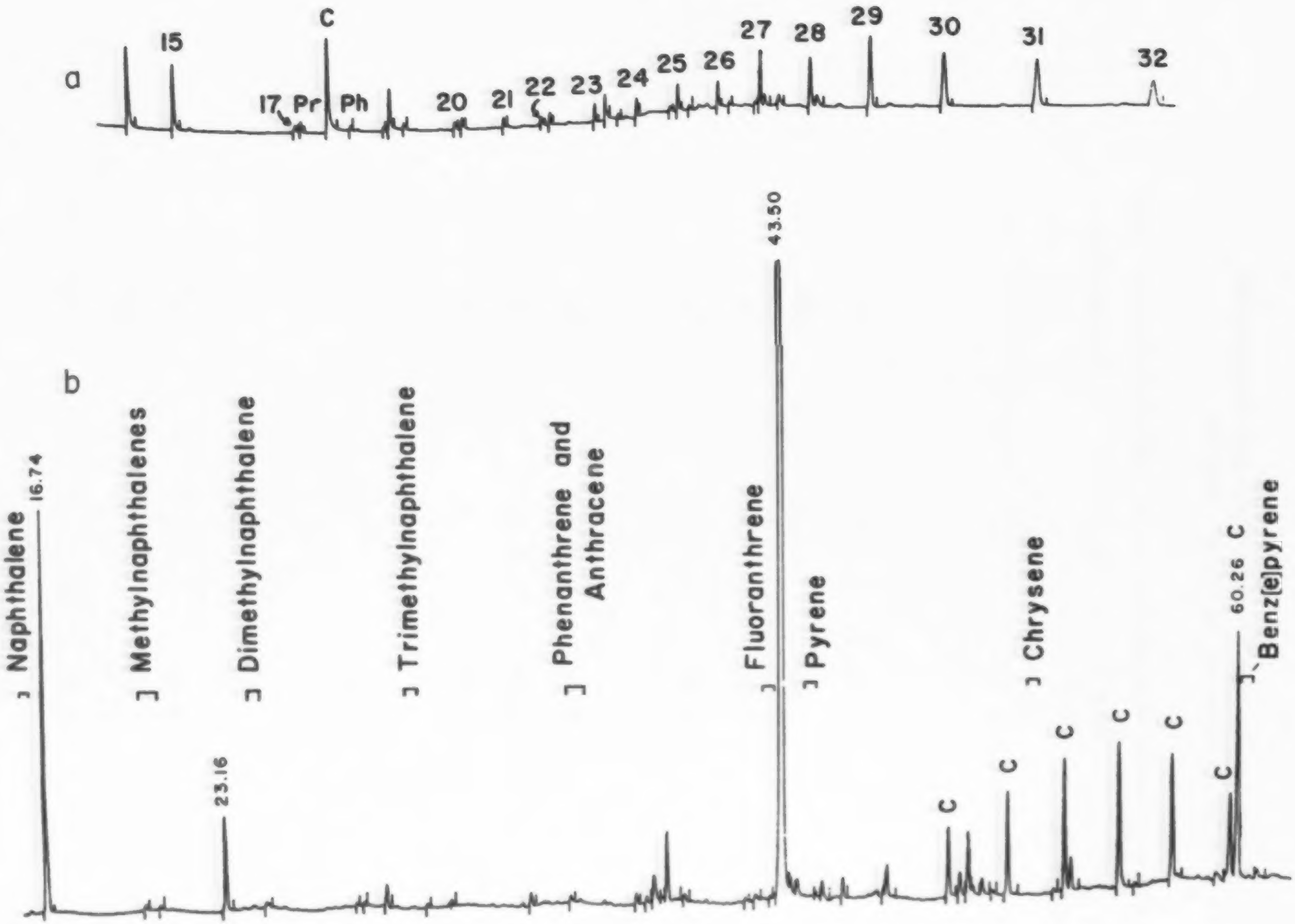

Figure 7.3 Gas chromatograms of the (a) saturated and (b) unsaturated fraction from station 9 located near Port Angeles (MESA-II). Normal alkanes are indicated by carbon chain length; peaks labeled "C" are known contaminants. Retention time windows of typical arenes are shown for reference purposes.

TABLE 7.4 Concentrations of normal alkanes and the isoprenoid hydrocarbons pristane and phytane at stations occupied during MESA-II.

Normal Alkanes	Station 9	Station 15	Station 17	Station 35
		(ng/g dry weight)		
C_{12}	< 50	< 26	< 18	< 28
C_{13}	↓	↓	↓	↓
C_{14}	↓	↓	↓	↓
C_{15}	1104	159	104	127
C_{16}	< 50	< 26	< 18	< 28
C_{17}	< 50	53	↓	< 28
Pristane	95	28	↓	82
C_{18}	< 50	< 26	↓	< 28
Phytane	↓	↓	↓	< 28
C_{19}	↓	↓	↓	32
C_{20}	57	↓	↓	36
C_{21}	< 50	↓	25	175
C_{22}	↓	↓	< 18	160
C_{23}	↓	↓	48	306
C_{24}	66	↓	25	378
C_{25}	128	41	57	456
C_{26}	123	< 26	33	412
C_{27}	298	↓	59	292
C_{28}	808	↓	110	238
C_{29}	1842	235	317	413
C_{30}	1860	110	282	274
C_{31}	2017	190	359	400
C_{32}	1215	< 26	144	< 28

reveals a slight odd-even preference in the above carbon range, but probably is not significant. We would interpret the character of the hydrocarbons to imply weathered petroleum or related products such as tar balls. Given the transportation activity in the Strait of Juan de Fuca, it is likely that tar balls would have been sampled along with the normal suspended detritus. By way of comparison, a much stronger odd-even preference is shown at the other stations sampled (Table 7.4), implying that a much larger fraction of the hydrocarbons obtained at these stations were derived from plant waxes (Ogner and Schnitzer, 1970).

We have also compared these results with those of MacLeod et al. (1976) taken from both contaminated and uncontaminated beach sediments near Port Angeles. The abundance of individual alkanes observed at station 9 are rather similar to the levels observed in contaminated intertidal sediments, but the most abundant alkane was C_{31} rather than C_{27} noted in the previous reference. Also, the contaminated sediments were characterized by normal paraffins generally found in the kerosene and light oil fraction of petroleum (Clark and Brown, 1977) and a large UCM centered near C_{28}. Neither of these features were present in the suspended matter analysis, but the quantity of sediment extracted was only 0.47 g, compared to 100 g of intertidal sediments analyzed (MacLeod et al., 1976).

The relatively high concentration of normal alkanes, characteristic of the heavy distillate oil fraction, may be due to the inclusion of tar balls. If this is so, then the reporting basis of the individual hydrocarbon shown in Table 7.4 is incorrect.

The unsaturated fraction is shown in Figure 7.3b. None of the major peaks were identifiable on the basis of retention indices; however, representative compounds are shown for reference purposes. The identity of the major peak occurring at 43.50 min. is unknown, but by comparative analogy with extracts of copepods and other zooplankton (Shaw, 1977), we would tentatively identify the compound as 3,6,9,12,15,18-heneicosahexaene (HEH), a polyolefin. This compound is also the most dominant hydrocarbon in 18 species of phytoplankton studied (Blummer et al., 1971), thus its occurrence in a sample containing plankton is not unexpected. We stress that this assignment is primarily based on its ubiquity in planktonic organisms and on its relative retention indices. It occurred in the aromatic fraction of all samples. Mass spectral analysis is needed to establish the structure of this compound. The peaks labeled "C" are contaminants, probably alkanes, and are believed to have leached out of the caps of the storage vials. They were observed in a few samples and also in several standards, but were not present in the procedural blanks.

A chromatographic trace of the aliphatic fraction from station 17 is shown in Figure 7.4a and the concentrations of the normal paraffins are given in Table 7.4. Of the biological hydrocarbons, only pentadecane (C_{15}) was significantly above the background levels. Its concentration was approximately 160 ng/g. Heptadecane and pristane, the isoprenoid C_{17} hydrocarbon, were also present in concentrations near the background levels. The most abundant paraffins present were nonacosane, triacontane and hentriacontane (C_{29}-C_{31}), not unlike that observed at the other stations sampled (Table 7.4). However, their

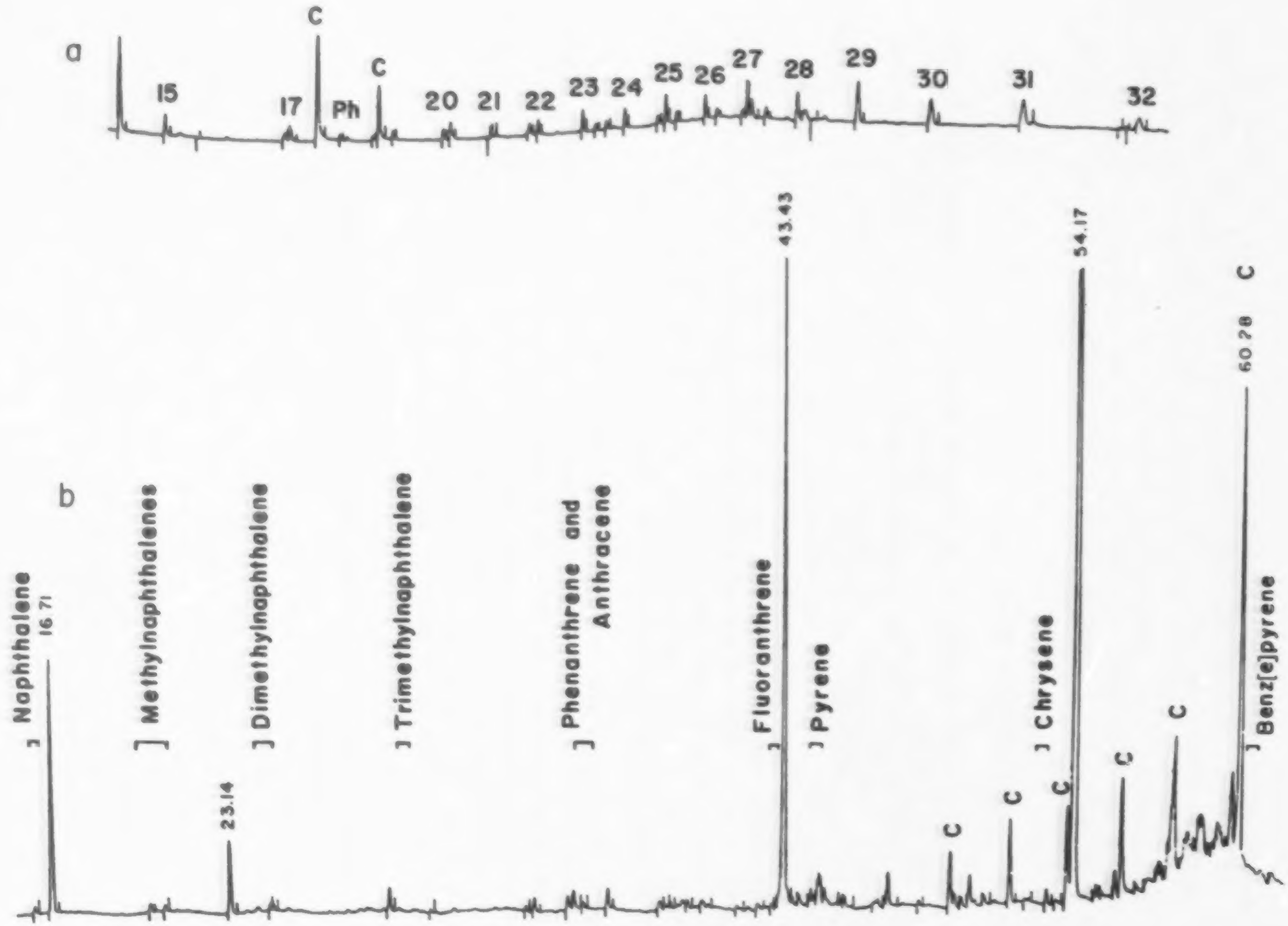

Figure 7.4 Gas chromatograms of the (a) saturated and (b) unsaturated fractions from station 17 located near Cherry Point (MESA-II). Normal alkanes are indicated by carbon chain length; peaks labeled "C" are known contaminants. Retention time windows of typical arenes are shown for reference purposes.

concentrations were approximately a factor of 10 less and indicated a much stronger odd-even preference. Both nonacosane (C_{29}) and triacontane (C_{31}) were present at concentrations near 200 ng/g.

The chromatogram of the aromatic fraction from station 17 is shown in Figure 7.4b. It was not unlike that obtained at station 9 with the exception of the major peak at retention indices 54.17 min. We assume that this is another biogenic component, but it is unclassified at this time. A UCM was observed in this chromatogram, part of which may be the result of contamination. No evidence of fresh petroleum was found in the aliphatic fraction, although the high molecular weight aromatics associated with oil may be more resistant to degradation.

7.4.4 Suspended Hydrocarbons - MESA III

Stations occupied and amounts of suspended material recovered during the summer cruise are presented in Table 7.2. Amounts of suspended material were generally small, reflecting the continuing drought conditions which accented the normally small runoff at this season of the year (see section 2). At station 10B, in Freshwater Bay, only 80 mg of material was recovered, although the concentrations of the saturates and unsaturates were relatively large (900 and 510 μg/g, respectively). As expected the largest quantity of suspended sediment recovered was from station 26, near the mouth of the Fraser River. However, the concentration of hydrocarbon was rather typical (see Table 7.3). Rather than discuss each station in detail, we will, as before, select stations 17 and 26 as representative, although the pertinent compositional data for the other stations will be shown in Tables 7.3 and 7.5.

The saturated hydrocarbon composition of suspended matter collected at station 17 is depicted in Figure 7.5a and Table 7.5. The most abundant hydrocarbons present were pentadecane (582 ng/g) and pristane (2069 ng/g) with lesser amounts of heptadecane and nonadecane. These particular components are most certainly of biological origin (Blumer et al., 1971), presumably derived from plankton. With the exception of a small amount of heptacosane (C_{27}), the remaining normal paraffins were near or below the minimum detection level of 30 ng/g.

A chromatographic analysis of the aromatic fraction is shown in Figure 7.5b. It is somewhat more complex than those shown previously but does reflect the major peak at retention indices 43.55 min. In addition, a suit of compounds is observed between retention indices 37-40 min., which falls between the retention indices of anthracene and methyphenanthrene. The identity of these compounds is unknown, but may represent biologically-derived olefinic hydrocarbons. Their source is most likely marine (i.e., plankton) rather than terrestrial because of the location of the station. There is also a remote possibility that the unsaturated compounds are of terrestrial origin, possibly suspended matter from the Fraser River, but it seems to us that marine organic matter would be dominant at this time of the year.

The absence of a complex aromatic spectra (e.g., alkyl naphthalenes; Hites and Biemann, 1972) and the absence of a smooth alkane envelope between

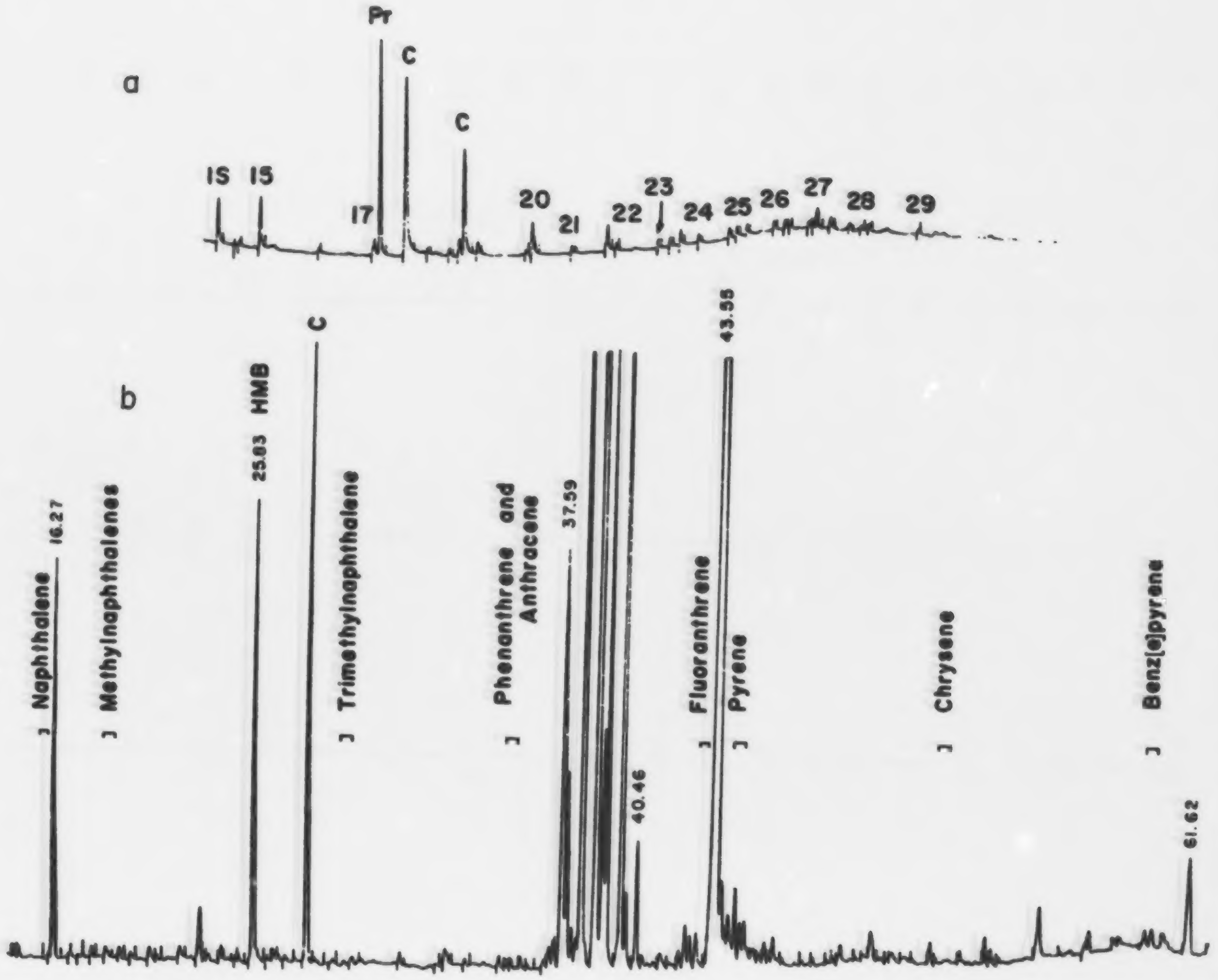

Figure 7.5 Gas chromatograms of the (a) saturated and (b) unsaturated fractions from station 17 located near Cherry Point (MESA-III). Normal alkanes are indicated by carbon chain length; peaks labeled "C" are known contaminants. Retention time windows of typical arenes are shown for reference purposes.

TABLE 7.5 Concentrations of normal alkanes and the isoprenoid hydrocarbons pristane and phytane at stations occupied during MESA-III.

Normal Alkanes	Station 10A	Station 15	Station 17	Station 26
		(ng/g dry weight)		
C_{12}	< 248	< 43	< 30	< 10
C_{13}	↓	↓	↓	< 10
C_{14}	↓	↓	↓	47
C_{15}	3183	282	582	3897
C_{16}	< 248	< 43	< 30	58
C_{17}	↓	243	152	257
Pr	↓	556	2069	911
C_{18}	851	68	< 30	64
Ph	< 248	< 43	< 30	221
C_{19}	< 248	↓	76	1032
C_{20}	544	↓	< 30	88
C_{21}	< 248	↓	↓	144
C_{22}	↓	↓	↓	209
C_{23}	↓	↓	↓	386
C_{24}	↓	↓	↓	536
C_{25}	↓	↓	↓	703
C_{26}	↓	68	↓	736
C_{27}	↓	86	95	752
C_{28}	↓	202	< 30	486
C_{29}	↓	499	↓	383
C_{30}	↓	508	↓	164
C_{31}	↓	756	↓	141
C_{32}	< 248	553	< 30	< 10

C_{15}-C_{26} (Farrington and Quinn, 1973) would suggest minimal hydrocarbon contribution from petroleum or related products.

The suspended hydrocarbon composition of the n-alkane fraction taken at station 26 is shown in Figure 7.6a. Individual compound concentrations are presented in Table 7.5. Several interesting features are present in the chromatogram (e.g., Figure 7.6a), including an abundance of odd carbon hydrocarbons in the range C_{15} to C_{20} and a smooth carbon envelope between C_{21} and C_{30}. The abundance of peaks between pristane and nonadecane are presumably planktonically derived hydrocarbons, including isoprenoids and phytadienes. As we have observed before (e.g., station 10B, Table 7.5), pentadecane was the most abundant hydrocarbon in the lighter fraction (carbon no. < 21). In a related study of the hydrocarbon composition of select species of phytoplankton, Blumer et al. (1971) found 3,6,9,12,15,18-heneicosahexaene ($C_{21:6}$) the predominant hydrocarbon produced by marine phytoplankton with lesser amounts of the normal alkanes in the range C_{12} to C_{25}. The dominant normal alkanes were pentadecane, heptadecane, and heneicosane, with the latter two compounds more universally present in the species studied. The assemblage of compounds between octadecane and eicosane presumably represents saturated and unsaturated isoprenoids derived from zooplankton (Blumer et al., 1971).

The heavier alkanes present in the sample show a uniform envelope beginning at heneicosane and ending at triacontane. The most abundant normal paraffins in the suite are pentacosane (C_{25}), hexacosane (C_{26}), and heptacosane (C_{27}); their concentrations are in excess of 700 ng/g. There is no odd-even preference. The origin of these hydrocarbons is not known, but the chromatographic pattern is similar to those observed for lubricating oils (Farrington and Quinn, 1973). Similar patterns have been observed in the Charles River, Boston (Hites and Biemann, 1972) and in recent bottom sediments obtained near the Fields Point waste treatment plant located on the Providence River (Van Vleet and Quinn, 1977). It has also been suggested that terrestrial plant material may contribute normal alkanes in the carbon range, although the odd-even preference is usually present (Ogner and Schnitzer, 1970). The ratio of odd carbon to even carbon in the range C_{22} to C_{32} is 1.11, nearly the same as that found by the above authors. Because the Fraser River is obviously supplying terrigenous plant material to the estuary and also is likely to be impacted by petroleum spillage, wastewater and industrial effluents as it passes through the metropolitan area of Vancouver, it seems likely that the source of hydrocarbons characterized in Figure 7.6a is not unequivocal. Additional studies are warranted to unravel the composition of suspended hydrocarbons in the Fraser River and to pinpoint their sources.

The aromatic fraction is depicted in Figure 7.6b. The large peak near fluoranthrene (RT = 43.50 min) is again evident together with a similar cluster of peaks between retention indices 37.50 and 40.0 min. The grouping and clustering of these compounds suggest that they are related genetically and are probably biological in origin. Because this particular sample appears to have both terrestrial and marine biogenic hydrocarbons (see Figure 7.6a), the origin of these hydrocarbons is not precisely definable. Within the above definition of biogenic hydrocarbons, we also include hydrocarbons resulting from microbial metabolism of organic detritus.

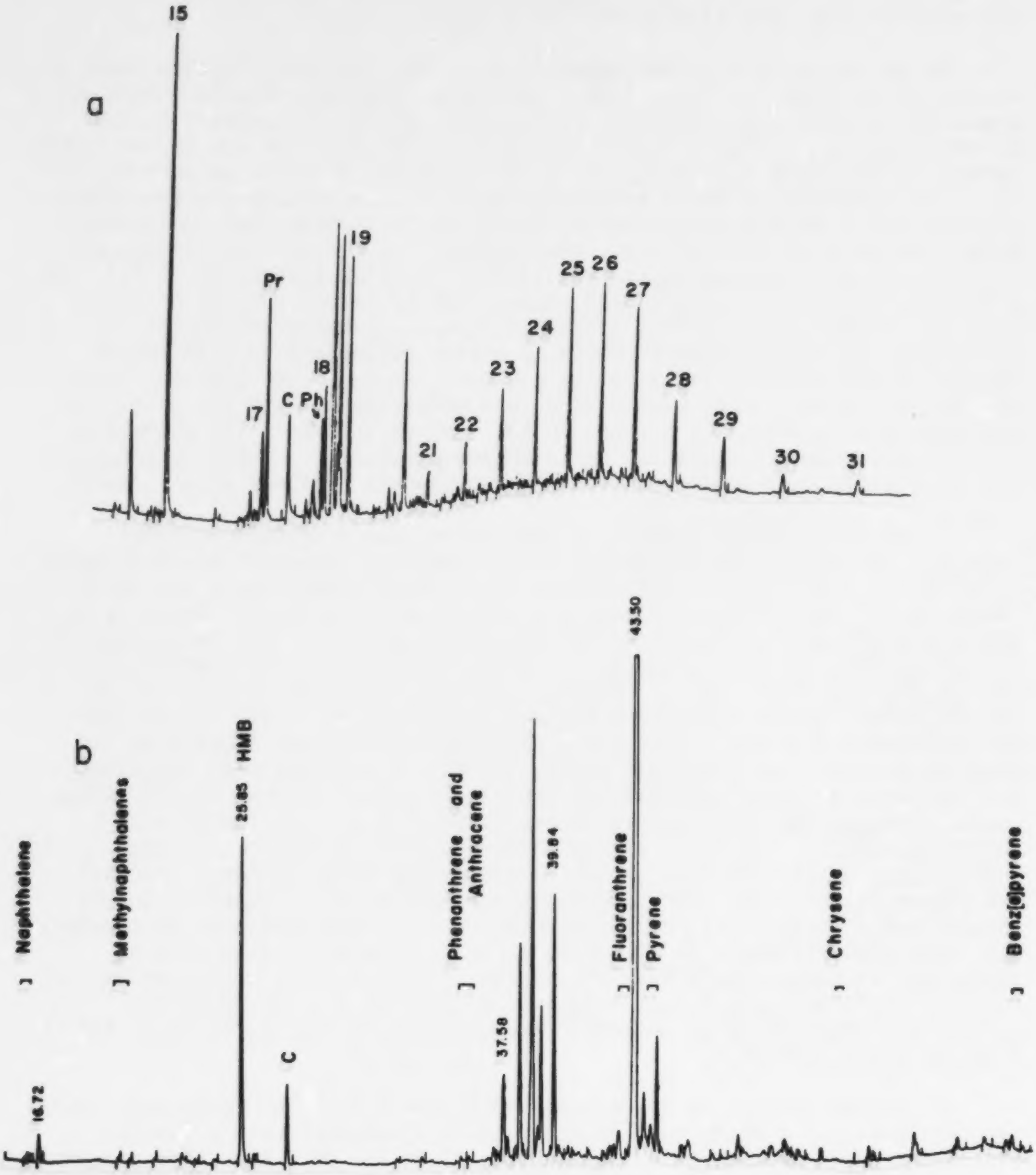

Figure 7.6 Gas chromatograms of the (a) saturated and (b) unsaturated fractions from station 26 located near the mouth of the Fraser River (MESA-III). Normal alkanes are indicated by carbon chain length; peaks labeled "C" are known contaminants. Retention time windows of typical arenes are shown for reference purposes.

The myriad of small, poorly defined peaks shown in Figure 7.6b represent aromatics and olefins present in the sample. Procedural blanks did not show the complexity of compounds evident in Figure 7.6b. The origin of these compounds is unknown, but conceivably could represent a low level input from petroleum or related products. Without further characterization, however, the origin of these compounds cannot be defined. The absence of a well-defined UCM does not suggest necessarily that petroleum hydrocarbons were absent. Analysis of the unsaturate fraction of Prudhoe Bay crude oil, using glass capillary columns, also did not reveal a UCM that might otherwise have been observed if packed columns had been used.

7.5 DISCUSSION

The purpose of this portion of the study was to evaluate the present levels of particulate hydrocarbons in northern Puget Sound and to characterize them compositionally. Five stations were identified for seasonal observations on the basis of current or future probable impact by petroleum. Since it has been shown that locally derived riverine sediments possess the capacity to accommodate crude oil (see section 6) and that this material subsequently may be used as a food source by detrital, suspension, and benthic feeders, it is important that an assessment of suspended hydrocarbons be conducted.

Based on this rather preliminary assessment, we would conclude that, at present, suspended matter in the eastern Strait of Juan de Fuca, San Juan Island passages, and the southern Strait of Georgia is minimally impacted by petroleum hydrocarbons. Recent studies conducted in Narragansett Bay and the Providence River estuary show both the suspended matter and the receiving bottom sediments to be contaminated by petroleum hydrocarbons, presumably arising from wastewater treatment facilities (Farrington and Quinn, 1973; Van Vleet and Quinn, 1977; Schultz and Quinn, 1977). Depending on the location in the estuary, the total hydrocarbon concentration ranged from 24 mg/g dry weight material to minimum values less than 1 mg/g dry weight material. The upper values are believed to be the result of effluent loading, whereas the smaller values are more representative of the relatively uncontaminated lower estuary (Schultz and Quinn, 1977). The highest values measured in this work were from stations 17 and 31 (MESA-I), where concentrations in excess of 6 mg/g dry weight were observed (Table 7.3). However, as previously stated, these data are suspect, and more typical values are 1 mg/g dry weight or less (Table 7.3).

In the previous studies cited above, chromatographic analysis of the alkane fraction derived from both suspended matter and bottom sediments showed a strong UCM centered near C_{26}. No such pattern was observed in any of our samples with the possible exception of station 26 (MESA-III). This may be an analytical artifact because we used glass capillary columns or because the HC component loadings were too small to result in peak overlap, or both. Suspended matter samples taken in the Strait of Juan de Fuca (station 9 and station 35, MESA-II) did show the possible presence of weathered petroleum residues (i.e., tar balls), but this remains speculation at this time (see Table 7.4).

We have also compared our results with the findings of an intertidal sediment study carried out by MacLeod et al. (1976) in the Port Angeles harbor and Dungeness Bay. The former area was known to be contaminated by petroleum; the latter was considered pristine. The concentration of total HC (saturated plus unsaturated) at the harbor intertidal site ranged from 1.5 mg/g dry weight to less than 0.2 mg/g dry weight, whereas the site in Dungeness Bay was characterized by HC concentrations uniformly less than .05 mg/g dry weight. Thus, the relative difference is important, not the absolute concentration. Although not reported, the intertidal beach sediments are presumably lower in carbon than the suspended matter in the overlying water. Thus, on a weight basis, it would be expected that the concentration of biogenic hydrocarbons would be greater in the suspended matter. Compositionally, the alkane fraction chromatograms we obtained at all study sites more nearly resemble those obtained by MacLeod et al. (1976) for the Dungeness Bay sediments (i.e., clean) as compared to the complex hydrocarbon composition observed for Port Angeles Harbor.

We also attempted to compare the hydrocarbon distributions and patterns obtained in this study with the comprehensive work currently being conducted by Dr. Shaw of IMS, Alaska on the Alaskan OCS. However, differences in methdology and the myriad of environments present in the nearshore areas of Alaska have prevented a direct comparison. Also, Dr. Shaw has not performed a systematic study of HC associated with suspended matter, but rather has focused his research efforts on biota and intertidal sediments. In general, the concentrations of aliphatics and aromatics in nearshore and intertidal sediments was less than 30 μg/g wet weight sediment (Shaw, 1977). Although the composition and abundance of the hydrocarbons are related to the organic carbon concentration, which was not given, the aforementioned hydrocarbon concentrations are considerably lower than that observed in Dungeness Bay by MacLeod et al. (1976). This is not surprising in view of the small input levels of natural hydrocarbons (e.g., lower primary productivity) and the equally small anthropogenic contribution.

In Table 7.6 is shown the ratio of hydrocarbons to particulate organic carbon. It is readily apparent that the hydrocarbons represent no more than 3% of the total organic carbon (station 15, MESA-III), but more typically less than 1%. A study of the HC/OC ratio in sediments derived from the Providence River estuary showed this ratio to vary longitudinally down the estuary (.07 to .02) as well as vertically in the sediment column (Van Vleet and Quinn, 1977). At their station 4, located most distant from the Fields Point waste treatment facility, the HC/OC ratio decreased from .024 at the surface (0-10 cm) to .0014 at depth (30-40 cm). These figures are in rather close agreement with the data shown in Table 7.6 and would suggest that contamination of suspended matter by petroleum hydrocarbons is minimal.

The relatively high organic carbon content of the suspended matter and the low C/N ratio both suggest that the carbon is of marine origin (Banse, 1974). This contention would support our findings that the major identifiable hydrocarbons in the alkane fraction below C_{21} are biogenic in origin, presumably arising from phytoplankton and zooplankton. Above C_{21} the normal paraffins are either the result of petroleum residues or plant waxes, or a mixture

TABLE 7.6 Summary of hydrocarbon concentrations, organic carbon, carbon: nitrogen ratios, and the ratio of extractable hydrocarbons to organic carbon at selected stations.

Station	Hydrocarbon Conc.[a] mg/g	Organic Carbon[b] %	C/N[c]	HC/OC
		MESA-I		
15	2.2	8.2	8.4	.026
		MESA-II		
9	0.79	6.9	6.7	.01
17	0.17	3.3	8.8	.005
		MESA-III		
17	0.20	9.1	8.1	.002
26	0.32	3.4	7.0	.009

[a] Total concentration of saturated and unsaturated hydrocarbons taken from Table 7.3.

[b] Percent organic carbon as dry weight.

[c] Organic carbon:nitrogen weight ratio.

thereof. Based on these few preliminary results, it is not possible to establish levels of petroleum hydrocarbons associated with suspended matter.

7.6 SUMMARY

During 1976 and 1977, a seasonal investigation was initiated to evaluate the ambient levels of suspended hydrocarbons with special emphasis on hydrocarbons of petroleum origin. For this work, five strategic locations were examined in the eastern Strait of Juan de Fuca, San Juan Island passages, and the southern Strait of Georgia. Sampling sites included the entrance to Puget Sound (Admiralty Inlet), Deception Pass, Cherry Point, the mouth of the Fraser River, and a central point in the Strait of Juan de Fuca near Port Angeles. Suspended matter was recovered with a continuous flow centrifuge and extracted for total hydrocarbons.

Of the samples taken, only gas chromatographic analysis of hydrocarbon extracts showed a predominance of biological compounds (e.g., pentadecane, heptadecane, pristane, etc.), including higher molecular weight alkanes believed to be of plant origin. In two samples, the presence of petroleum hydrocarbons was implied, not conclusively shown. Suspended matter taken from the Strait of Juan de Fuca was characteristically high in normal paraffins in the carbon range C_{25}-C_{32}, which may be plant waxes or weathered petroleum residues. The dominant alkane was hentriacontane (C_{31}); its concentration approximately 2 μg/g dry weight sediment.

Material collected from the mouth of the Fraser River contained abundant amounts of both biological hydrocarbons and a heavier fraction that chromatographically appears to be similar to motor oil (C_{22}-C_{32}). In this range, the most abundant normal paraffin was pentacosane (0.7 μg/g dry weight). Again, this particular fraction of the aliphatic hydrocarbons may represent a contribution from plant waxes.

The total amount of extractable hydrocarbons varied from 0.2 mg/g dry weight to 1.4 mg/g dry weight. These concentrations fall between those observed in pristine Alaskan shelf sediments and those observed in the Providence River-Narragansett Bay estuary system. On the basis of these few data and the limited sample size (0.5-5 g dry weight), we were not able to unequivocally define the presence of petroleum hydrocarbons, although a few samples were suggestive. Larger suspended matter samples are required with attention given to definitive marker compounds in both the aliphatic and aromatic fractions. Systematic studies of point sources would be highly beneficial in defining the fate of oil in natural systems as well as their characterization as a function of time and space.

8. LANDSAT IMAGERY

8.1 INTRODUCTION

It is evident from the discussions in the previous sections of this report that suspended sediments, originating from the Fraser and Skagit Rivers, can play a major role in the dispersal and deposition of some fractions of petroleum that may be released as a result of oil transportation through the Strait of Georgia-Strait of Juan de Fuca system. Consequently, a comprehensive understanding of the dispersal mechanisms and trajectories of suspended sediments from these rivers is essential to any model which attempts to predict the fates and potential impacts of oil in these waters. The suspended matter distribution studies, which have been described elsewhere in this report and represent the first comprehensive survey of its kind in the study region, provide useful data on the seasonal variations of particulate distributions. However, due to the physical limitations of operating from a single vessel the data are not entirely synoptic and must be integrated over several tidal cycles. In order to obtain truly synoptic information other forms of data must be obtained.

In recent years several advances in remote sensing techniques have provided scientists with the ability to collect synoptic information about water circulation and sediment dispersal patterns which heretofore have been unobtainable. The multispectral scanner images from the LANDSAT-1 and LANDSAT-2 satellites have been especially useful for the study of suspended matter transport processes in coastal and estuarine waters (Kritkos et al., 1974; Klemas et al., 1974; Gatto, 1976; and Johnson et al., 1977).

Table 8.1 shows the major characteristics of the LANDSAT satellites and multispectral scanner. The multispectral scanner has four spectral bands. The green band (0.5-0.6 μm) and the red band (0.6-0.7 μm) provide information about the dispersal patterns of suspended matter from major source regions such as rivers, streams, and coastal outfalls. The far red band (0.7-0.8 μm) only shows the core of the sediment plume and the near infrared band (0.8-1.1 μm) shows the shoreline. The data from the multispectral scanner is transmitted to a receiving station and then is converted to a photographic product.

In order to provide synoptic information about variations of suspended sediment distributions, water trajectories, and tidal mixing patterns, all usable LANDSAT imagery from 1972 to the present were collected and correlated with corresponding data on water and sediment discharge (U.S. Geological Survey and Water Survey of Canada), water circulation (appropriate published literature as cited), tides and tidal currents (Tide Tables, National Ocean Survey), and suspended sediment distributions (this report). LANDSAT MSS bands 4 and 5 were found to be ideal for studying the dispersal of turbid water. The sediment plumes, which appear lighter in tone than less turbid water in the images, are natural tracers of the low salinity water that exists offshore from the Fraser and Skagit estuaries. However, the LANDSAT imagery only provides information about the upper few meters of the water column. Fortunately, previous studies have shown that the brackish water is

TABLE 8.1 Principal characteristics of the LANDSAT satellite and multispectral scanner

System Parameters	Specific Specifications
Satellite	
Altitude	915 km
Type of Orbit	circular, sun synchronous
Orbits per Day	14
Coverage Cycle	18 days
Time of Observation	approx. 1000 a.m. at 50° north latitude
Size of Area Imaged	185 x 185 km
Field of View	11.56°
Side Lap	67%
Overlap Along Orbit	10%
Multispectral Scanner	
Image Distortion	2%
Ground Resolution	80 to 120 meters
Position Accuracy	900 meters
Spectral Bands, Bandwidths (μm), and Nominal Color	4: 0.5-0.6; green 5: 0.6-0.7; red 6: 0.7-0.8; far red 7: 0.8-1.1; near infrared

generally confined to the upper 5 meters or less (Waldichuk, 1957; Tabata, 1972; and Schumacher et al., 1978), and therefore, the LANDSAT imagery can be used to study the migration patterns of the low salinity water provided the sediment loading is sufficiently higher than the surrounding water.

8.2 SEASONAL VARIATIONS

The amount of useful information about seasonal variations of suspended sediment distributions and dispersal patterns that can be obtained from LANDSAT imagery is somewhat limited because most cloud-free days occur during the summer; and, as a result, the majority of available images are from that season. However, two high quality images* from January 1973 (Figs. 8.1 and 8.2) and one from March 1976 (Fig. 8.3) are available. Therefore, some general statements about sediment dispersal patterns for winter, spring, and summer can be made.

When the fresh water and sediment discharge from the Fraser River are high, particularly during the spring floods and during the ebbing tide, the longitudinal pressure head at the river mouth produces a well-defined turbid plume which extends outward into the Stait of Georgia. The orientation of the plume axis can be used to determine the direction of flow. During the months of May through August, the southward flow of Main Arm and Middle Arm is so strong that the resultant plume maintains its identity for a considerable distance and, in some cases, traverses the entire length of the Strait. Figures 8.4, 8.6, and 8.9 are examples of this phenomenon. Depending upon local changes in tidal currents, the plumes extend either to the southeast or southwest from the river mouth. Tidal mixing is rapid and numerous eddies are apparent.

At the mouths of Middle Arm and North Arm there was some evidence of flow to the northwest in most of the images. This feature is particularly evident in Figures 8.6 and 8.7. These plumes appear to maintain their identity as far north as Point Grey and the entrance to Burrard Inlet.

The Skagit River plume flows into Skagit Bay and Saratoga Passage during the summer months (Figs. 8.4 thru 8.9). Some plume material passes through Deception Pass into Rosario Strait during ebb tide (Fig. 8.8).

The winter plumes from the Fraser and Skagit Rivers, as shown in the LANDSAT images from January 1973 and March 1976 (Figs. 8.1 thru 8.3), are much less distinct than that observed during summer. For instance, the Fraser River plumes in January and March are only visible in the nearshore regions just a few kilometers seaward of the river mouth, where the primary flow pattern is to the southeast. During this period, the discharge of both water and suspended sediments are at a minimum. Average discharge rates for water and

---

*Specific characteristics of the images are uniquely identified in the figures by numbered markers and are described both in the text and in the figure captions.

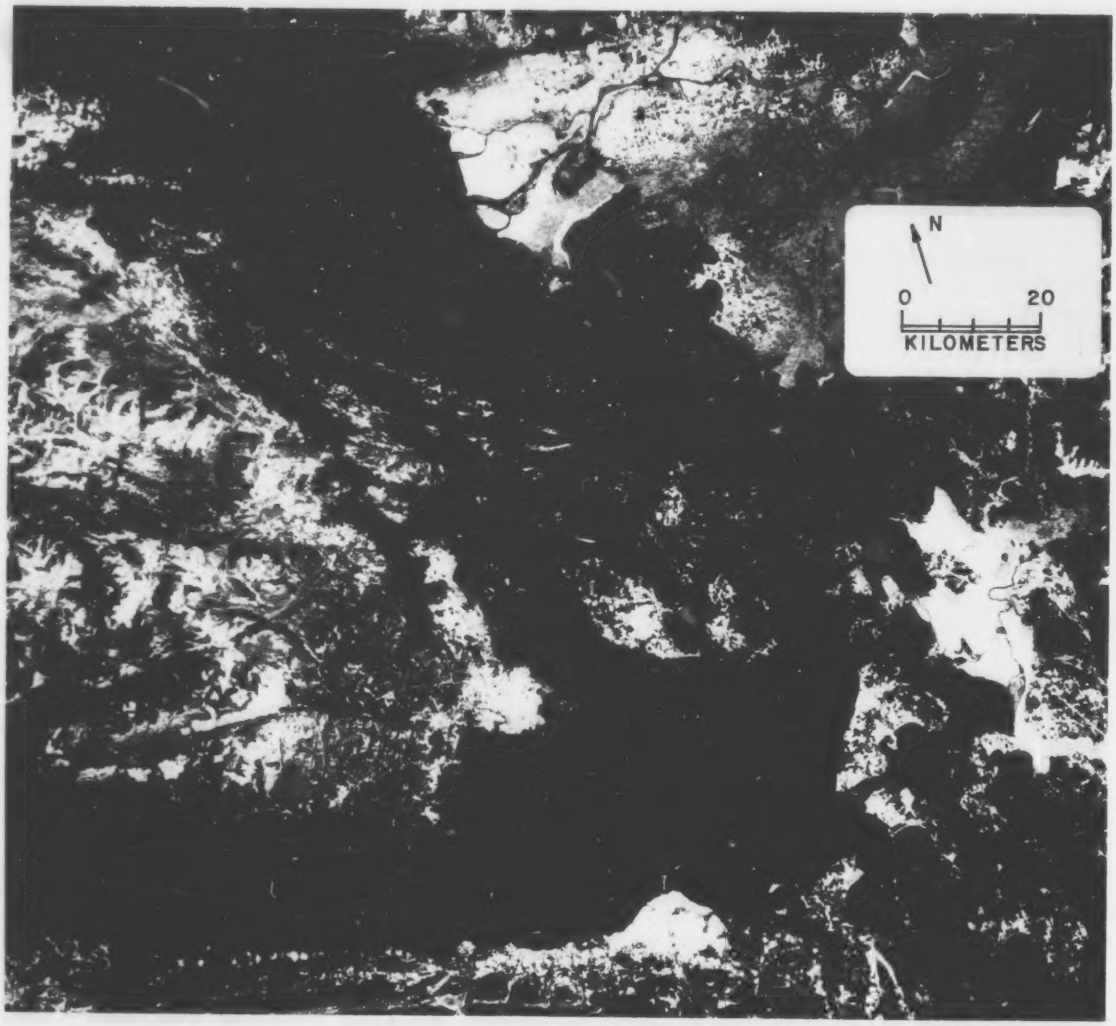

Fig. 8.1 MSS Band 5 of LANDSAT image 1169-18373 on Jan. 8, 1973 between slack water and minor ebb current. Time of image acquisition was 1037 PST. The image shows little evidence of sediment dispersal from the Fraser River into the Strait of Georgia, reflecting the lower water and sediment discharge during the winter season. The image is free of cloud cover.

TIDAL CURRENT:	Slack Water	Max. Current	Vel. (kts)	TIDES:	Time	Ht.(m)
		0515	1.7		High at 0834	2.9
	0906	1209	1.7		Low at 1429	1.6

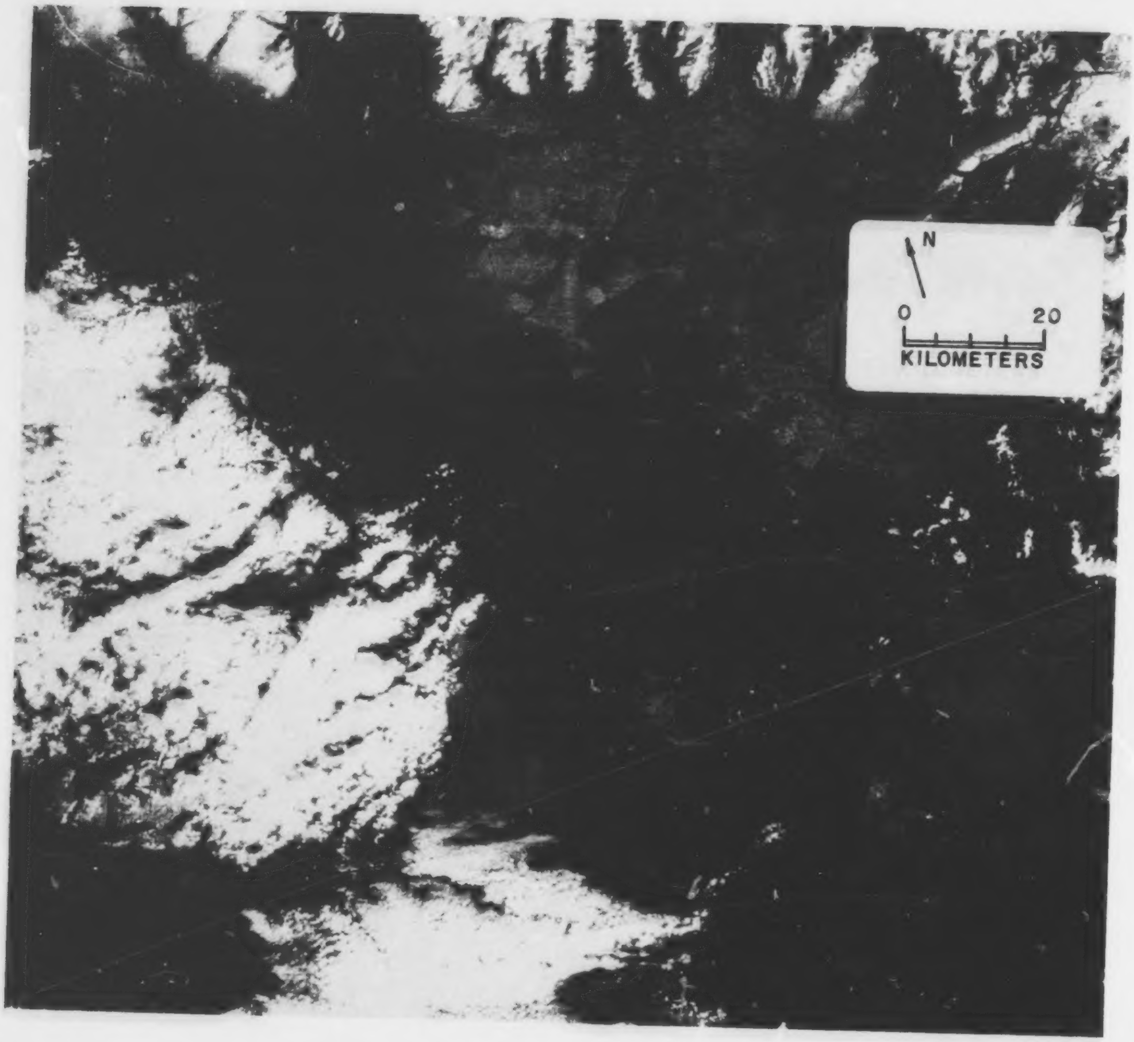

Fig. 8.2 MSS Band 5 of LANDSAT image 1187-18374 on Jan. 26, 1973. Time of image acquisition was 1037 PST, between slack water and major ebb current. The image shows limited dispersal of suspended sediments into the Strait of Georgia from the Fraser River.

TIDAL CURRENT:

Slack Water	Max. Current	Vel. (kts)
0508	0733	0.9
1008	1501	2.3

TIDES:

Time	Ht.(m)
High at 0905	2.6
Low at 1811	0.4

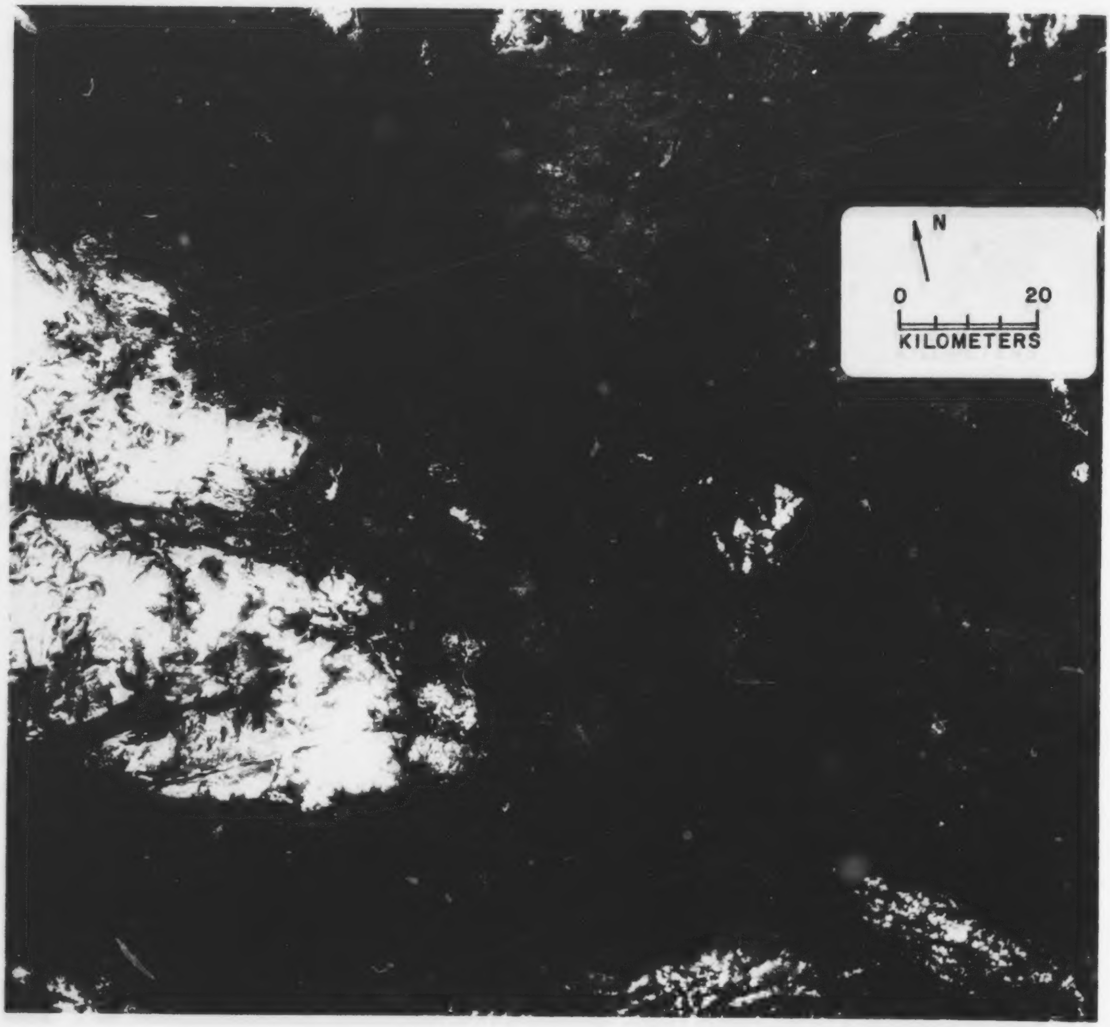

Fig. 8.3 MSS Band 4 of LANDSAT image 2417-18220 on Mar. 14, 1976. Time of image acquisition was 1022 PST, between minor ebb current and slack water. The image shows limited dispersal of suspended sediments into the nearshore waters south and southeast of the mouths of Main, Middle and North Arms.

TIDAL CURRENT:	Slack Water	Max. Current	Vel. (kts)	TIDES:	Time	Ht. (m)
	0454	0806	1.8		Low at 0808	0.8
	1150	1322	0.8		High at 1402	1.9

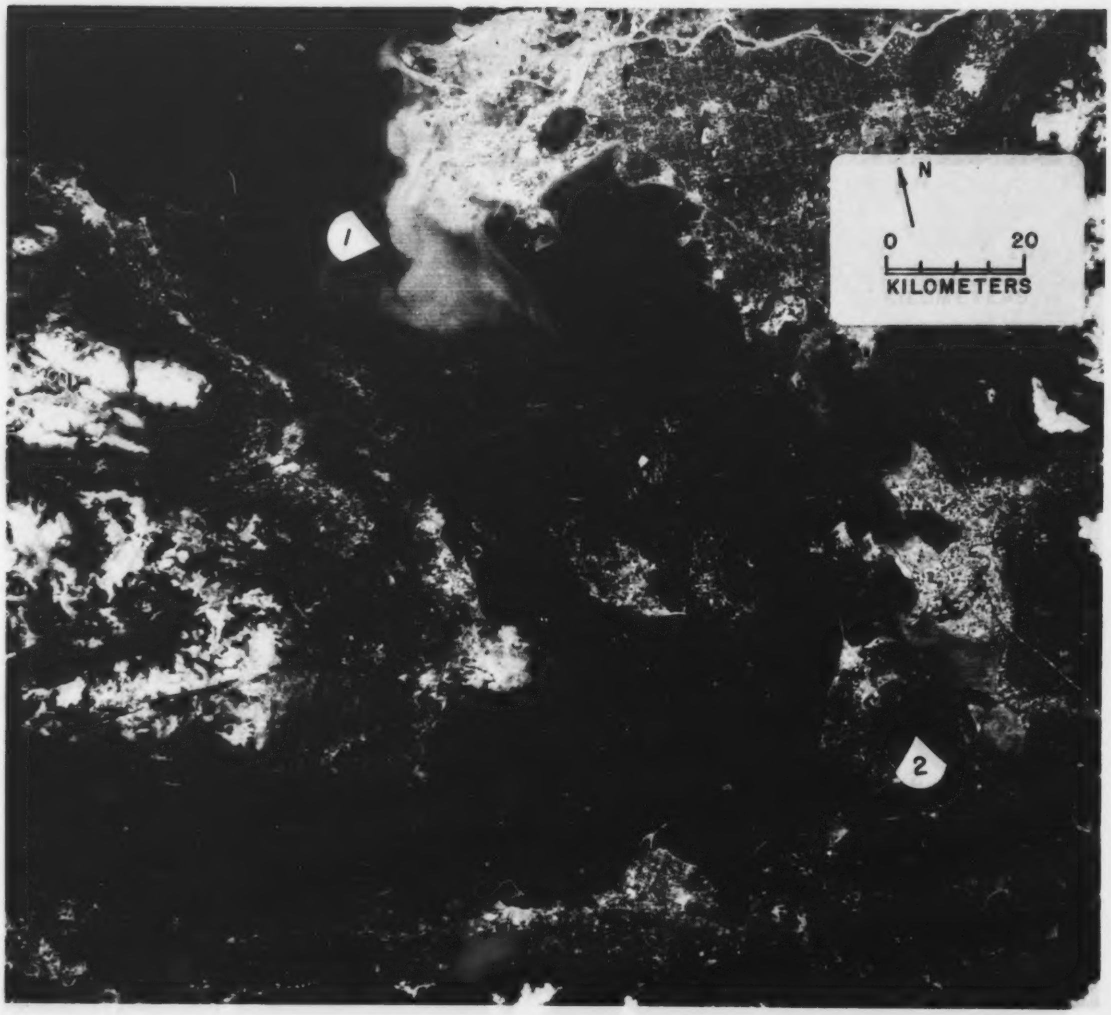

Fig. 8.4 MSS Band 5 of LANDSAT image 2111-18254 showing a southeasterly dispersal (1) of suspended sediments from the Fraser River into the Strait of Georgia on May 13, 1975. Time of image acquisition was 1025 PST, between major ebb current and slack water. The dispersal pattern shows movement of Fraser River sediments into Haro Strait, primarily through Boundary Pass. Sediment discharge from the Skagit River into Skagit Bay and Saratoga Passage is evident (2). 10% cloud cover is observed in the lower right corner of image.

TIDAL CURRENT:	Slack Water	Max. Current	Vel. (kts)	TIDES:	Time	Ht.(m)
	0506	1000	2.9		High at 0449	2.4
	1404	1643	2.4		Low at 1246	-0.5

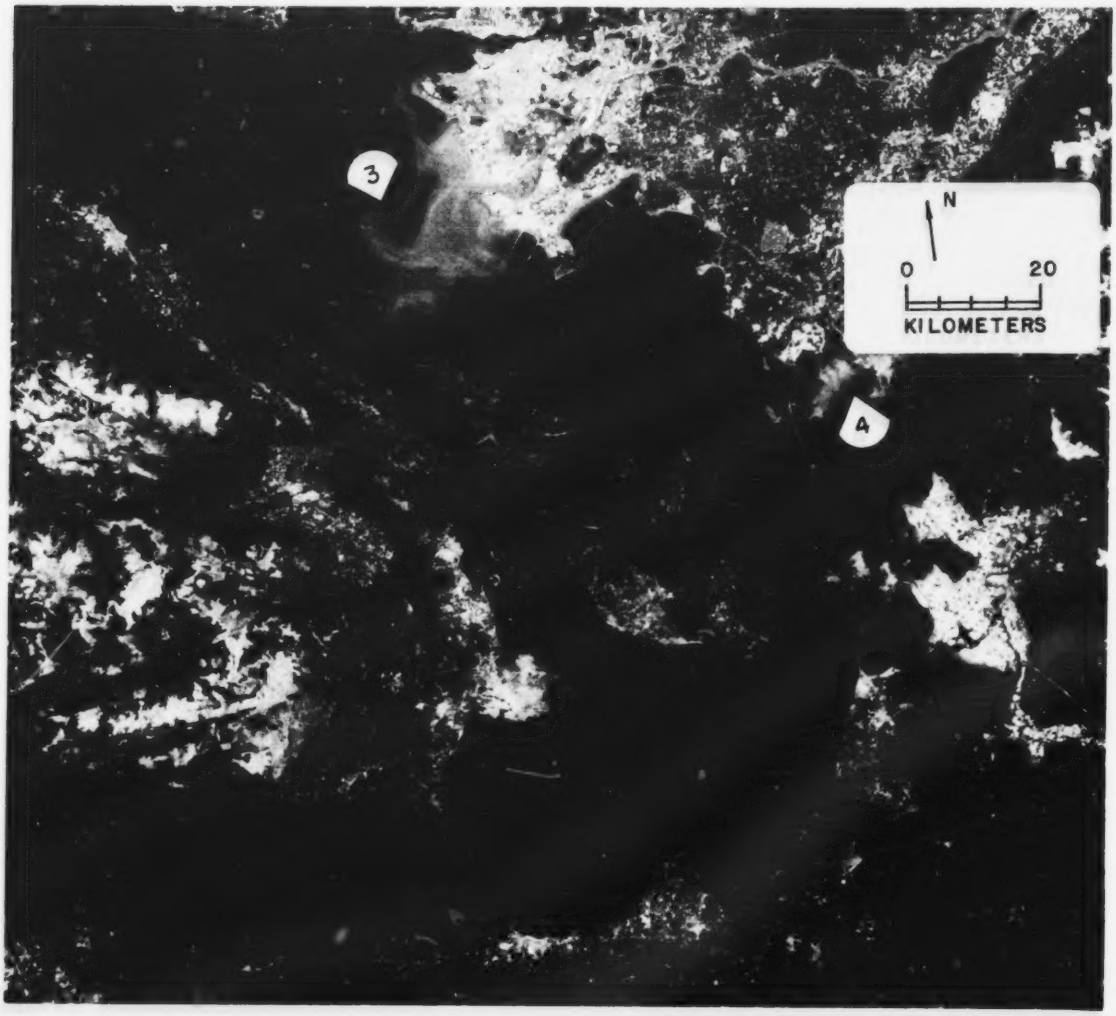

Fig. 8.5 MSS Band 5 of LANDSAT image 2129-18254 showing a southwesterly dispersal of suspended sediments from the Fraser River into the Strait of Georgia on May 31, 1975. Time of image acquisition was 1025 PST, just after flood current. An anticyclonic gyre can be observed due west of Pt. Roberts (3). Sediment discharge from the Nooksack River can be seen in Bellingham Bay (4). Image is free of cloud cover.

TIDAL CURRENT:	Slack Water	Max. Current	Vel. (kts)	TIDES:	Time	Ht.(m)
		0650	weak and variable		High at 0821	1.7
		1256	1.6		Low at 1522	0.3

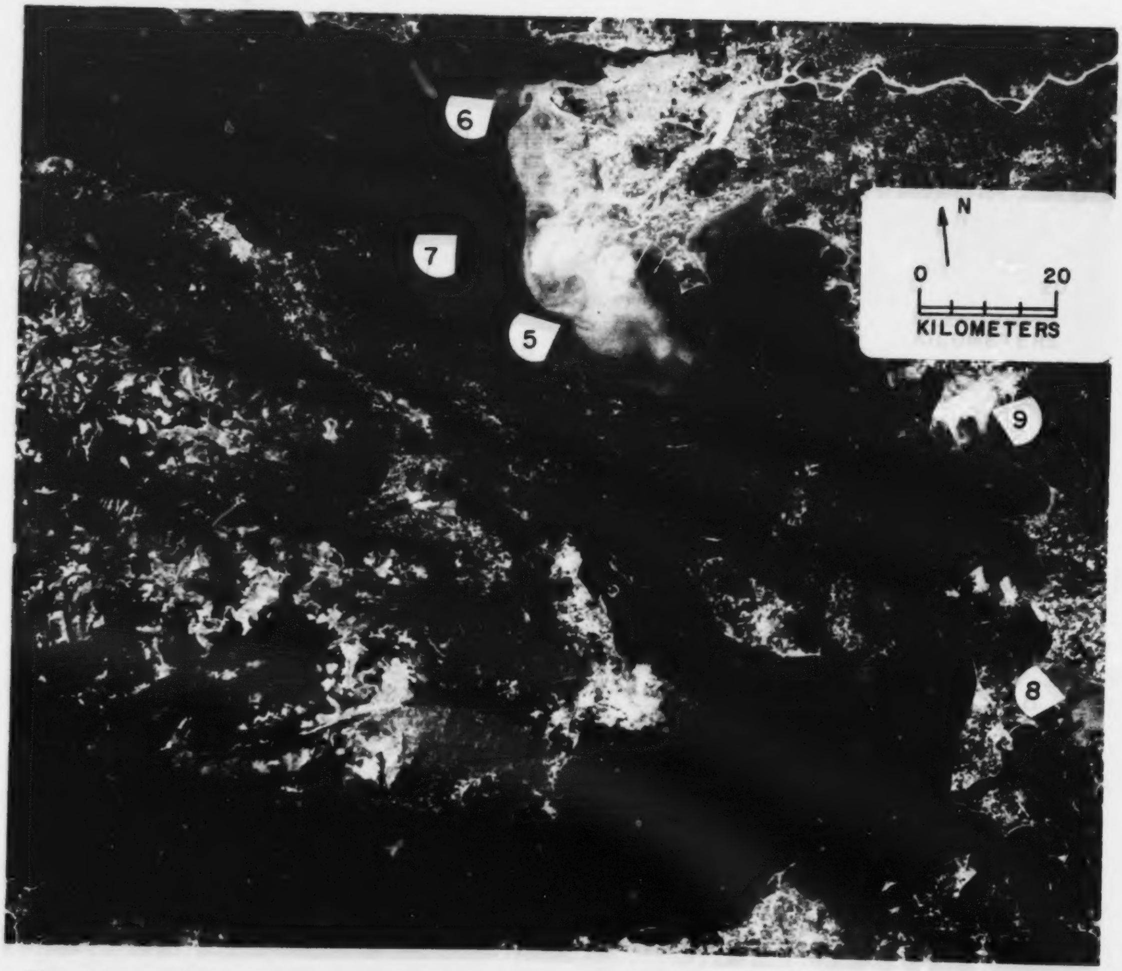

Fig. 8.6 MSS Band 5 of LANDSAT image 1727-18290 showing a southeasterly dispersal (5) of suspended sediments from the Fraser River into the Strait of Georgia on July 20, 1974. Time of image acquisition was 1029 PST, between major ebb current and slack water. The dispersal pattern suggests movement of Fraser River sediments along Saturna, Mayne, and Galiano Islands and into Trincomali Channel from Porlier Pass. Suspended sediments from the North Arm appear to flow to the northwest and to the northeast into Burrard Inlet (6). A cyclonic eddy (7) can be observed north of Galiano Island. Sediment discharge from the Skagit River into Skagit Bay (8), and from the Nooksack River into Bellingham Bay (9) is clearly visible. Several tidal fronts are also observed in the Strait of Juan de Fuca.

TIDAL CURRENT:

Slack Water	Max. Current	Vel. (kts)
0429	0912	3.1
1303	1534	2.0

TIDES:

Time	Ht.(m)
Low at 1147	-0.7
High at 1904	2.7

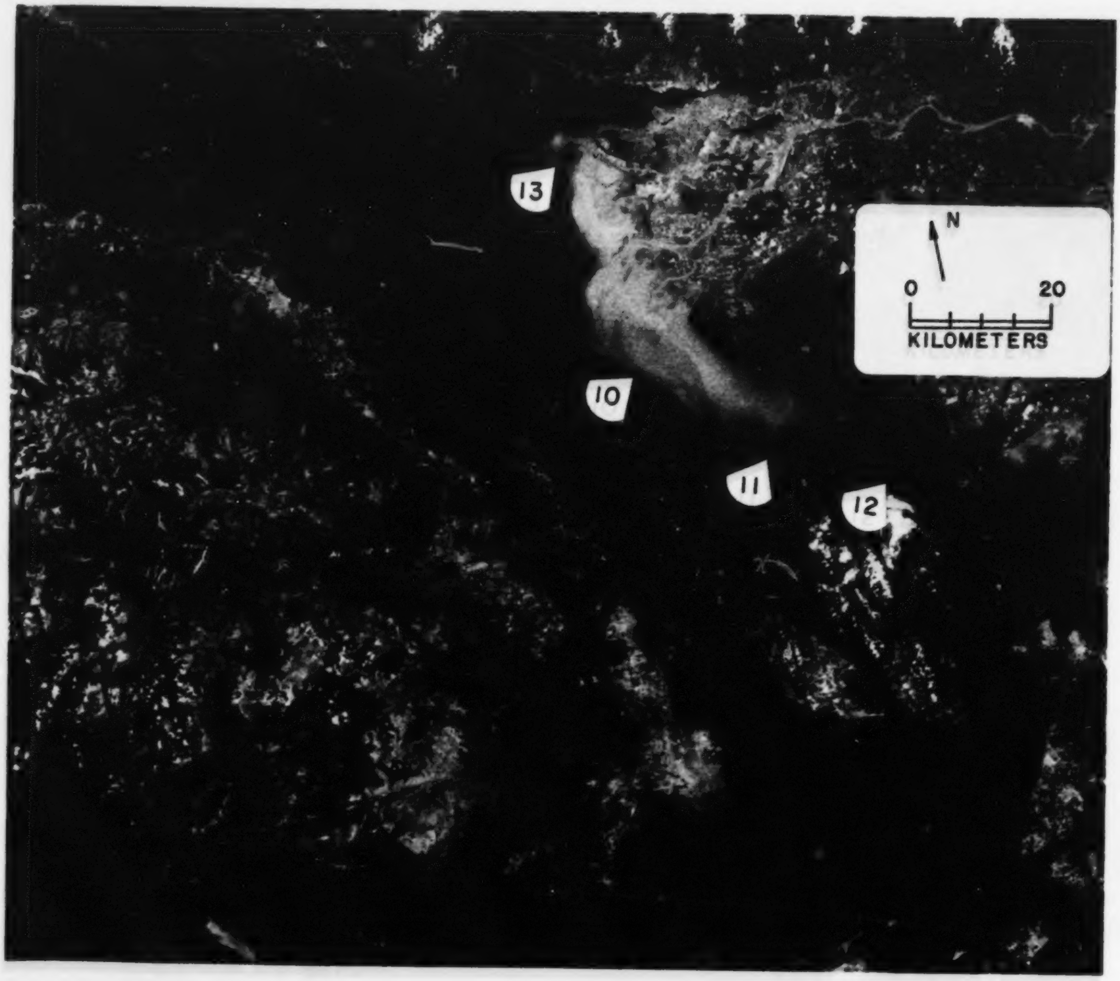

Fig. 8.7 MSS Band 5 of LANDSAT image 5465-17484 showing a southeasterly dispersal (10) of suspended sediments from the Fraser River into the Strait of Georgia on July 27, 1976. Time of image acquisition was 1048 PST, between major ebb current and slack water. The dispersal pattern suggests movement of Fraser River sediments into Haro Strait from the passages on either side of Mayne and Saturna Islands (11), and into Rosario Strait from the southeastern Strait of Georgia (12). Suspended sediments discharging into the Strait from North Arm appear to flow northward past Pt. Grey where it bifurcates, a portion flowing to the northwest, and the remaining flowing to the northeast into Burrard Inlet (13).

TIDAL CURRENT:

Slack Water	Max. Current	Vel. (kts)
0408	0904	2.7
1224	1517	1.8

TIDES:

Time	Ht.(m)
High at 0225	1.9
Low at 0931	-0.7

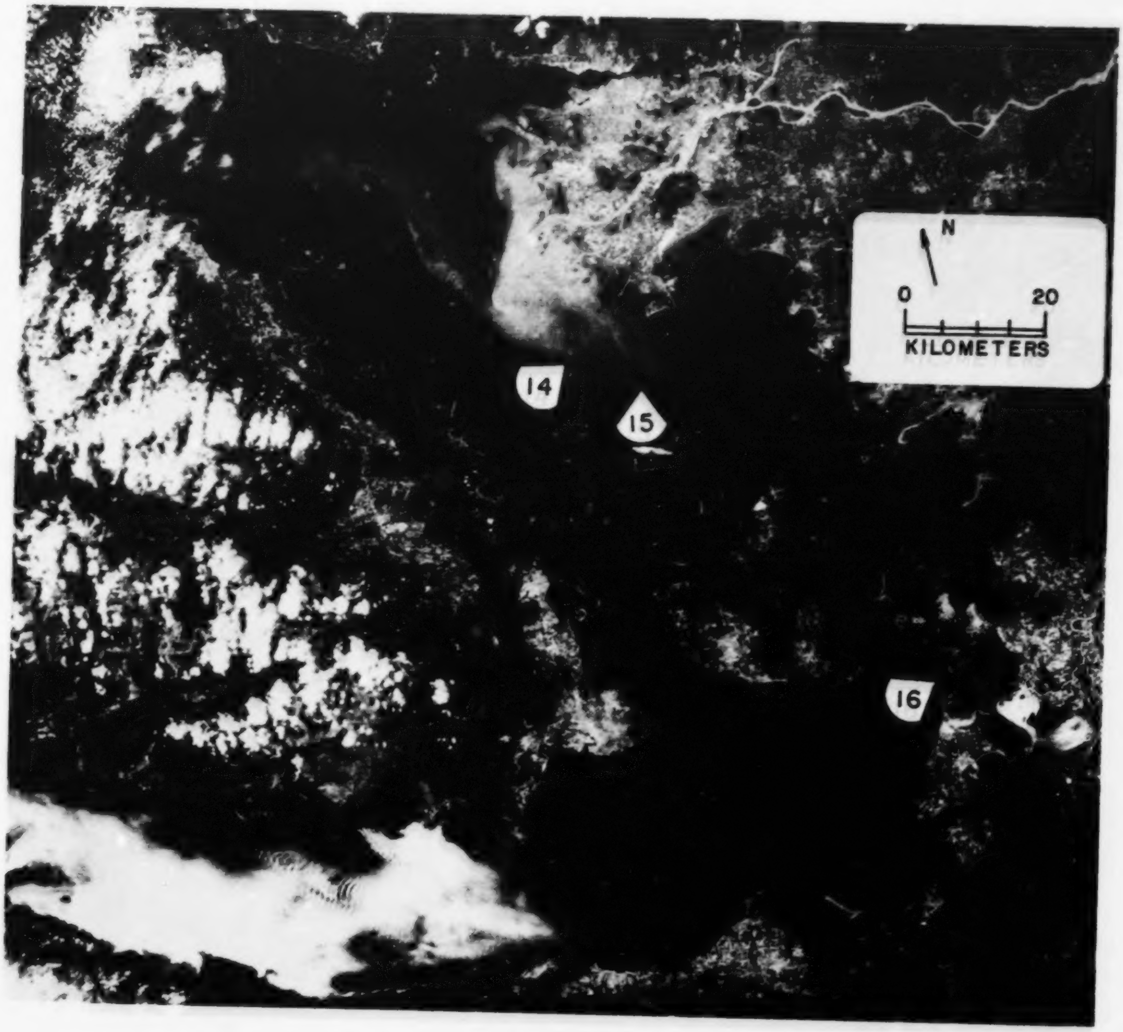

Fig. 8.8 MSS Band 4 of LANDSAT image 2921-18025 showing southeasterly dispersal (14) of suspended sediments from the Fraser River into the Strait of Georgia on July 31, 1977. Time of image acquisition was 1002 PST, between major ebb current and slack water. A tidal front is clearly indicated in the center of the Strait of Georgia (15). Suspended sediments can be observed discharging into Skagit Bay and through Deception Pass into Rosario Strait (16).

TIDAL CURRENT:	Slack Water	Max. Current	Vel. (kts)	TIDES:	Time	Ht.(m)
		0921	3.1		High at 0437	2.4
	1306	1531	1.8		Low at 1149	-0.4

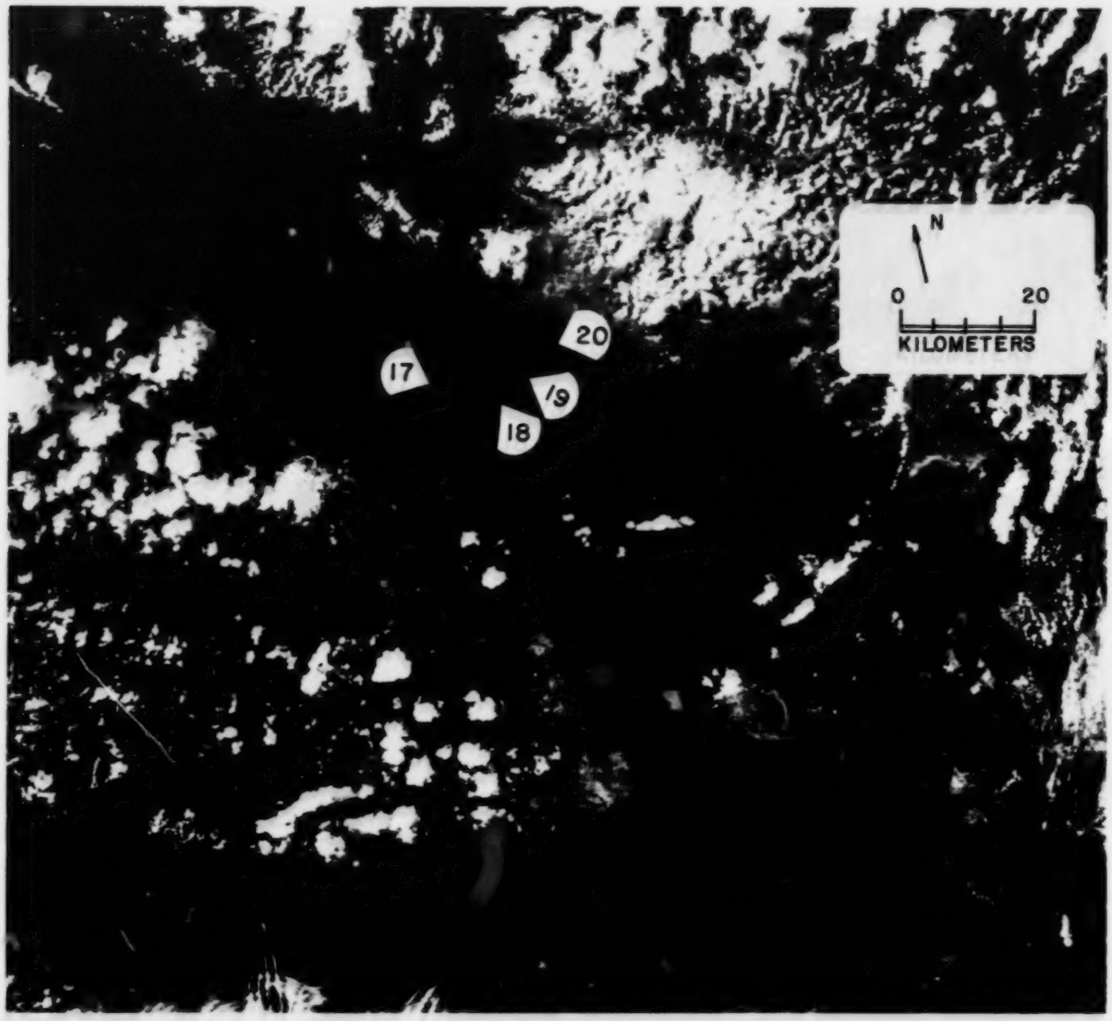

Fig. 8.9 MSS Band 5 of LANDSAT image 2957-18004 showing a southwesterly dispersal (17) of suspended sediments from the Fraser River into the Strait of Georgia on Sept. 5, 1977. Time of image acquisition was 1000 PST, between major flood current and slack water. The dispersal pattern suggests southwesterly flow associated with the flood current. Three small cyclonic eddies can be observed north of Mayne Island (18, 19 and 20). 40% cloud cover is visible over most land masses.

TIDAL CURRENT:	Slack Water	Max. Current	Vel. (kts)	TIDES:	Time	Ht.(m)
		0756	0.7		Low at 0414	0.4
	1201	1502	0.7		High at 1227	1.9

sediments are approximately 10-30% of the mean annual rates (see Fig. 2.2). This means that both the longitudinal pressure gradient and the suspended sediment concentrations are greatly reduced in winter. Consequently, the forces which drive the Fraser River plume into the Strait of Georgia are diminished in winter, resulting in more rapid mixing of the plume and concurrent dilution of suspended sediment concentrations to background levels. These conclusions are substantiated by the results of the seasonal surveys of suspended matter concentrations in the vicinity of the Fraser River which were presented earlier in this report. The background concentration of suspended matter in the study region was found to be approximately 1.0 mg/ℓ. Near the mouth of the Fraser River particulate concentrations ranged between 2.5 and 9.0 mg/ℓ during the November and August surveys (see, for example, stations 25, 26, and 27 in Figs. 5.4 and 5.6). However, in March the particulate concentration for station 25 was 0.9 mg/ℓ or approximately the same as background values for this region and time of year, indicating rapid dilution of the Fraser River plume as it discharges into the Strait.

The Skagit River also shows a minimum in water and sediment discharge during the winter period (Fig. 2.3). However, the percentage decrease is not as large as the winter decrease of the Fraser River (the average water and sediment discharge rates for the Skagit River during the months of January through March are 50-70% of the mean annual rates); and, as a result, the seasonal variations of the Skagit River plume are not nearly as pronounced. The LANDSAT images for January 1973 and March 1976 show evidence for movement of suspended sediments from the Skagit River into the nearshore regions of Skagit Bay (Figs. 8.2 and 8.3). This material mixes rapidly with the offshore water and the plumes do not maintain their identity beyond Deception Pass.

8.3 TIDAL VARIATIONS

As indicated in Table 8.1, the LANDSAT satellites maintain a sunsynchronous orbit around the earth in such a manner as to arrive at the same location at approximately the same time of day once every 18 days. Because the average tidal interval is about 12 hours 25 minutes, the tides will be out of phase by approximately one quarter cycle each time the satellite passes over. This means that over the course of several years the LANDSAT imagery for a given location should include all tidal stages if proper atmospheric conditions have prevailed. Since their deployment in 1972 and 1975, the LANDSAT satellites have produced approximately eight or nine high quality images which can be used for describing tidal effects on the dispersion of the Fraser River plume.

Figures 8.3 through 8.9 show examples of LANDSAT imagery which are of sufficient quality to be useful for studying tidal processes. The ebb tides are represented by Figures 8.3, 8.4, 8.6, and 8.8 and flood tides are indicated in Figures 8.5 and 8.9. The tidal stage corresponding to each of the LANDSAT images has been determined and is included in the figure captions. Patos Island was used as a reference point for determination of the tidal stage because: (1) it is centrally located with respect to the northern part of the study region and, consequently, differences in tidal stages are relatively small (e.g., the tides at the mouth of Main Arm precede those at Patos Island by about 2-4 minutes, whereas the tides at Deception Pass precede those at Patos Island by about 77 minutes); and (2) it provided the most complete set of data on tides and tide currents.

During ebb tide, distinct sediment plumes originating from Main Arm and Middle Arm flow seaward in a southwesterly direction to a point approximately midway between Steveston and Porlier Pass where the plumes are diverted in a southeasterly direction by the ebb flow in the Strait. Figures 8.4, 8.6, and 8.7 are examples of this process. The sediment plumes migrate with the flow across the Strait and through the passages between Orcas, Saturna, Mayne, and Galiano Islands into Haro Strait. In one case the tidal flow was so strong that the sediment plume could be traced as far east as the passage between Orcas and Lummi Islands (Fig. 8.7). However, the prevailing northwesterly winds were steady at about 30 mph and may have added to this effect (Pacific Weather Center, Environment Canada).

Numerous cyclonic and anticylonic eddies are associated with the plumes. These eddies, which are probably the result of interactions between inertial, tidal, and coriolis forces, maintain their integrity for several hours. For instance, in Figure 8.6, a cyclonic eddy is observed in the region north of Galiano Island. Since it appears to be detached from the major plume emanating from the Fraser River, it probably represents a relict bolus that moved into the region during a previous tide. This means that at least during some seasons, boluses of low salinity water derived from the Fraser River are probably capable of maintaining their identity for periods longer than a single tidal cycle.

The sediment plume emanating from North Arm during ebb tide flows to the north and west past Point Grey (Figs. 8.6 and 8.7). Beyond Point Grey the plume bifurcates, with a portion of the plume moving to the northwest and the remaining material flowing to the northeast into Burrard Inlet.

The dispersal pattern of the Fraser River plume during flood tide has some characteristics which are very similar to the pattern for ebb tide and some which are uniquely different. As indicated in Figures 8.5 and 8.9, the sediment plumes originating from Main Arm and Middle Arm flow seaward in a southwesterly direction. However, instead of being diverted to the southeast, as is the case during ebb tide, the flood current drives the sediment plume across the Strait and to the northwest along the northern coast of Galiano Island. Some material from the plume passes into Trincomall Channel from Porlier Pass and the remaining material continues to flow to the northwest, mixing with and being diluted by the less turbid water of the northwestern Strait.

There is evidence for some small cyclonic and anticyclonic eddies in the plumes associated with the flooding tide. These eddies are interpreted as evidence for interactions between the longitudinal pressure gradient, associated with the fresh water input from the Fraser River, and the tidal and coriolis forces associated with water movement in the Strait during flood tide (Tabata, 1972). It is interesting to note that the anticyclonic eddies in the LANDSAT images are most pronounced when the tidal and coriolis forces are additive. The large anticyclonic eddy due west of Point Roberts in Figure 8.5 is an example of this situation. The plume appears to be split into two parts, presumably by tidal and coriolis forces. These processes increase the rate of lateral mixing and subsequent dilution of the plume.

The sediment-laden plume from North Arm flows to the north around Point Grey and into Burrard Inlet during flood tide. There is no evidence from the LANDSAT images of sediment movement to the northwest during this stage of the tide.

8.4 SUMMARY AND CONCLUSIONS

LANDSAT images, obtained during the period between 1972 and 1977, have been utilized to study the surface trajectories of sediment plumes originating from the Fraser and Skagit Rivers. These plumes are natural tracers of flow patterns of low salinity water and suspended matter that is discharged into northern Puget Sound from these rivers.

Three separate plumes can be observed emanating from the distributaries of the Fraser River. The plumes from Main Arm and Middle Arm join together to form a well-defined jet which can be traced across the Strait of Georgia and through Porlier, Active, and Boundary Passes. During ebb tide the plume is directed to the southeast from a point about midway between Steveston and Porlier Pass. The flood tide drives the plume across the Strait and to the northwest along the northern coast of Galiano Island. The presence of a well-defined jet is indicative of the significance of the longitudinal pressure and inertial forces. When water and sediment discharge is high, particularly during the spring runoff period, these forces predominate and the plumes maintain their identity for considerable distances. When discharge is low these forces are weak and tidal, coriolis, and wind forces predominate, causing rapid mixing and corresponding dilution of the plumes. The plume from North Arm moves to the northwest past Point Grey where it bifurcates, with some material flowing to the northwest during ebb tide and the remaining material moving into Burrard Inlet. The northward flow of the plume from the North Arm is probably the result of a combination of a number of forces including inertial, pressure, and coriolis.

The existence of a number of separate plumes in some of the images suggests that eddies of sediment-laden water are probably capable of maintaining their identity for periods longer than a single cycle. This implies that a dynamic balance exists between the inertial and pressure forces associated with these boluses and the coriolis and tidal forces associated with circulation patterns in the Strait. From observations of photographs taken near the mouth of Main Arm, Tabata (1972) suggests that this balance is maintained by the daily surge of fresh water from the river merging with the already present low salinity water lying along the southwestern side of the Strait. Our data support these conclusions, at least for the periods of high runoff. While the winter data are very limited, there is no evidence for multiple plumes, indicating that mixing is rapid and the lifetimes of the plumes are very short, probably less than one tidal cycle.

The plumes from the distributaries of the Skagit River are most pronounced in early summer, during the peak runoff. During this period suspended sediments from the Skagit River can be traced as far south as the middle of Saratoga Passage and as far north as Deception Pass, where Skagit River sediments flow into Rosario Strait during ebb tide. During the period of low discharge, the Skagit River plume is confined to the nearshore regions of Skagit Bay.

In conclusion, the salient features of the dispersal patterns and trajectories of suspended sediments from the Fraser and Skagit Rivers have been examined using LANDSAT imagery. A number of conclusions about the characteristics of the circulation patterns and suspended sediment distributions have been inferred from the images which cannot be verified until extensive seaborne observations are initiated. In the future, attempts should be made to augment the LANDSAT observations with corresponding sea truth data collected in a synoptic manner.

ACKNOWLEDGMENTS

We wish to express our sincere gratitude to Dr. W. Macleod, Dr. D. Brown, and to S. Ramos of the NOAA Analytical Facility for their technical and analytical support of the hydrocarbon program.

The authors also express appreciation to M. Lamb for the preparation of the LANDSAT images and for the compilation of the hydrological data; to G. Massoth for his help in data reduction and analyses; and to J. Nevins for the analysis of suspended matter mineralogies. Special appreciation is extended to S. Hamilton, A. Chapdelaine, and C. Katz for their assistance in hydrocarbon analysis, scanning electron microscopy, and graphics.

This work was supported by the Office of Energy, Minerals, and Industry, Office of Research and Development, U.S. Environmental Protection Agency through an interagency agreement with the Environmental Research Laboratories of NOAA.

BIBLIOGRAPHY

Atkinson, L. P., and F. A. Richards. 1967. The Occurrence and Distribution of CH_4 in the Marine Environment. Deep-Sea Res. 14:673-686.

Baier, R. E. 1970. Surface Quality Assessment of Natural Bodies of Water. Proc. Conf. Great Lakes Res. 13:114-127.

Banse, K. 1974. On the Interpretation of Data for the Carbon to Nitrogen Ratio of Phytoplankton. Limnol. Oceanogr. 19:695-699.

Bassin, N. J., and T. Ichiye. 1977. Flocculation Behavior of Suspended Sediments and Oil Emulsions. J. Sed. Petrol. 47:671-677.

Blumer, M. 1971. Scientific Aspects of the Oil Spill Problem. Environ. Affairs. 1:54-73.

Blumer, M., R.R.L. Guillard, and T. Chase. 1971. Hydrocarbons of Marine Phytoplankton. Mar. Biol. 8:183-189.

Broecker, W. S., and T. H. Peng. 1974. Gas Exchange Rates Between Air and Sea. Tellus. 29:21-35.

Brooks, J. M. 1977. The Flux of Light Hydrocarbons into the Gulf of Mexico via Runoff. In: Marine Pollutant Transfer, pp. 185-200, H. L. Windom and R. A. Duce, eds. Lexington Books, D. C. Heath Co., Lexington, Mass. 391 pp.

Brooks, J. M., A. D. Fredericks, W. M. Sackett, and J. W. Swinnerton. 1973. Baseline Concentrations of Light Hydrocarbons in Gulf of Mexico. Environ. Sci. Technol. 7:639-642.

Brooks, J. M., and W. M. Sackett. 1973. Sources, Sinks and Concentrations of Light Hydrocarbons in the Gulf of Mexico. J. Geophys. Res. 78:5248-5258.

Brooks, J. M., and W. M. Sackett. 1976. Significance of Low-molecular-weight Hydrocarbons in Marine Waters. In: Proc. 7th International Meeting Organic Geochemistry. pp. 455-468.

Castellan, G. W. 1964. Physical Chemistry. Addison-Wesley Publishing Co., Reading, Mass. 717 pp.

Chang, P., S. Pond, and S. Tabata. 1976. Subsurface Currents in the Strait of Georgia, West of Sturgeon Bank. J. Fish. Res. Bd. Can. 33:2218-2241.

Chipman, W. A., and P. S. Galtsoff. 1949. Effects of Oil Mixed with Carbonized Sand on Aquatic Animals. U.S. Dept. Inter. Spec. Sci. Rept., Fisheries No. 1. 49 pp.

Clark, R. C., and D. W. Brown. 1977. Petroleum: Properties and Analyses in Biotic and Abiotic Systems. In: Effects of Petroleum on Arctic and Subarctic Marine Environments and Organisms, Vol. I, pp. 1-90. D. C. Malins, ed. Academic Press, Inc., New York. 321 pp.

Clark, R. C., and W. D. MacLeod. 1977. Inputs, Transport Mechanism, and Observed Concentrations of Petroleum in the Marine Environment. In: Effects of Petroleum on Arctic and Subarctic Marine Environments and Organisms, Vol. I, pp. 91-224. D. C. Malins, ed. Academic Press, New York. 321 pp.

Cline, J. D. 1977. Identification of Natural and Anthropogenic Petroleum Sources Utilizing Low Molecular Weight Hydrocarbons, C_1-C_4. OCSEAP/ERL Quarterly Rept. 153, June-Sept., Boulder, Colo.

Cline, J. D., and M. L. Holmes. 1977. Submarine Seepage of Natural Gas in Norton Sound, Alaska. Sci. 198:1149-1153.

Conover, R. J. 1971. Some Relations Between Zooplankton and Bunker C. Oil in Chedabucto Bay Following the Wreck of the Tanker "Arrow." J. Fish. Res. Bd. Can. 28:1327-1330.

EPA. 1977. Review of Environmental Issues of the Transportation of Alaskan North Slope Crude Oil, EPA-600/7-77-046. Office of Energy, Minerals and Industry, Office of Research and Development, EPA, Washington, D.C. 123 pp.

Farrington, J., and J. G. Quinn. 1973. Petroleum Hydrocarbons in Narragansett Bay, Part I: Survey of Hydrocarbons in Sediments and Clams, Mercenaria mercenaria. Estuarine Coast. Mar. Sci. 1:71-79.

Farrington, J. W., and J. G. Quinn. 1973. Petroleum Hydrocarbons and Fatty Acids in Wastewater Effluents. J. Water Pollut. Contr. Fed. 45:704-712.

Forrester, W. D. 1971. Distribution of Suspended Particles Following the Wreck of the Tanker "Arrow." J. Mar. Res. 29:151-170.

Gatto, L. W. 1976. Circulation and Sediment Distribution in Cook Inlet, Alaska. In: Assessment of Arctic Marine Environment Selected Types. pp. 205-228. D. W. Hood and D. C. Burrell, eds. Occasional Pub. No. 4, Univ. Alaska, Fairbanks, Alaska.

Geyer, R. A., and W. M. Sweet, Jr. 1973. Natural Hydrocarbon Seepage in the Gulf of Mexico. Trans. Gulf Coast Ass. Geol. Soc. 23:158-169.

Gordon, D. C., and P. D. Keizer. 1974. Hydrocarbon Concentrations in Sea-water along the Halifax-Bermuda Section: Lessons Learned Regarding

Sampling and Some Results. In: Marine Pollution Monitoring (Petroleum). Natl. Bur. Stand. Spec. Publ. 409. pp. 113-115.

Hartung, R., and G. W. Klinger. 1968. Sedimentation of Floating Oil. Michigan Acad. Sci. Art. Lett. 53:23-27.

Herlinveaux, R. H., and J. P. Tully. 1961. Some Oceanographic Features of Juan de Fuca Strait. J. Fish. Res. Bd. Can. 18:1027-1071.

Hites, R. A., and K. Biemann. 1972. Water Pollution: Organic Compounds in the Charles River, Boston. Sci. 178:158-160.

Huang, C. P., and H. A. Elliott. 1977. The Stability of Emulsified Crude Oils as Affected by Suspended Particles. In: Fate and Effects of Petroleum Hydrocarbons in Marine Organisms and Ecosystems, pp. 413-420. D. A. Wolfe, ed. Pergamon Press, New York. 478 pp.

Jeffrey, L. M., and D. W. Hood. 1958. Organic Matter in Seawater: An Evaluation of Various Methods of Isolation. J. Mar. Res. 17:247-271.

Johnson, R. W., I. W. Duedall, R. W. Glasgow, and J. R. Proni. 1977. Quantitative Mapping of Suspended Solids in Wastewater Sludge Plumes in the New York Bight Apex. J. Water Poll. Contr. Fed. 49:2063-2073.

Klemas, V., D. Bartlett, W. Philpot, R. Rogers, and L. Reed. 1974. Coastal and Estuarine Studies with ERTS-1 and SKYLAB. Remote Sensing of Environ. 3:153-174.

Kolpack, R. L. 1971. Biological and Oceanographical Survey of Santa Barbara Channel Oil Spill, 1969-1970. Vol. II. Physical, Chemical, Geological Studies. Allen Handcock Foundation, Univ. Southern Calif.

Kreider, R. E. 1971. Identification of Oil Leaks and Spills. In: Proc. Joint Conf. Prev. Contr. of Oil Spills, pp. 119-124. Amer. Petrol. Inst., Washington, D.C.

Kritokos, H., L. Yorinks, and H. Smith. 1974. Suspended Solids Analysis Using ERTS-A Data. Remote Sensing of Environ. 3:69-75.

Lamontagne, R. A., J. W. Swinnerton, V. J. Linnenbom, and W. D. Smith. 1973. Methane Concentrations in Various Marine Environments. J. Geophys. Res. 78:5317-5324.

Lamontagne, R. A., J. W. Swinnerton, and V. J. Linnenbom. 1974. C_1-C_4 Hydrocarbons in the North and South Pacific. Tellus. 26:71-77.

Link, W. K. 1952. Significance of Oil and Gas Seeps in World Oil Exploration. Amer. Ass. Petrol. Geol., Bull. 36:1055-1540.

McAuliffe, C. D. 1966. Solubility in Water of Paraffin, Cycloparaffin, Olefin, Acetylene, Cycloolefin, and Aromatic Hydrocarbons. J. Phys. Chem. 70:1267-1275.

McAuliffe, C. 1969. Solubility in Water of Normal C_9 and C_{10} Alkane Hydrocarbons. Sci. 158:478-479.

McAuliffe, C. D. 1977. Dispersal and Alteration of Oil Discharged on a Water Surface. In: Fate and Effects of Petroleum Hydrocarbons in Marine Organisms and Ecosystems, pp. 19-35. D. A. Wolfe, ed. Pergamon Press, Elmsford, New York. 478 pp.

MacLeod, W. D., D. W. Brown, R. G. Jenkins, L. S. Ramos, and V. D. Henry. 1976. A Pilot Study on the Design of Petroleum Hydrocarbon Baseline Investigation for Northern Puget Sound and Strait of Juan de Fuca. NOAA Tech. Memo. ERL MESA-8, NTIS, Springfield, Virginia. 53 pp.

Meyers, P. A., and J. G. Quinn. 1973. Factors Affecting the Association of Fatty Acids with Mineral Particles in Seawater. Geochim. Cosmochim. Acta. 37:1745-1759.

NAS. 1975. Petroleum in the Marine Environment, E. G. Wilson, ed. National Academy of Science, Washington, D.C. 107 pp.

Ogner, G., and M. Schnitzer. 1970. The Occurrence of Alkanes in Fulvic Acid, a Soil Humic Fraction. Geochim. Cosmochim. Acta. 34:921-928.

Pacific Northwest River Basins Commission. Puget Sound Task Force. March 1970. Comprehensive Study of Water and Related Land Resources, Puget Sound and Adjacent Waters, State of Washington, Appendix III, Hydrology and Natural Environment.

Parker, B. 1977. Tidal Hydrodynamics in the Strait of Juan de Fuca-Strait of Georgia. NOAA Tech. Rept. NOS-69, NOAA/DOC, Washington, D.C. 56 pp.

Parker, C. A. 1970. The Ultimate Fate of Crude Oil at Sea--Uptake of Oil by Zooplankton. AML Rept. B. 198 pp.

Poirier, O. A., and G. A. Thiel. 1941. Deposition of Free Oil by Sediments Settling in Sea Water. Bull. Am. Assoc. Petrol. Geol. 25:2170-2180.

Reeburgh, W. S., and D. T. Heggie. 1977. Microbial Methane Consumption Reactions and Their Effect on Methane Distributions in Freshwater and Marine Environments. Limnol. Oceanogr. 22:1-9.

Rohrback, B. G., and W. E. Reed. 1975. Evaluation of Extraction Techniques for Hydrocarbons in Marine Sediments. Inst. Geophys. Planet. Physics. Publ. No. 1537. University of California, Los Angeles.

Sackett, W. M. 1977. Use of Hydrocarbon Sniffing in Offshore Exploration. J. Geochem. Explor. 7:243-254.

Schultz, D. M., and J. G. Quinn. 1977. Suspended Material in Narragansett Bay: Fatty Acid and Hydrocarbon Composition. Organic Geochem. 1:27-36.

Scranton, M. I., and J. W. Farrington. 1977. Methane Production in the Waters Off Walvis Bay. J. Geophys. Res. 82:4947-4953.

Sharp, J. H. 1974. Improved Analysis for "Particulate" Organic Carbon and Nitrogen from Seawater. Limnol. Oceanogr. 19:984-989.

Shaw, D. 1977. Hydrocarbons: Natural Distribution and Dynamics on the Alaskan Outer Continental Shelf. In: Environmental Assessment of Alaskan Continental Shelf, Vol. XIII, pp. 507-727. U.S. Dept. of Commerce/U.S. Dept. of Interior, OCSEAP, Boulder, Colo. 857 pp.

Schumacher, J. D., C. A. Pearson, R. A. Charnell, and N. P. Laird. 1978 (in press). Regional Response to Forcing in Southern Strait of Georgia. Estuar. Coast. Mar. Sci.

Smith, H. M. 1968. Qualitative and Quantitative Aspects of Crude Oil Composition. Bur. Mines, Bull. 642. U.S. Dept. Interior, U.S. Government Printing Office, Washington, D.C. 136 pp.

Sternberg, R. W., E. T. Baker, D. A. McManus, S. Smith, and D. R. Morrison. 1974. An Integrating Nephelometer for Measuring Particle Mass Concentrations in the Deep Sea. Deep-Sea Res. 21:887-892.

Swinnerton, J. W., and V. J. Linnenbom. 1967. Determination of C_1-C_4 Hydrocarbons in Seawater by Gas Chromatogr. 5:570-573.

Tabata, S. 1972. The Movement of Fraser River Influenced Surface Water in the Strait of Georgia as Deduced from a Series of Aerial Photographs. Dept. Environ. Water Management, Service Mar. Sci. Branch, Pac. Regional Pac. Mar. Sci., Rept. 72-6. 69 pp.

Tully, J. P. 1942. Surface Non-tidal Currents in the Approaches to Juan de Fuca Strait. J. Fish Res. Bd. Can. No. 83. 169 pp.

Van Olphen, H. 1963. Clay Colloid Chemistry. Interscience Publishers, New York. 301 pp.

Van Vleet, E. A., and J. G. Quinn. 1977. Input and Fate of Petroleum Hydrocarbons Entering the Providence River and Upper Narragansett Bay from Wastewater Effluents. Environ. Sci. Technol. 11:1086-1092.

Waldichuk, M. 1957. Physical Oceanography of the Strait of Georgia, British Columbia. J. Fish. Res. Bd. Can. 14:321-486.

Water Resources Data for Washington. 1976. U.S. Dept. Int., Geol. Surv. Water Resources Division. Tacoma, Washington.

Water Survey of Canada. Sediment Data, Canadian Rivers, Inland Waters Directorate, Ottawa, Canada, 1967-1976.

Water Survey of Canada. Water Data, Canadian Rivers, Inland Waters Directorate, Ottawa, Canada, 1967-1976.

Wilson, D. F., J. W. Swinnerton, and R. A. Lamontagne. 1970. Production of Carbon Monoxide and Gaseous Hydrocarbons in Seawater: Relation to Dissolved Organic Carbon. Sci. 168:1577-1579.

Winter, D. F., K. Banse, and G. C. Anderson. 1975. The Dynamics of Phytoplankton Blooms in Puget Sound, a Fjord in the Northwestern United States. Mar. Biol. 19:139-176.

APPENDIX A

Seasonal Distributions and Abundances of Low Molecular Weight Aliphatics in the Waters of Northern Puget Sound

A.1 INTRODUCTION

The development of petroleum resources in Alaska is likely to result in the increased transshipment of crude oil and refined products to and from Washington refineries. As a consequence of this, oil and refined products are apt to enter the waters of Northern Puget Sound in ever-increasing quantities as import and export volumes increase.

Crude oil contains four broad classes of compounds: straight chain and branched alkanes, cycloparaffins, aromatics, and heterocyclics (Clark and MacLeod, 1977). Within the paraffin fraction, a wide range of molecular weights is usually found, depending on the source and maturation history of the oil. The lightest hydrocarbon found in petroleum, and more abundantly in natural gas, is methane. Homologs of methane (ethane, propane, butanes, etc.) are also present, usually in diminishing amounts. During production, the liquid fraction of petroleum is normally separated from the gas and water portions, but the separated crude oil still retains significant concentrations of the light hydrocarbons in solution.

When petroleum is accidentally spilled, several physical, biochemical, and chemical processes begin to operate immediately to degrade the oil. Among them are evaporation, solution, photooxidation, emulsification, adsorption, and biodegradation (NAS, 1975). The most volatile fractions of oil, including the LMW compounds, are readily volatilized into the atmosphere (McAuliffe, 1977), but some also go into solution because of their relatively high solubility (McAuliffe, 1966).

It is presently believed that the most toxic fractions of crude oil are the low boiling point aliphatics (Blumer, 1971). While the LMW aliphatic hydrocarbons are of less toxicity than the previously mentioned fractions, they are soluble, and, therefore, become useful marker compounds for the dissolved or emulsified fractions of oil.

The occurrence of the LMW aliphatics and aromatics in water may arise from both natural and anthropogenic sources. Natural marine sources include microbial production (i.e., marsh gas; Atkinson and Richards, 1967) and leakage from natural seeps (Link, 1952; Geyer and Sweet, 1973).

Because the low molecular weight hydrocarbons are ubiquitous components of petroleums (Smith, 1968), and because they are readily monitored, these compounds have been used commercially (Sackett, 1977) and environmentally (Brooks and Sackett, 1973) to detect the incipient introduction of petroleum into marine waters. Documented in numerous reports, scientists from Texas A&M University have shown the LMWH to be valuable tracers of anthropogenic petroleum and related products in the Gulf of Mexico via shipping, production, and transfer operations (Brooks et al., 1973; Brooks and Sackett, 1976; Brooks, 1977 and references contained therein). Estuaries and shelf waters along the U.S. coastline have been impacted in particular, as suggested by the unusually high concentrations of the C_2-C_4 homologs of methane (Brooks et al., 1973).

For these reasons as well as the successes that have been achieved in the coastal waters of Alaska in documenting petroleum sources (Cline and Holmes, 1977), a survey of the waters of the eastern Strait of Juan de Fuca, San Juan Island Passages, and the southern Strait of Georgia was initiated as a supplementary program. Also, because the LMW aliphatics are proving to be valuable monitoring parameters, a seasonal assessment of current levels of LMW hydrocarbon in the waters of northern Puget Sound seemed advisable.

The components measured in this study include dissolved methane, ethane, ethene, propane, propene, iso- and n-butanes. Only a portion of the results will be discussed for the purpose of brevity, but the results are typical and representative. All of the data acquired during the three cruises have been digitized on punch cards and submitted to NODC/EDS for inclusion in their data bank.

A.2 METHODOLOGY

The volatile hydrocarbons are removed from sea water according to a modified procedure of Swinnerton and Linnenbom (1967). Briefly, the procedure is: Hydrocarbons are removed in a stream of ultra-pure He (120-140 mℓ/min) and condensed on a single activated alumina trap maintained at -196°C. Approximately 10 minutes of stripping are required to quantitatively remove the hydrocarbons (> 98%) from solution, after which time the trap is warmed to 90-100°C and the absorbed gases are allowed to pass into the gas chromatograph (GC).

The alkanes are chromatographed on a 60/80 mesh Poropak Q^R column (3/16" x 4', stainless steel) at a flow rate of 60 mℓ/min and detected sequentially as they emerge from the columns. In order to obtain peak resolution between the alkanes and alkenes, the Poropak Q^R column was connected in series with a short column (3/16" x 2", stainless steel) of activated alumina impregnated with 1% silver nitrate by weight. This modification, coupled with temperature programming from 110-150°C, has resulted in sharper peaks, better separation and reduced retention times for all components. The GC utilized was a Hewlett Packard^R model 5711, equipped with dual FID's.

The analysis of the samples was conducted in the laboratory rather than on shipboard. To prevent microbial oxidation of the hydrocarbons, samples were pickled with 100 mg sodium azide and analyzed within 2 weeks of the cruise termination.

A.3 RESULTS AND DISCUSSION

A plot of stations sampled for LMW aliphatics is shown in Figure A.1. These stations were selected as being representative from the complete grid shown in Figure 5.1. Only the surface distributions of methane (near bottom also), ethane, and ethene will be presented as little additional information is gained by considering the entire suite of hydrocarbons observed. If hydrocarbon pollution was indicated, the concentrations and abundances of C_3 and C_4 homologs of methane would be important.

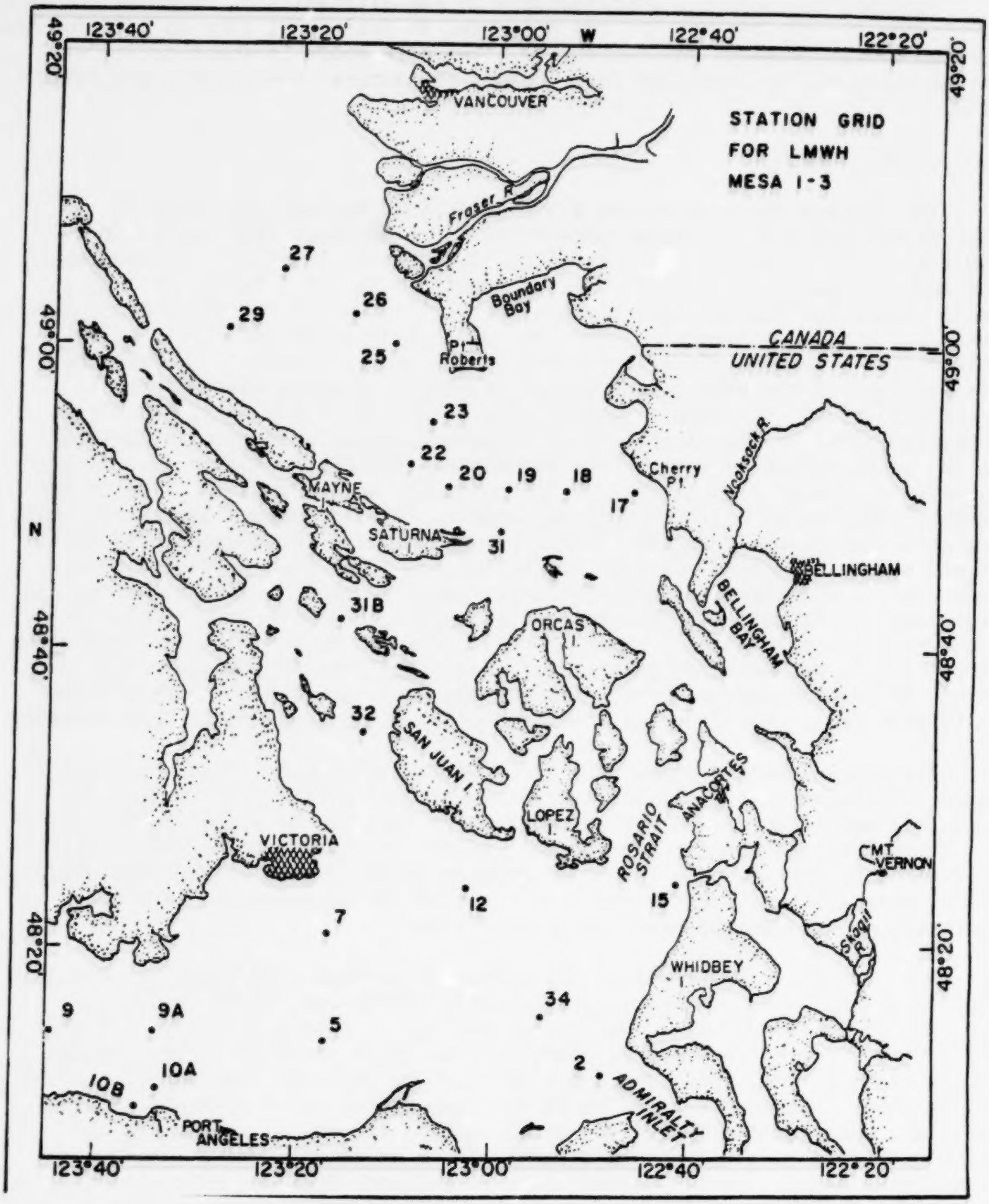
123°40'
123°20'
123°00'
W
122°40'
122°20'
49°20'
49°00'
48°40'
48°20'
N
STATION GRID
FOR LMWH
MESA 1-3
VANCOUVER
Fraser R.
Boundary Bay
Pt. Roberts
CANADA
UNITED STATES
Cherry Pt.
Nooksack R.
BELLINGHAM
BELLINGHAM BAY
MAYNE I.
SATURNA I.
ORCAS I.
SAN JUAN I.
LOPEZ I.
ROSARIO STRAIT
ANACORTES
MT VERNON
Skagit R.
WHIDBEY I.
VICTORIA
PORT ANGELES
ADMIRALTY INLET
27
29
26
25
23
22
20
19
18
17
31
31B
32
12
15
7
9
9A
5
34
10A
10B
2

Figure A.1. Locations selected for seasonal LMW hydrocarbon observations. Samples were not taken at every station during each of the three cruises. This sampling grid represents a subset of the station sampling protocol shown in Figure 5.1.

Seasonal and vertical distributions of LMW aliphatics at selected stations (2, 5, 15, 17, 23, 26, and 32) are presented in Tables A.1 through A.7, for the purpose of completeness and continuity. The data shown in these tables will not be discussed in detail as they support the general conclusions presented below.

A.3.1 LMWH - MESA I

The surface and near bottom distributions of methane are shown in Figures A.2 and A.3. Surface concentrations in November 1976 varied from 250 nℓ/ℓ (STP) to nearly 800 nℓ/ℓ (STP); the highest level was observed south and west of the Fraser River. These concentrations are a factor of 5 to 16 above saturation values (Lamontagne et al., 1973), which for these water temperatures and salinities ($T = 10^{\circ}C$; $S = 32^{\circ}/oo$) is approximately 50 nℓ/ℓ (STP) given a methane partial pressure of 1.4 ppmv. A plot of the methane distribution in the near bottom waters (Figure A.3) shows that methane is equally high, ranging from a low 345 nℓ/ℓ to a high of 849 nℓ/ℓ. The large supersaturation of dissolved methane represents a net production of methane in the water column or from bottom sediments. Methane, or marsh gas, is produced by microbial fermentation of low molecular weight organic acids or the direct reduction of CO_2 (Reeburgh and Heggie, 1977). Because these reactions are catalyzed by strict anaerobic microorganisms, the bottom sediments are a likely source. However, because the water column was poorly stratified at this time of the year and rather strongly tidally-induced vertical mixing was prevalent, it is unlikely that bottom sediments alone were responsible for these high concentrations. Based on recent studies by Scranton and Farrington (1977), it is now believed that significant quantities of methane are produced within microenvironments. These microenvironments are organic particles and aggregates (e.g., fecal pellets) within which anoxic conditions would prevail.

The concentrations shown here are significantly higher than the shelf waters of Alaska (Cline, 1977), but rather typical of the shelf waters of Louisiana and Texas, which are believed to be impacted by petroleum production and transportation (Brooks and Sackett, 1973). Because Puget Sound is characterized by seasonally high levels of primary production (Winter et al., 1975), these concentrations, particularly in light of the abundances of the other hydrocarbons, are not believed to be excessive.

The distributions of ethane and ethene in surface waters are presented in Figures A.4 and A.5. The range of the concentration of ethane is 0.4 nℓ/ℓ to 1.0 nℓ/ℓ (STP) (Figure A.4), whereas ethene varies from 1.6 nℓ/ℓ to 3.1 nℓ/ℓ. These concentrations are rather comparable to those observed in the Alaskan shelf waters (Cline, 1977) and are what would be expected from normal biological activity. Ethene is known to be produced biologically (Lamontagne et al., 1973) and photochemically (Wilson et al., 1970) in natural sea water, and these measurements are rather similar to those in other parts of the ocean (Lamontagne et al., 1974). Also, there is evidence from our extensive studies in the Alaskan shelf waters that during periods of intense phytoplankton blooms, ethene is reduced to ethane or ethane is produced directly as the result of high biological activity (Cline, 1977).

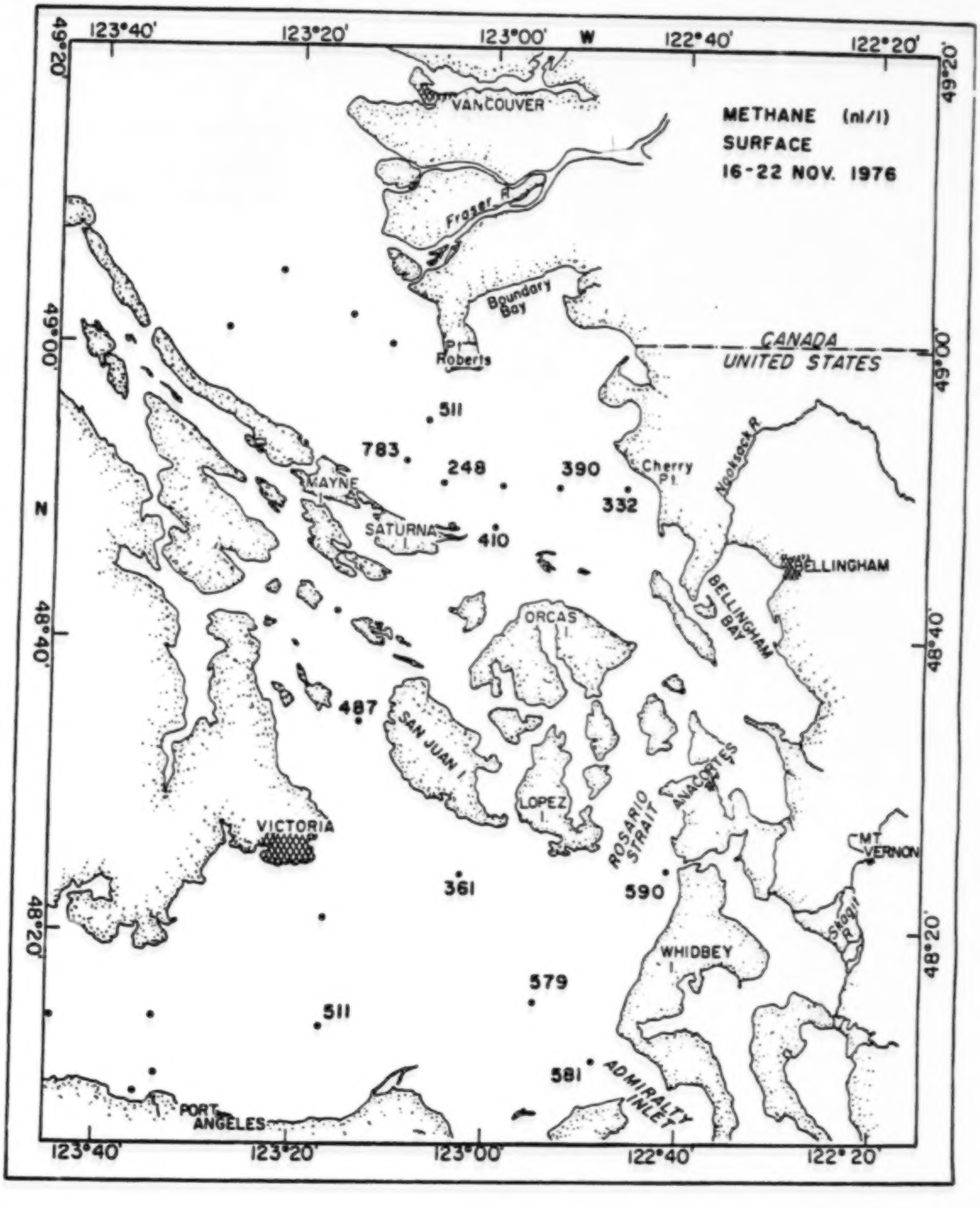
123°40'
123°20'
123°00'
W
122°40'
122°20'
49°20'
49°00'
48°40'
48°20'
N
METHANE (nl/l)
SURFACE
16-22 NOV. 1976
VANCOUVER
Fraser R.
Boundary Bay
Pt. Roberts
CANADA
UNITED STATES
Nooksack R.
Cherry Pt.
BELLINGHAM
BELLINGHAM BAY
MAYNE I.
SATURNA I.
ORCAS I.
SAN JUAN I.
LOPEZ I.
ROSARIO STRAIT
ANACORTES
MT VERNON
Skagit R.
WHIDBEY I.
VICTORIA
PORT ANGELES
ADMIRALTY INLET
511
783
248
390
332
410
487
361
590
579
511
581

Figure A.2. Areal surface distribution of dissolved methane (nℓ/ℓ, STP) during 16-22 Nov. 1976 (MESA-I).

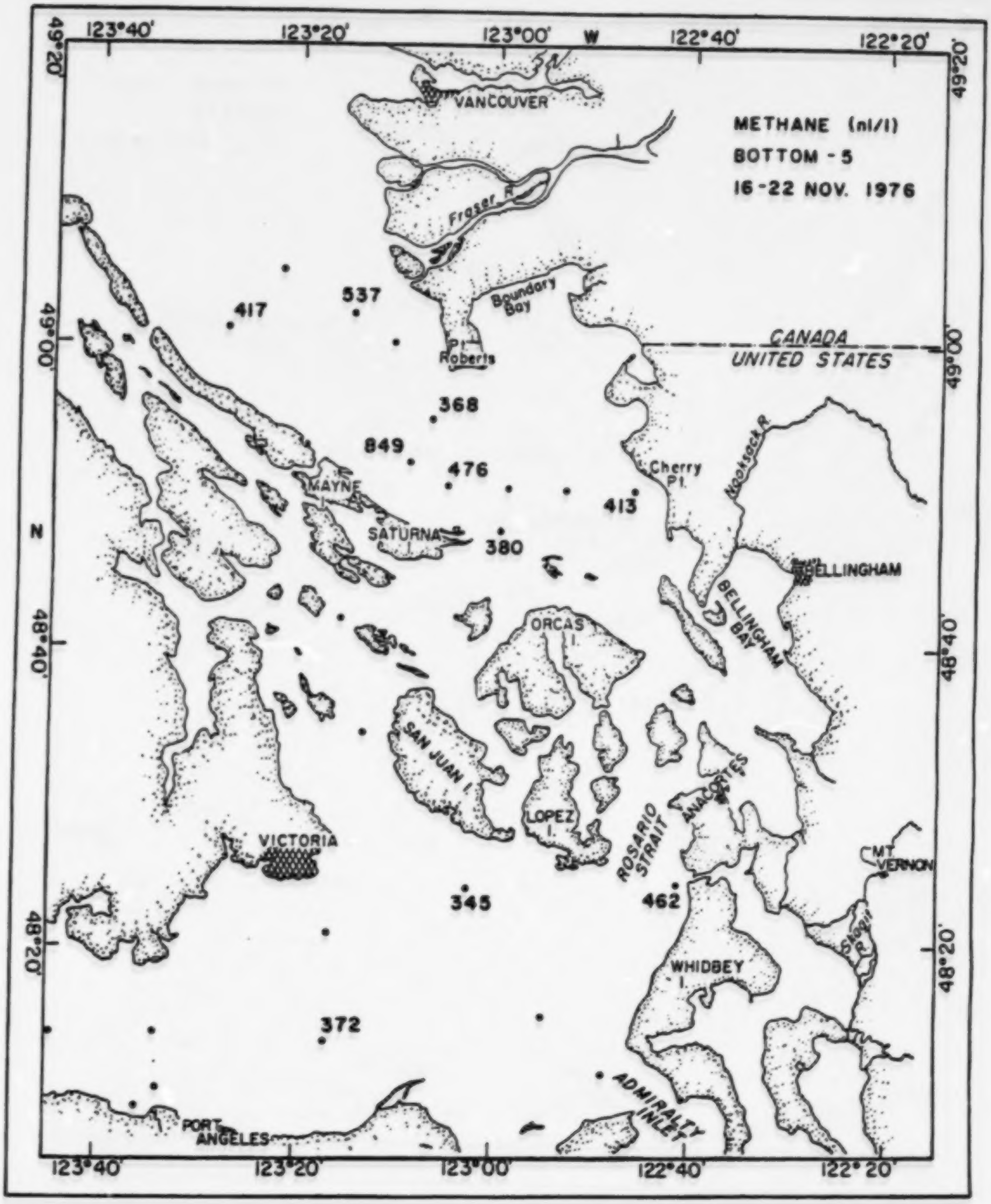
METHANE (nl/l)
BOTTOM - 5
16-22 NOV. 1976
123°40'
123°20'
123°00'
W
122°40'
122°20'
49°20'
49°00'
48°40'
48°20'
N
VANCOUVER
Fraser R.
Boundary Bay
Pt. Roberts
CANADA
UNITED STATES
Cherry Pt.
Nooksack R.
BELLINGHAM
BELLINGHAM BAY
MAYNE
SATURNA
ORCAS I.
SAN JUAN I.
LOPEZ I.
ROSARIO STRAIT
ANACORTES
MT VERNON
Skagit R.
WHIDBEY I.
VICTORIA
PORT ANGELES
ADMIRALTY INLET
417
537
368
849
476
413
380
345
462
372

Figure A.3. Distribution of dissolved methane (nℓ/ℓ, STP) within 5 m of the bottom during 16-22 Nov. 1976 (MESA-I).

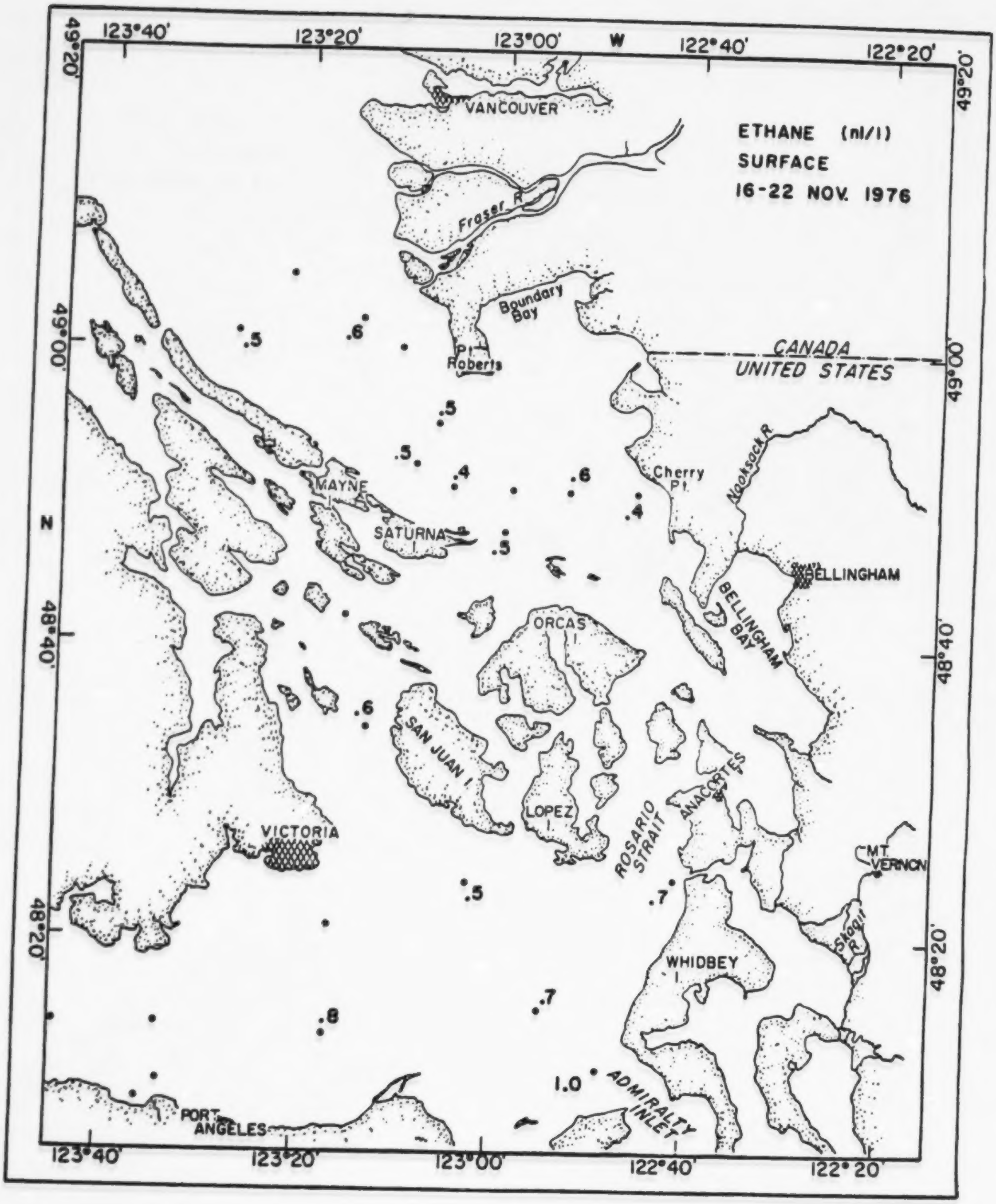

ETHANE (nl/l)
SURFACE
16-22 NOV. 1976
123°40'
123°20'
123°00'
W
122°40'
122°20'
49°20'
49°00'
48°40'
48°20'
N
VANCOUVER
Fraser R.
Boundary Bay
Pt. Roberts
CANADA
UNITED STATES
Cherry Pt.
Nooksack R.
BELLINGHAM
BELLINGHAM BAY
MAYNE
SATURNA I.
ORCAS I.
SAN JUAN I.
LOPEZ I.
ROSARIO STRAIT
ANACORTES
MT. VERNON
Skagit R.
VICTORIA
WHIDBEY I.
PORT ANGELES
ADMIRALTY INLET
.5
.6
.5
.5
.4
.6
.4
.5
.6
.5
.7
.7
.8
1.0

Figure A.4. Areal surface distribution of dissolved ethane (nℓ/ℓ, STP) during 16-22 Nov. 1976 (MESA-I).

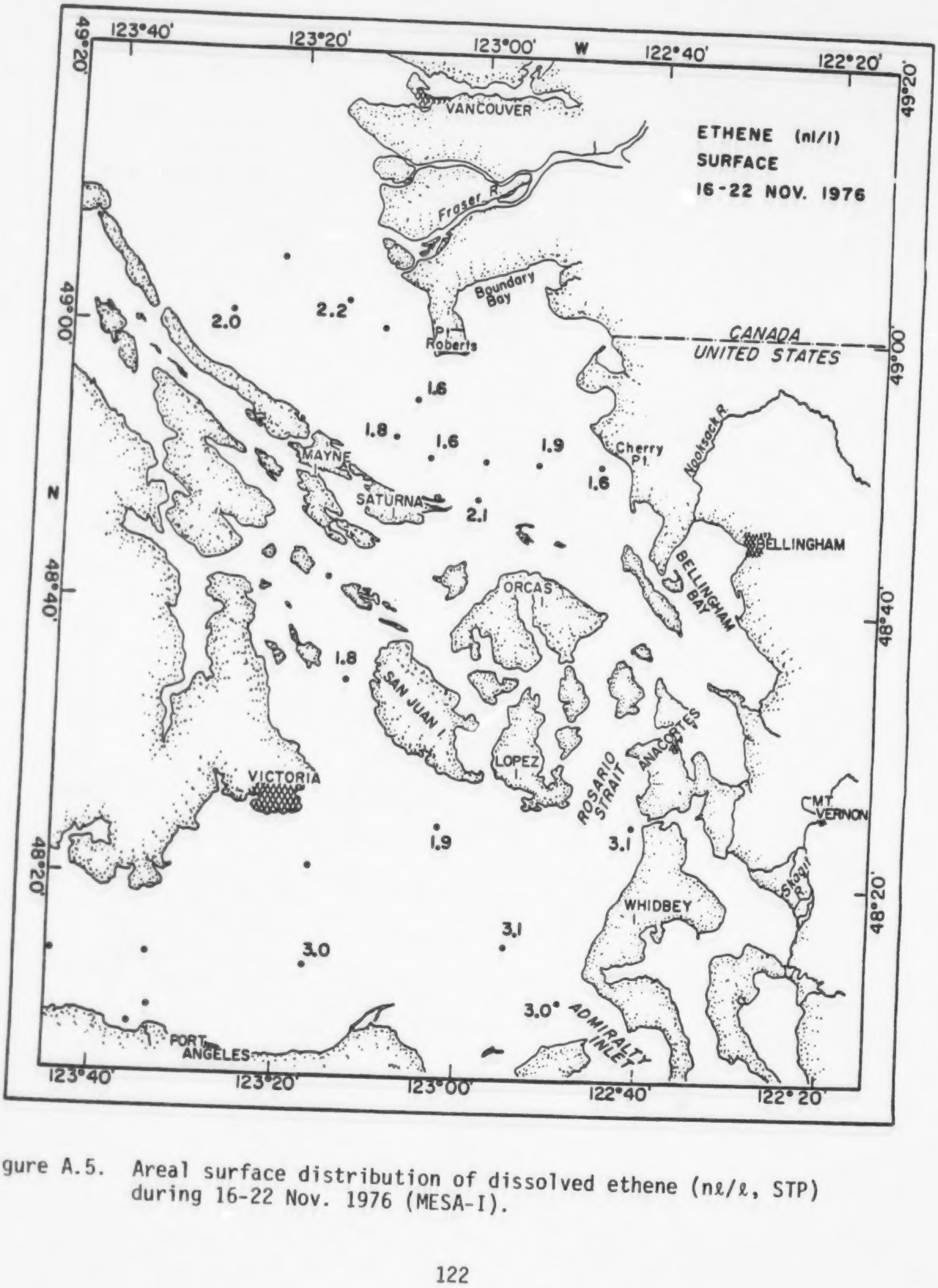
ETHENE (nl/l)
SURFACE
16-22 NOV. 1976
123°40'
123°20'
123°00'
W
122°40'
122°20'
49°20'
49°00'
48°40'
48°20'
N
VANCOUVER
Fraser R.
Boundary Bay
Pt. Roberts
CANADA
UNITED STATES
Cherry Pt.
Nooksack R.
BELLINGHAM
BELLINGHAM BAY
MAYNE I.
SATURNA I.
ORCAS I.
SAN JUAN I.
LOPEZ I.
ROSARIO STRAIT
ANACORTES
MT. VERNON
Skagit R.
WHIDBEY I.
VICTORIA
PORT ANGELES
ADMIRALTY INLET
2.0
2.2
1.6
1.8
1.6
1.9
1.6
2.1
1.8
1.9
3.1
3.1
3.0
3.0

Figure A.5. Areal surface distribution of dissolved ethene (nℓ/ℓ, STP) during 16-22 Nov. 1976 (MESA-I).

A.3.2 LMWH - MESA II

The areal distributions and abundances of methane are shown in Figures A.6 and A.7 for the early spring of 1977. Range of values in the surface waters was 140 nℓ/ℓ to 330 nℓ/ℓ in the near-bottom waters. These levels are significantly less than those observed during the previous fall and suggest a reduced level of biological activity during the observational period. Supersaturation of methane in the surface layers ranged from 3 to 6.

The surface distribution of ethane during March was nearly the same as that observed in the previous fall (Figure A.8). Again the range was 0.4 nℓ/ℓ to 0.6 nℓ/ℓ and suggests little or no input of petroleum containing this compound. Ethene, a hydrocarbon related to marine biological activity, ranged from 1.0 nℓ/ℓ to 1.5 nℓ/ℓ, significantly less than the amounts observed during the previous cruise (Figure A.9). These low levels are rather similar to those observed in late fall in the Alaskan shelf waters (Cline, 1977) and suggest minimal biological activity.

A.3.3 LMWH - MESA III

The surface and near-bottom distributions of methane for August 1977 are presented in Figures A.10 and A.11. In the surface layers, the concentration of methane varied from 120 nℓ/ℓ to approximately 3600 nℓ/ℓ near the Fraser River. More typical values were in the range 400-600 nℓ/ℓ, similar to that observed in fall 1976. The high concentration observed near the Fraser River may be the result of river input or simply related to high levels of primary production. In a study of the Houston Ship Canal, Brooks (1977) observed concentrations of methane as high as 22,000 nℓ/ℓ or a factor of 6 greater than that observed here. It will be shown below that the anomalously high value is probably due to increased biological activity.

Near-bottom concentrations (Figure A.11) varied from 365 nℓ/ℓ to 970 nℓ/ℓ, again near the Fraser River. These again are similar to those concentrations found in the fall of 1977.

Surface concentrations of ethane were slightly elevated above those observed in November 1976 and March 1977 (Figure A.12), but again not out of the normal range observed in known pristine environments (Cline, 1977). The range of concentrations of ethane was 0.4 nℓ/ℓ to 1.5 nℓ/ℓ, the higher concentrations found near Admiralty Inlet, Deception Pass, and Victoria. The absence of high concentrations of ethane near the Fraser River suggests that the unusually high concentration of methane observed there was of marine biological origin.

Figure A.13 shows the surface distribution of ethene. Values ranged from a low of 2 nℓ/ℓ to a high of 20 nℓ/ℓ near Admiralty Inlet. These concentrations are the highest we have ever measured and represent some of the highest concentrations seen anywhere in the oceans (Swinnerton and Lamontagne, 1974). We speculate that these high concentrations are the result of high biological activity, a high radiant energy flux, and low winds at the time of the measurements. The first two factors are known to produce ethene (Wilson et al., 1970); the latter simply retards the flux across the air-sea boundary (Broecker and Peng, 1974).

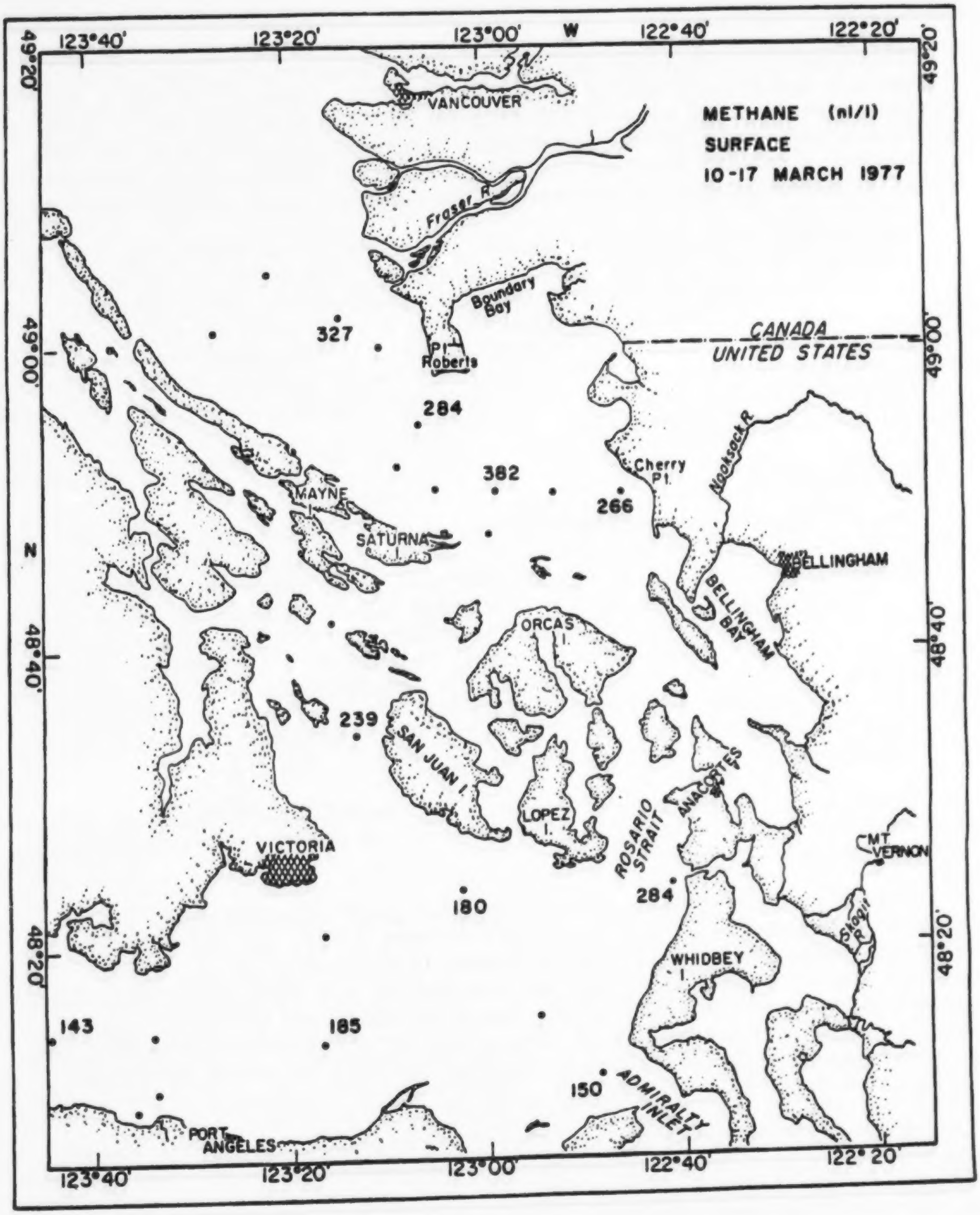
METHANE (nl/l)
SURFACE
10-17 MARCH 1977
123°40'
123°20'
123°00'
W
122°40'
122°20'
49°20'
49°00'
48°40'
48°20'
N
VANCOUVER
Fraser R.
Boundary Bay
Pt. Roberts
CANADA
UNITED STATES
Nooksack R.
Cherry Pt.
BELLINGHAM
BELLINGHAM BAY
MAYNE I.
SATURNA I.
ORCAS I.
SAN JUAN I.
LOPEZ I.
ROSARIO STRAIT
ANACORTES
MT VERNON
Skagit R.
VICTORIA
WHIDBEY I.
ADMIRALTY INLET
PORT ANGELES
327
284
382
266
239
180
284
143
185
150

Figure A.6. Areal surface distribution of dissolved methane (nℓ/ℓ, STP) during 10-17 Mar. 1977 (MESA-II).

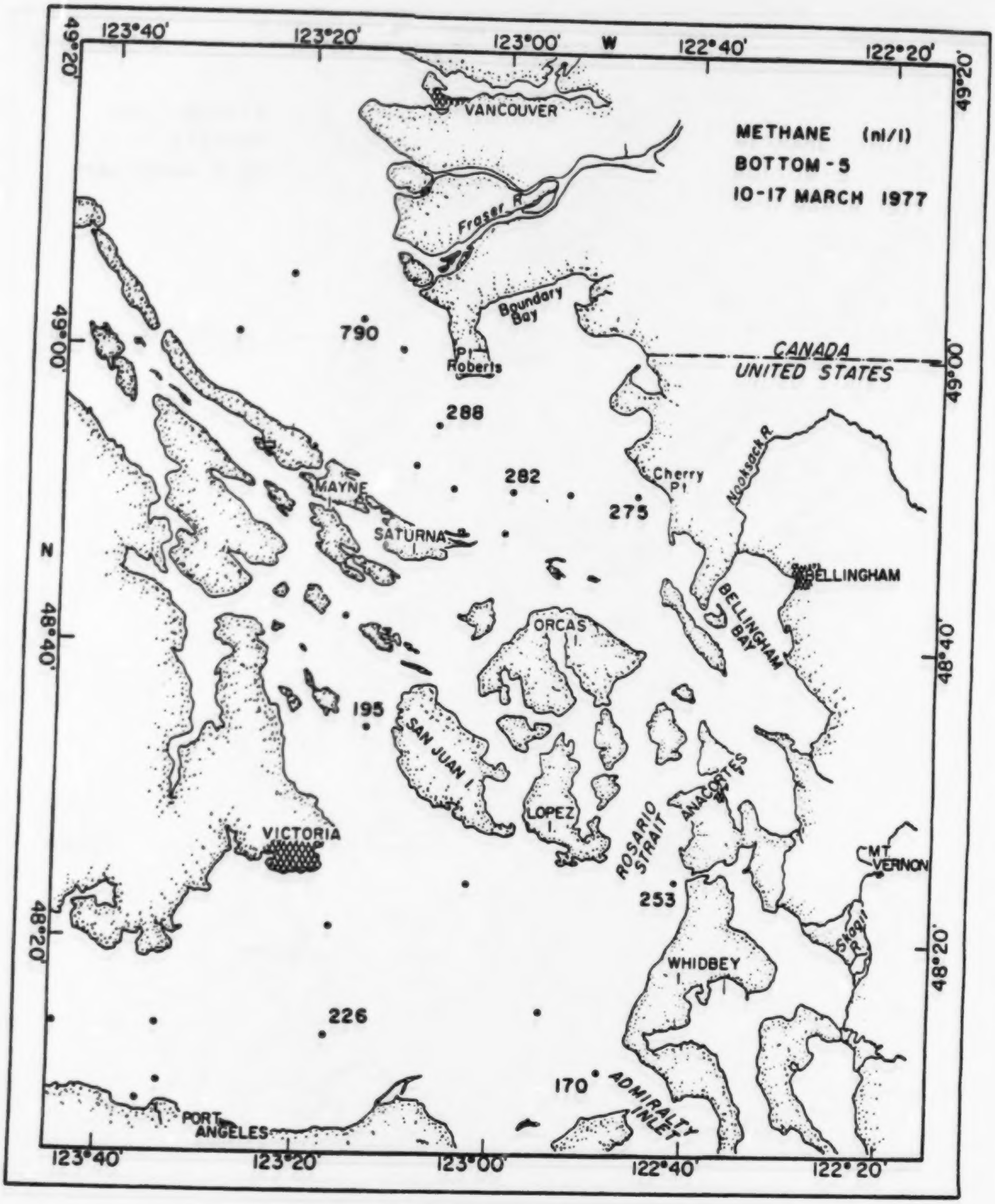

METHANE (nl/l)
BOTTOM - 5
10-17 MARCH 1977
123°40'
123°20'
123°00'
122°40'
122°20'
49°20'
49°00'
48°40'
48°20'
N
W
VANCOUVER
Fraser R.
Boundary Bay
Pt. Roberts
CANADA
UNITED STATES
Cherry Pt.
Nooksack R.
BELLINGHAM
BELLINGHAM BAY
MAYNE I.
SATURNA I.
ORCAS I.
SAN JUAN I.
LOPEZ I.
ROSARIO STRAIT
ANACORTES
MT VERNON
Skagit R.
WHIDBEY I.
VICTORIA
PORT ANGELES
ADMIRALTY INLET
790
288
282
275
195
253
226
170

Figure A.7. Distribution of dissolved methane (nℓ/ℓ, STP) within 5 m of the bottom during 10-17 Mar. 1977 (MESA-II).

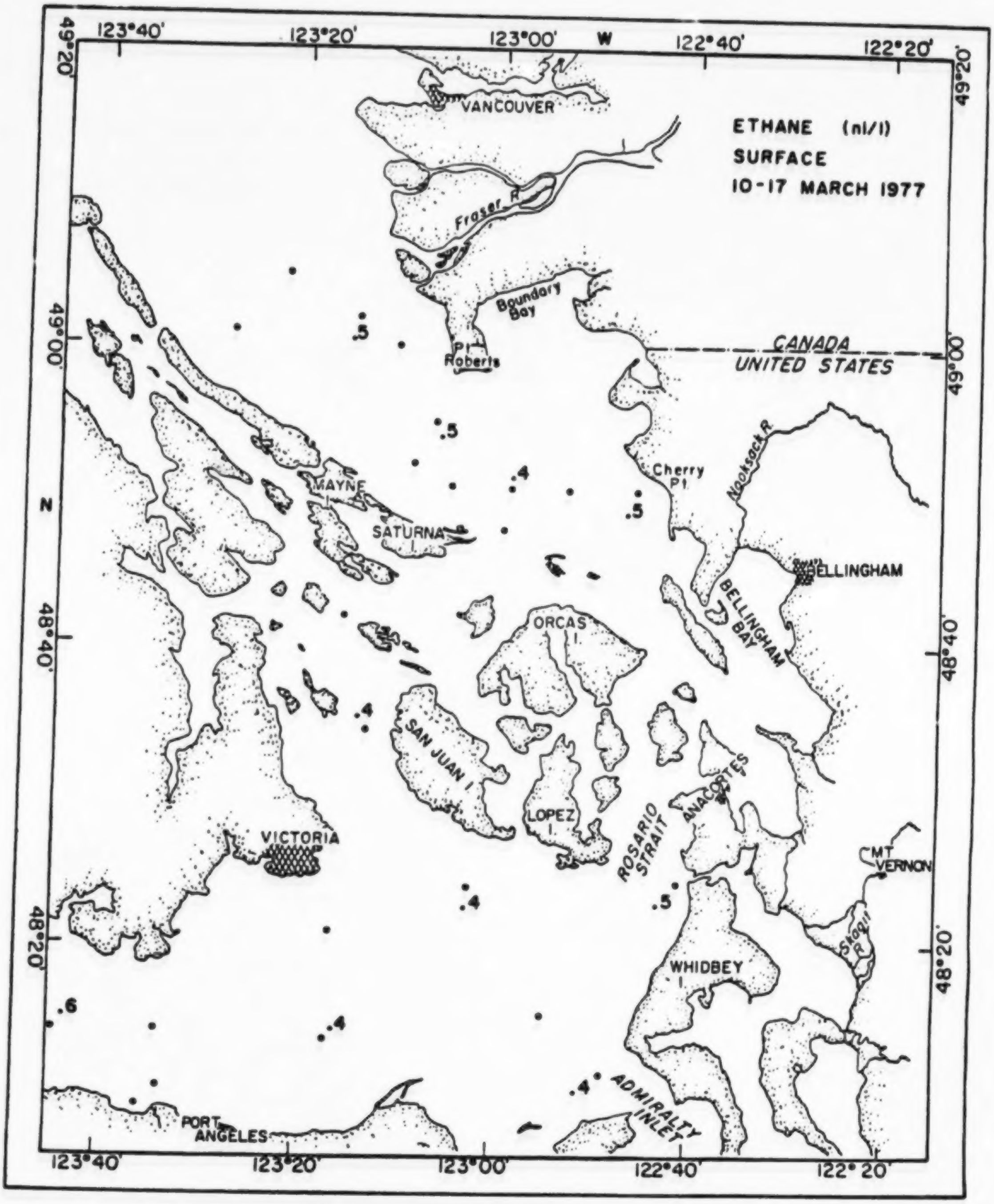
ETHANE (nl/l)
SURFACE
10-17 MARCH 1977
123°40'
123°20'
123°00'
W
122°40'
122°20'
49°20'
49°00'
48°40'
48°20'
N
VANCOUVER
Fraser R.
Boundary Bay
Pt. Roberts
CANADA
UNITED STATES
Cherry Pt.
Nooksack R.
BELLINGHAM
BELLINGHAM BAY
MAYNE I.
SATURNA I.
ORCAS I.
SAN JUAN I.
LOPEZ I.
ROSARIO STRAIT
ANACORTES
MT VERNON
Skagit R.
WHIDBEY I.
VICTORIA
PORT ANGELES
ADMIRALTY INLET
.5
.5
.4
.5
.4
.4
.5
.6
.4
.4

Figure A.8. Areal surface distribution of dissolved ethane (nℓ/ℓ, STP) during 10-17 Mar. 1977 (MESA-II).

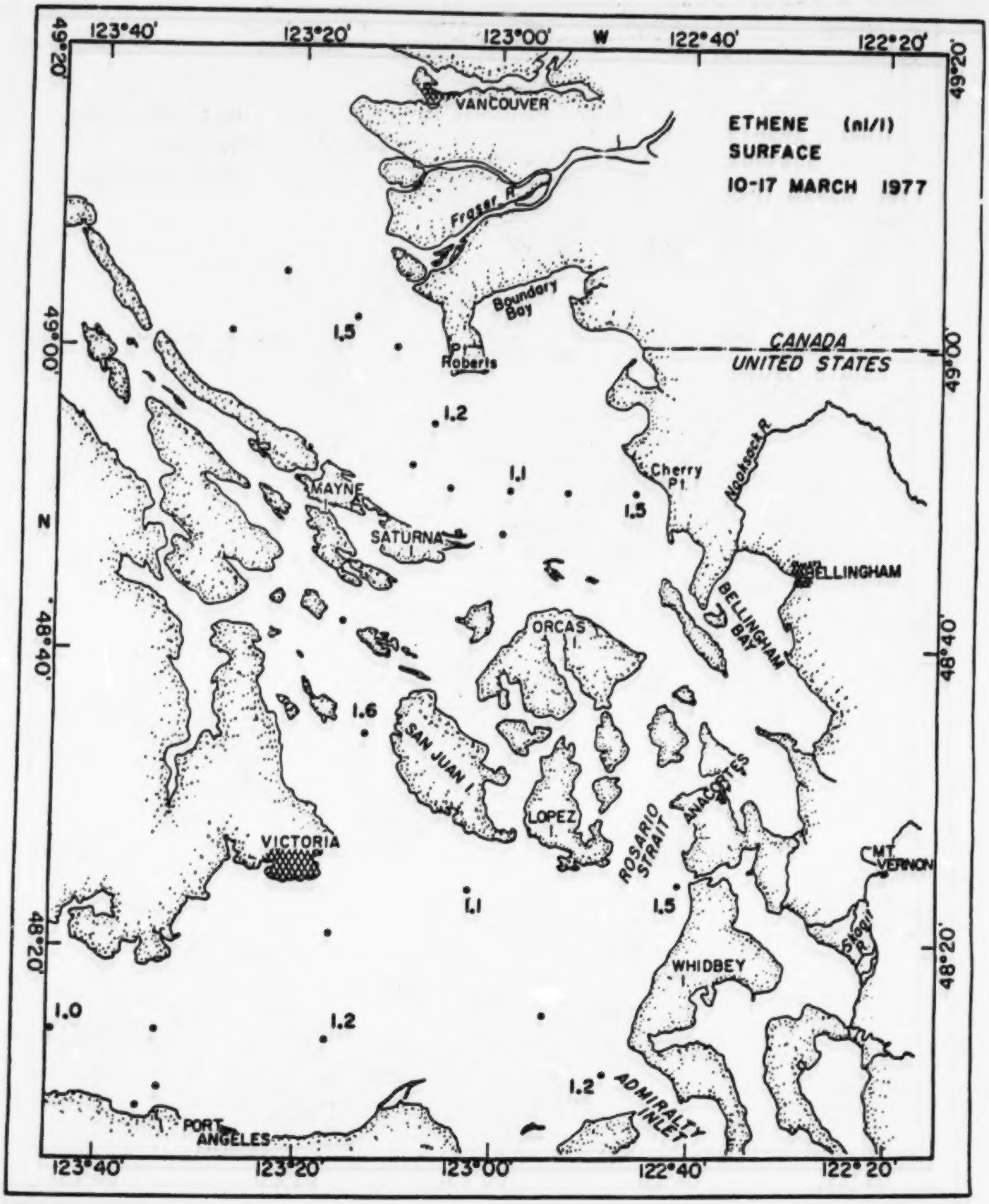

ETHENE (nl/l)
SURFACE
10-17 MARCH 1977
123°40'
123°20'
123°00'
W
122°40'
122°20'
49°20'
49°00'
N
48°40'
48°20'
VANCOUVER
Fraser R.
Boundary Bay
Pt. Roberts
CANADA
UNITED STATES
Nooksack R.
Cherry Pt.
MAYNE I.
SATURNA I.
BELLINGHAM
BELLINGHAM BAY
ORCAS I.
SAN JUAN I.
LOPEZ I.
ROSARIO STRAIT
ANACORTES
MT VERNON
VICTORIA
WHIDBEY I.
Skagit R.
PORT ANGELES
ADMIRALTY INLET
1.5
1.2
1.1
1.5
1.6
1.1
1.5
1.0
1.2
1.2

Figure A.9. Areal surface distribution of dissolved ethene (nℓ/ℓ, STP) during 10-17 Mar. 1977 (MESA-II).

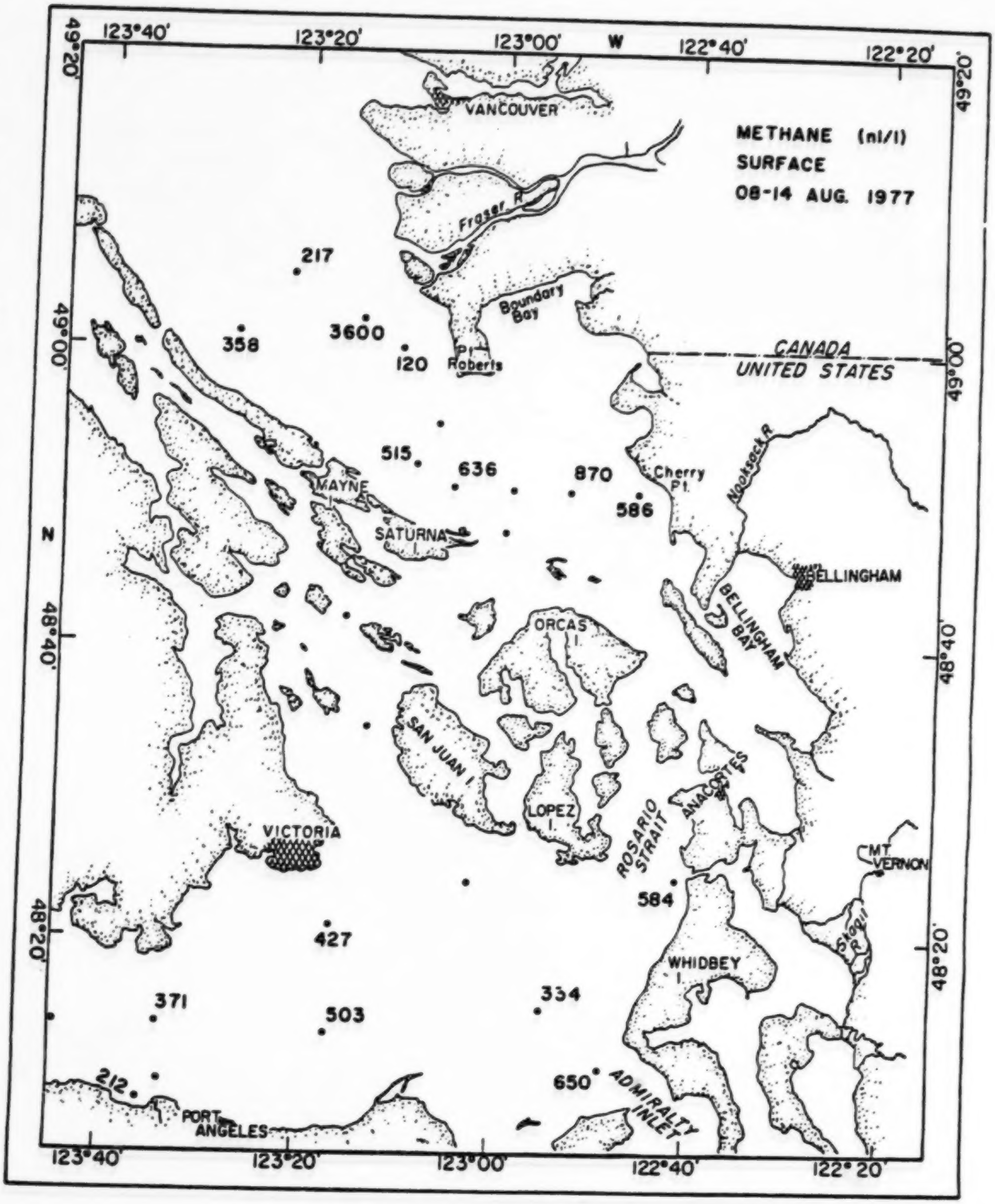
METHANE (nl/l)
SURFACE
08-14 AUG. 1977
123°40'
123°20'
123°00'
W
122°40'
122°20'
49°20'
49°00'
48°40'
48°20'
N
VANCOUVER
Fraser R.
Boundary Bay
Pt. Roberts
CANADA
UNITED STATES
Nooksack R.
Cherry Pt.
BELLINGHAM
BELLINGHAM BAY
MAYNE
SATURNA I.
ORCAS I.
SAN JUAN I.
LOPEZ I.
ROSARIO STRAIT
ANACORTES
VICTORIA
MT. VERNON
Skagit R.
WHIDBEY I.
ADMIRALTY INLET
PORT ANGELES
217
358
3600
120
515
636
870
586
584
427
371
503
334
212
650

Figure A.10. Areal surface distribution of dissolved methane (nℓ/ℓ, STP) during 8-14 Aug. 1977 (MESA-III).

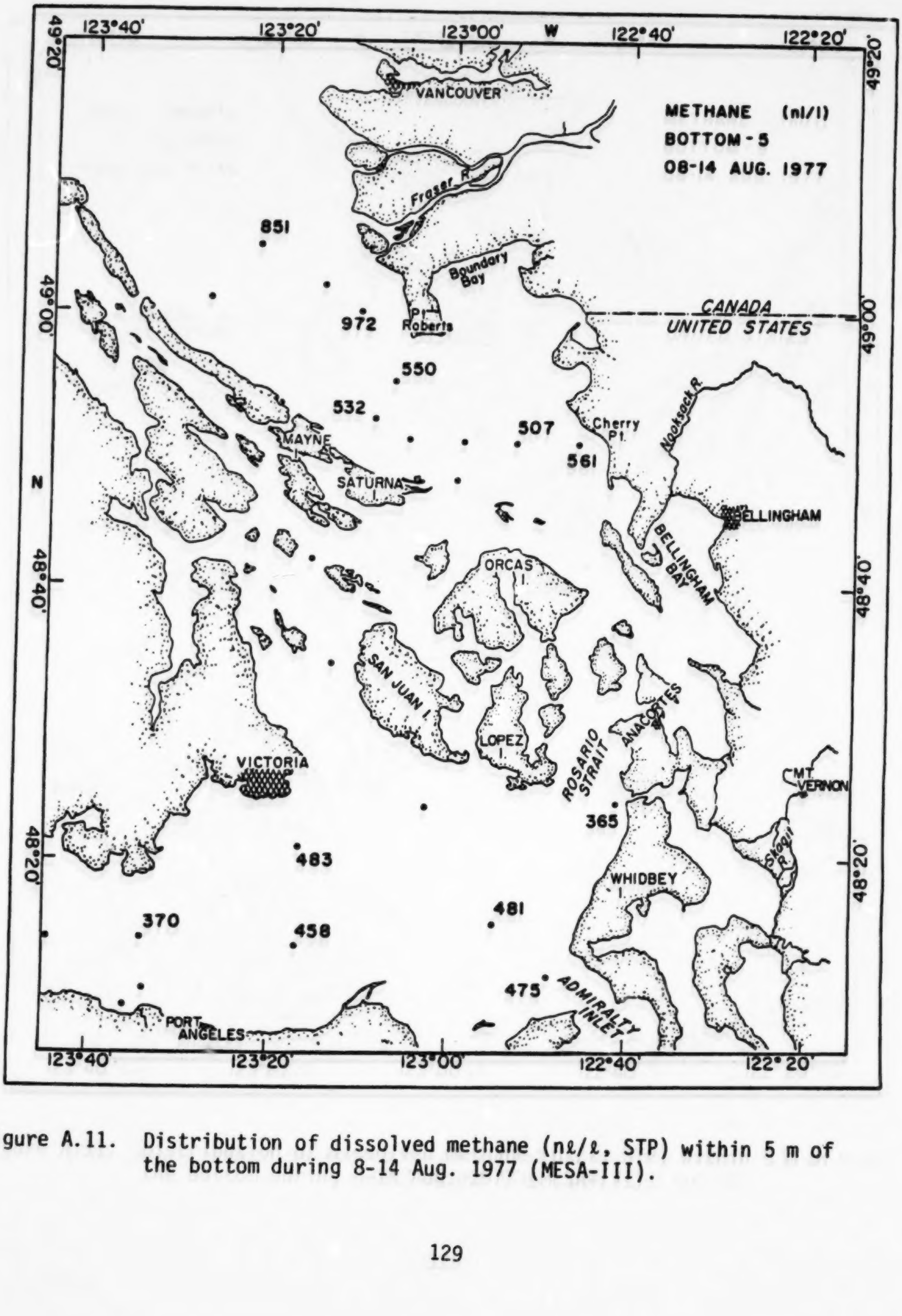
METHANE (nl/l)
BOTTOM - 5
08-14 AUG. 1977
123°40'
123°20'
123°00'
122°40'
122°20'
49°20'
49°00'
48°40'
48°20'
W
N
VANCOUVER
Fraser R.
Boundary Bay
Pt. Roberts
CANADA
UNITED STATES
Cherry Pt.
Nooksack R.
BELLINGHAM
BELLINGHAM BAY
MAYNE
SATURNA I.
ORCAS I.
SAN JUAN I.
LOPEZ I.
ROSARIO STRAIT
ANACORTES
MT VERNON
Skagit R.
WHIDBEY I.
VICTORIA
PORT ANGELES
ADMIRALTY INLET
851
972
550
532
507
561
365
483
370
458
481
475

Figure A.11. Distribution of dissolved methane (nℓ/ℓ, STP) within 5 m of the bottom during 8-14 Aug. 1977 (MESA-III).

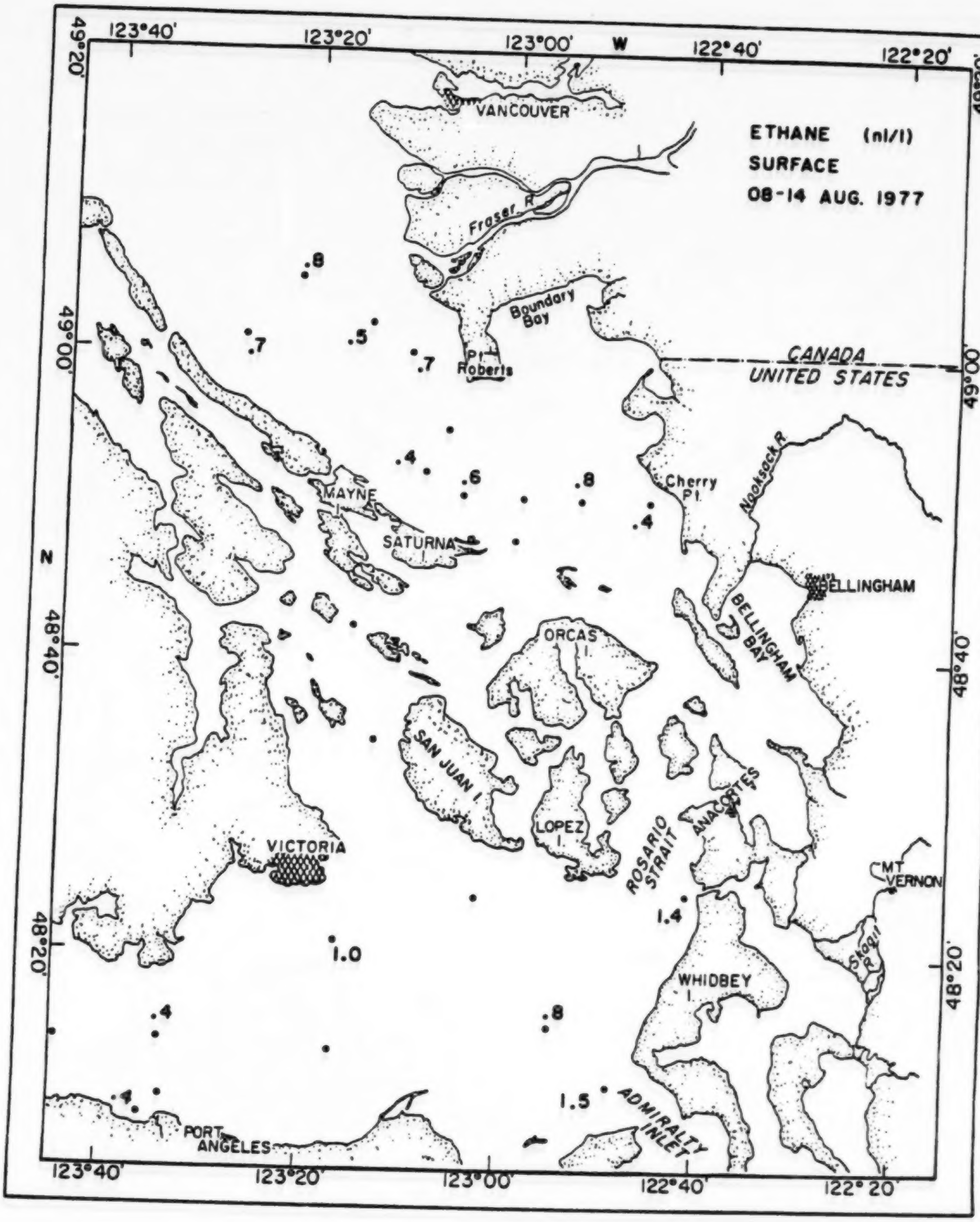
ETHANE (nl/l)
SURFACE
08-14 AUG. 1977
123°40'
123°20'
123°00'
W
122°40'
122°20'
49°20'
49°00'
48°40'
48°20'
N
VANCOUVER
Fraser R.
Boundary Bay
Pt. Roberts
CANADA
UNITED STATES
Cherry Pt.
Nooksack R.
BELLINGHAM
BELLINGHAM BAY
MAYNE
SATURNA I.
ORCAS I.
SAN JUAN I.
LOPEZ I.
ROSARIO STRAIT
ANACORTES
MT VERNON
Skagit R.
WHIDBEY I.
VICTORIA
PORT ANGELES
ADMIRALTY INLET
.8
.7
.5
.7
.4
.6
.8
.4
1.4
1.0
.4
.8
.4
1.5

Figure A.12. Areal surface distribution of dissolved ethane (nℓ/ℓ, STP) during 8-14 Aug. 1977 (MESA-III).

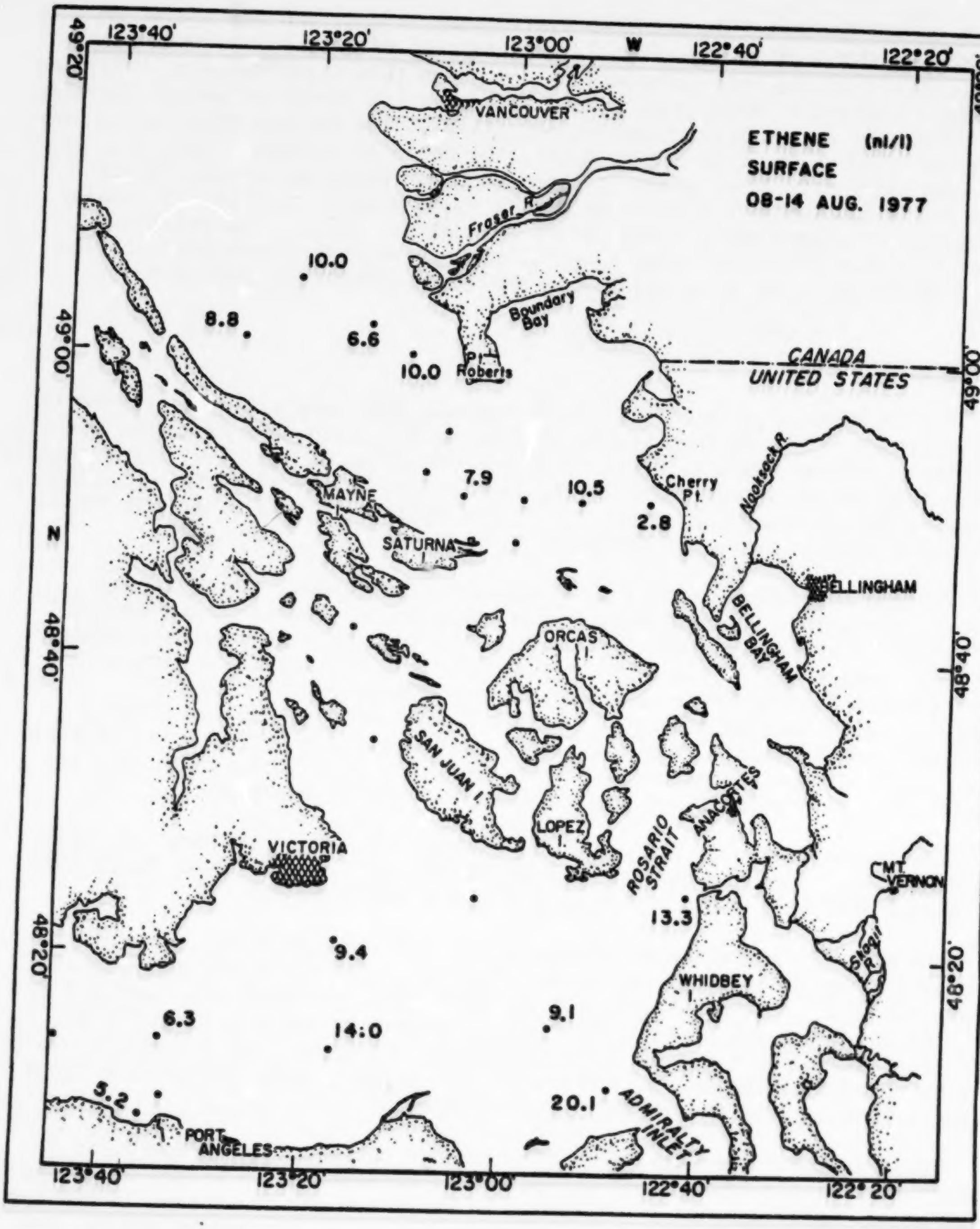
ETHENE (nl/l)
SURFACE
08-14 AUG. 1977
123°40'
123°20'
123°00'
W
122°40'
122°20'
49°20'
49°00'
48°40'
48°20'
N
VANCOUVER
Fraser R.
Boundary Bay
Pt. Roberts
CANADA
UNITED STATES
Nooksack R.
Cherry Pt.
BELLINGHAM
BELLINGHAM BAY
MAYNE I.
SATURNA I.
ORCAS I.
SAN JUAN I.
LOPEZ I.
ROSARIO STRAIT
ANACORTES
MT VERNON
Skagit R.
WHIDBEY I.
VICTORIA
PORT ANGELES
ADMIRALTY INLET
10.0
8.8
6.6
10.0
7.9
10.5
2.8
13.3
9.4
6.3
14.0
9.1
5.2
20.1

Figure A.13. Areal surface distribution of dissolved ethene (nℓ/ℓ, STP) during 8-14 Aug. 1977 (MESA-III).

A useful parameter in which to distinguish natural and petrogenic LMWH is the ethane:ethene ratio ($C_{2:0}/C_{2:1}$). The success of this ratio depends on the low abundance of olefinic compounds in petroleum (Clark and MacLeod, 1977) and the small biological production of the saturated low molecular weight hydrocarbons in marine waters (Lamontagne et al., 1974). The surface distribution for the study site is shown in Figure A.14. The ratio is uniformly near 0.1, except near Admiralty Inlet where it rises to 0.7. Based on our studies of known petroleum input in Alaskan waters, a ratio greater than one is usually indicative of a petrogenic input (Cline and Holmes, 1977). The relatively high ratio near Admiralty Inlet suggests some petrogenic ethane contribution from Puget Sound, but it is relatively small and within the ambient noise level.

A.4 SUMMARY

The low molecular weight aliphatic hydrocarbons were measured seasonally in the waters of the eastern Strait of Juan de Fuca, San Juan passages, and the southern Strait of Georgia. This study was conducted as a part of the suspended matter program and served to delineate the current levels of dissolved methane, ethane, ethene, propane, propene, iso- and n-butanes. These dissolved constituents are useful markers of petroleum hydrocarbons.

Methane and ethene, two of the hydrocarbons observed, showed strong seasonal variations in distribution that could be related to normal seasonal variations in biological activity. Methane in surface waters range from near 140 nℓ/ℓ in March 1977 to a high of 3600 nℓ/ℓ in August of 1977. The mean concentration for the three observational periods were 480 ± 150 nℓ/ℓ (November 1976) and 245 ± 80 nℓ/ℓ (August 1977); the high and low values (3600 nℓ/ℓ and 120 nℓ/ℓ) from the August period were not included in the estimate. Mean surface concentrations were nearly the same in November 1976 and August 1977, with a factor of two decrease observed in March 1977.

The concentration of ethene in the surface layers was uniform temporally and spatially. The mean surface concentrations for November 1976, March 1977, and August 1977 were 0.6 ± 0.2 nℓ/ℓ, 0.5 ± 0.1 nℓ/ℓ, and 0.7 ± 0.4 nℓ/ℓ.

The mean concentration of ethene in the surface layers was low and uniform during the first two observational periods, then increased abruptly in August of 1977. The mean levels for November 1976 and March 1977 were 2.2 ± 0.6 nℓ/ℓ and 1.3 ± 0.2 nℓ/ℓ, respectively, increasing abruptly to 9.6 ± 4.2 nℓ/ℓ in August 1977. The cause of this increase is not known, but is believed to be related to high biological activity and light levels. Both factors are known to be responsible for the production of ethene.

Based on these few data, much of which was not shown for brevity, it appears that little hydrocarbon pollution was evident in the waters of northern Puget Sound. Although incipient levels of petroleum may be present in the system, the distributions and abundances of the low molecular weight alkanes and alkenes are within the normal biological background levels.

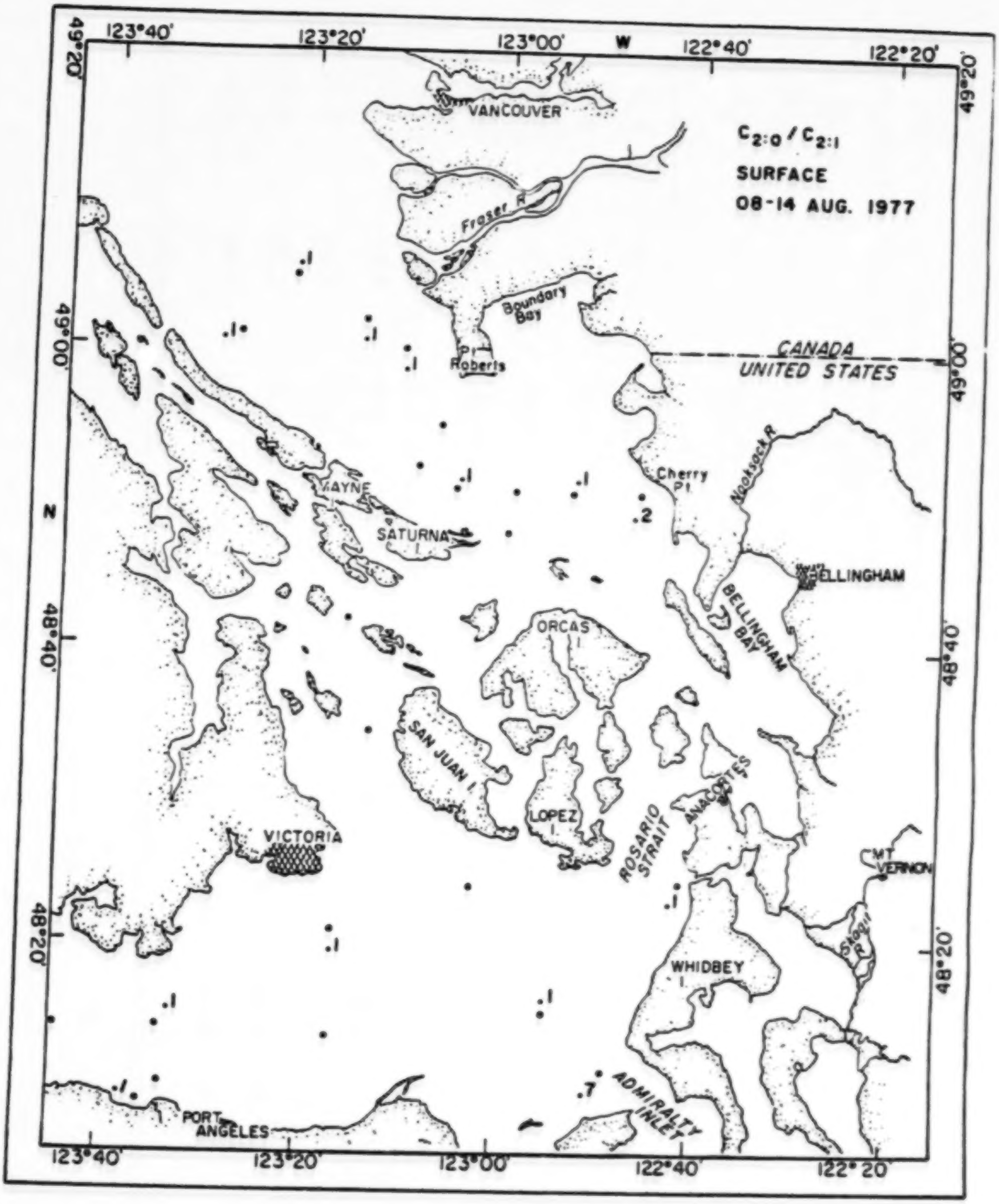
123°40'
123°20'
123°00'
W
122°40'
122°20'
49°20'
VANCOUVER
$C_{2:0}/C_{2:1}$
SURFACE
08-14 AUG. 1977
Fraser R.
Boundary Bay
Pt. Roberts
CANADA
UNITED STATES
49°00'
N
Cherry Pt.
Nooksack R.
MAYNE
SATURNA I.
BELLINGHAM
BELLINGHAM BAY
ORCAS I.
48°40'
SAN JUAN I.
LOPEZ I.
ROSARIO STRAIT
ANACORTES
VICTORIA
MT. VERNON
48°20'
WHIDBEY I.
Skagit R.
PORT ANGELES
ADMIRALTY INLET
.1
.1
.1
.1
.1
.1
.2
.1
.1
.1
.1
.1
.7

Figure A.14. The areal surface ethane/ethene ratio ($C_{2:0}/C_{2:1}$) during 8-14 Aug. 1977 (MESA-III).

TABLE A.1 Seasonal distributions of selected hydrocarbons at station 2 (48°11.3'N 122°48.6'W)

	Depth (m)	S (°/oo)	T (°C)	Methane	Ethane	Ethene	Propane	Propene	Ethane/Ethene
						(nℓ/ℓ) STP			
MESA I Nov. 1976	0	-	-	581	0.97	3.00	1.11	1.06	0.32
	40	-	-	548	0.88	2.38	0.93	-	0.37
MESA II March 1977	0	-	-	150	0.39	1.16	0.37	0.89	0.34
	10	-	-	145	0.46	1.21	0.41	0.65	0.38
	20	-	-	137	0.32	0.96	0.22	0.51	0.33
	50	-	-	170	0.45	1.01	0.31	0.72	0.44
MESA III Aug. 1977	0	30.47	11.30	650	1.47	20.10	1.09	4.63	.07
	10	31.50	10.22	605	0.85	7.54	0.63	2.48	0.11
	20	31.85	9.66	540	0.68	6.05	0.62	2.05	0.11
	47	32.49	8.79	475	0.40	3.94	0.58	1.42	0.10

TABLE A.2 Seasonal distributions of selected hydrocarbons at station 5 (48°14.0'N 123°17.2'W)

	Depth (m)	S (°/oo)	T (°C)	Methane	Ethane	Ethene (nℓ/ℓ)	Propane STP	Propene	Ethane/Ethene
MESA I Nov. 1976	0	30.97	9.13	511	0.76	3.06	-	-	0.25
	10	31.11	9.03	528	0.83	2.40	0.67	1.31	0.34
	20	31.16	8.97	531	0.78	2.19	0.63	-	0.36
	60	-	-	420	0.72	-	-	-	-
	110	-	-	372	0.95	1.30	0.76	0.64	0.73
MESA II March 1977	0	-	-	185	0.45	1.22	0.32	0.68	0.37
	10	-	-	182	0.43	1.19	0.30	0.78	0.36
	20	-	-	196	0.48	1.25	0.32	0.76	0.38
	40	-	-	202	0.48	1.08	0.32	0.75	0.44
	60	-	-	206	0.47	1.07	0.47	0.67	0.44
	114	-	-	226	0.58	0.97	0.44	0.55	0.60
MESA III Aug. 1977	0	30.36	11.42	503	-	1.40	0.54	2.36	-
	10	30.37	11.38	491	0.75	7.41	0.58	2.44	0.10
	20	31.11	10.65	538	0.69	7.79	0.61	2.35	0.09
	60	32.47	8.62	473	0.44	3.74	0.42	1.20	0.12
	127	33.37	7.32	458	0.28	1.52	0.31	0.78	0.18

TABLE A.3 Seasonal distributions of selected hydrocarbons at station 15 ($48^{o}24.2'$N $122^{o}41.0'$W)

	Depth (m)	S ($^{o}/oo$)	T (^{o}C)	Methane	Ethane	Ethene (nℓ/ℓ) STP	Propane	Propene	Ethane/Ethene
MESA I Nov. 1976	8	-	-	474	0.79	2.07	0.63	0.99	0.38
MESA II March 1977	10	-	-	284	0.46	1.50	0.34	0.83	0.31
	20	-	-	290	0.46	1.45	0.34	0.82	0.32
	40	-	-	278	0.46	1.38	0.32	0.78	0.33
	60	-	-	261	0.49	1.32	0.34	0.71	0.37
	73	-	-	253	0.49	1.23	0.35	0.66	0.40
MESA III Aug. 1977	0	29.72	11.92	584	1.40	13.30	0.97	-	0.10
	10	30.45	10.68	560	0.86	7.25	0.75	-	0.12
	20	30.91	10.16	601	0.86	7.25	0.63	-	0.12
	30	31.29	9.84	676	0.72	7.44	-	-	0.10
	40	31.80	9.32	672	0.63	6.33	-	-	0.10
	60	32.00	10.24	365	0.45	4.75	0.80	-	.09

TABLE A.4 Seasonal distributions of selected hydrocarbons at station 17 (48°50.6'N 122°46.2'W)

	Depth (m)	S (° oo)	T (°C)	Methane	Ethane	Ethene (nℓ/ℓ) STP	Propane	Propene	Ethane/Ethene
MESA I Nov. 1976	0	29.39	8.68	332	0.45	1.60	0.43	0.80	0.28
	10	29.39	8.91	359	0.45	1.67	0.47	0.79	0.27
	20	29.84	8.91	418	0.54	1.94	0.53	0.88	0.28
	32	29.92	8.91	413	0.56	1.68	0.54	0.88	0.33
MESA II March 1977	0	-	-	266	0.47	1.49	0.36	0.87	0.32
	10	-	-	272	0.46	1.33	0.36	0.80	0.34
	20	-	-	276	0.47	1.41	0.37	0.80	0.33
	40	-	-	275	0.46	1.33	0.38	0.74	0.34
MESA III Aug. 1977	0	24.44	19.82	586	0.45	2.84	0.90	1.19	0.16
	10	26.05	15.68	561	0.30	1.99	0.82	0.82	0.15
	21	27.84	13.10	561	0.31	1.77	0.72	0.55	0.18

TABLE A.5 Seasonal distributions of selected hydrocarbons at station 23 (48°55.0'N 123°6.5'W)

	Depth (m)	S (°/oo)	T (°C)	Methane	Ethane	Ethene (nℓ/ℓ) STP	Propane	Propene	Ethane/Ethene
MESA I Nov. 1976	1	30.89	9.01	511	0.46	1.59	0.60	1.04	0.30
	11	31.32	9.04	301	0.36	1.61	0.42	0.87	0.22
	21	31.35	9.08	174	0.34	1.60	0.47	0.86	0.21
	61	32.29	8.89	379	0.54	1.64	0.68	0.71	0.33
	111	32.80	8.65	368	0.64	1.88	-	-	0.34
MESA II March 1977	0	-	-	284	0.46	1.17	0.30	0.77	0.39
	10	-	-	273	0.43	1.20	0.30	0.74	0.36
	20	-	-	262	0.45	1.17	0.31	0.74	0.39
	40	-	-	256	0.46	1.21	0.34	0.76	0.38
	60	-	-	267	0.46	1.27	0.35	0.73	0.36
	119	-	-	288	0.49	1.26	0.38	0.71	0.39
MESA III Aug. 1977	10	28.18	12.70	358	0.78	7.13	0.66	2.06	0.11
	20	29.01	11.30	352	0.56	5.22	0.62	1.67	0.11
	30	29.30	11.34	180	0.40	3.80	0.74	1.50	0.10
	114	30.96	9.76	550	0.58	4.55	0.63	1.52	0.13

TABLE A.6 Seasonal distributions of selected hydrocarbons at station 26 (49°2.0'N 123°15.5'W)

	Depth (m)	S (°/oo)	T (°C)	Methane	Ethane	Ethene	Propane	Propene	Ethane/Ethene
						(nℓ/ℓ) STP			
MESA I Nov. 1976	0	26.41	8.51	-	0.64	2.20	0.60	1.28	0.29
	10	32.23	9.05	439	0.45	1.59	0.60	0.92	0.28
	20	32.39	8.99	528	0.50	1.81	1.22	1.51	0.28
	60	32.52	8.89	537	0.56	1.79	0.49	1.03	0.31
MESA II March 1977	0	-	-	327	0.54	1.46	0.36	1.29	0.37
	10	-	-	326	0.91	1.46	0.47	0.95	0.62
	20	-	-	242	0.33	0.96	0.34	0.83	0.34
	40	-	-	137	0.32	0.90	0.41	0.89	0.36
	60	-	-	161	0.33	0.90	0.42	0.97	0.37
	188	-	-	790	0.45	1.18	0.38	0.81	0.38
MESA III Aug. 1977	0	23.67	15.38	273	0.92	8.86	0.81	2.81	0.10
	84	30.44	9.88	339	0.65	4.65	0.58	1.52	0.14

TABLE A.7 Seasonal distributions of selected hydrocarbons at station 32 (48°34.3'N 123°13.5'W)

	Depth (m)	S (°/oo)	T (°C)	Methane	Ethane	Ethene (nℓ/ℓ) STP	Propane	Propene	Ethane/Ethene
MESA I Nov. 1976	0	-	-	487	0.64	1.76	0.63	1.01	0.36
	5	-	-	405	0.61	1.88	0.55	0.84	0.32
	10	-	-	487	0.60	2.51	0.68	0.95	0.24
	20	-	-	431	0.66	2.29	0.65	0.88	0.29
	60	-	-	388	0.63	2.13	0.63	0.81	0.30
	200	-	-	382	0.67	2.05	0.64	0.81	0.33
MESA II March 1977	0	-	-	239	0.44	1.60	0.32	0.95	0.28
	20	-	-	243	0.46	1.49	0.33	0.84	0.32
	50	-	-	227	0.45	1.27	0.33	0.76	0.35
	100	-	-	223	0.51	1.46	0.46	0.98	0.35
	150	-	-	209	0.60	1.18	0.38	0.83	0.51
	225	-	-	195	0.49	1.20	0.40	0.88	0.41
MESA III August 1977					No Data				